IntechOpen Series
Veterinary Medicine and Science, Volume 17

Animal Science Annual Volume 2023

Edited by Edward Narayan

Animal Science Annual Volume 2023

Edited by Edward Narayan

Contributors
Khursheed Ahmad, Arbab Sikandar, Amar Nasir, Alan Vincelette, Elise Renders, Diksha Kandpal, Deepika Lather, Vikas Nehra, Babulal Jangir, Muhammad Fahad Raza

Notice
Statements and opinions expressed in the chapters are these of the individual contributors and not necessarily those of the editors or publisher. No responsibility is accepted for the accuracy of information contained in the published chapters. The publisher assumes no responsibility for any damage or injury to persons or property arising out of the use of any materials, instructions, methods or ideas contained in the book.

We are IntechOpen,
the world's leading publisher of Open Access books
Built by scientists, for scientists

6,700+
Open access books available

181,000+
International authors and editors

195M+
Downloads

156
Countries delivered to

Our authors are among the
Top 1%
most cited scientists

12.2%
Contributors from top 500 universities

Interested in publishing with us?
Contact book.department@intechopen.com

Numbers displayed above are based on latest data collected.
For more information visit www.intechopen.com

Veterinary Medicine and Science

Volume 17

Aims and Scope of the Series

Paralleling similar advances in the medical field, astounding advances occurred in Veterinary Medicine and Science in recent decades. These advances have helped foster better support for animal health, more humane animal production, and a better understanding of the physiology of endangered species to improve the assisted reproductive technologies or the pathogenesis of certain diseases, where animals can be used as models for human diseases (like cancer, degenerative diseases or fertility), and even as a guarantee of public health. Bridging Human, Animal, and Environmental health, the holistic and integrative "One Health" concept intimately associates the developments within those fields, projecting its advancements into practice. This book series aims to tackle various animal-related medicine and sciences fields, providing thematic volumes consisting of high-quality significant research directed to researchers and postgraduates. It aims to give us a glimpse into the new accomplishments in the Veterinary Medicine and Science field. By addressing hot topics in veterinary sciences, we aim to gather authoritative texts within each issue of this series, providing in-depth overviews and analysis for graduates, academics, and practitioners and foreseeing a deeper understanding of the subject. Forthcoming texts, written and edited by experienced researchers from both industry and academia, will also discuss scientific challenges faced today in Veterinary Medicine and Science. In brief, we hope that books in this series will provide accessible references for those interested or working in this field and encourage learning in a range of different topics.

Meet the Series Editor

Rita Payan Carreira earned her Veterinary Degree from the Faculty of Veterinary Medicine in Lisbon, Portugal, in 1985. She obtained her Ph.D. in Veterinary Sciences from the University of Trás-os-Montes e Alto Douro, Portugal. After almost 32 years of teaching at the University of Trás-os-Montes and Alto Douro, she recently moved to the University of Évora, Department of Veterinary Medicine, where she teaches in the field of Animal Reproduction and Clinics. Her primary research areas include the molecular markers of the endometrial cycle and the embryo–maternal interaction, including oxidative stress and the reproductive physiology and disorders of sexual development, besides the molecular determinants of male and female fertility. She often supervises students preparing their master's or doctoral theses. She is also a frequent referee for various journals.

Meet the Topic Editor

Dr. Edward Narayan graduated with a Ph.D. in Biology from the University of the South Pacific. He pioneered non-invasive reproductive and stress endocrinology tools for amphibians through the novel development and validation of non-invasive enzyme immunoassays. These assays evaluate reproductive hormonal cycles and stress hormone responses to environmental stressors. Dr. Narayan leads the Stress Lab (Comparative Physiology and Endocrinology) at the University of Queensland, a dynamic research platform focusing on comparative vertebrate physiology, stress endocrinology, reproductive endocrinology, animal health and welfare, and conservation biology. Edward has supervised over 40 research students and has published over 100 peer-reviewed research articles.

Contents

Preface

Animal Science is an important field of biological sciences that covers research on captive and wildlife species, including domesticated animals. The research presented consists of primary studies in various animal biology fields such as genetics, nutrition, behavior, welfare, and animal production, to name a few.

The contributing authors come from diverse animal science fields, including animal welfare and health, ecology, neurobiology, anatomy, and physiology. This volume features a total of five peer-reviewed articles, published in Volume 2023 of Animal Science.

Chapter 1, titled "Ecology and Conservation of Mountain Ungulate in the Western and Trans-Himalayas, India", provides information on the status, ecology, and conservation of 20 ungulate species inhabiting the Himalayan region.

Chapter 2, titled "Alimentary System of Native Goat Breeds of Pakistan", provides an anatomical description of the alimentary system of goats in Pakistan. The chapter covers information on gross and microscopic anatomical features of the alimentary canal and highlights health and clinical issues associated with the goat alimentary system.

Chapter 3, titled "Pathology of Protein Misfolding Diseases in Animals", describes and discusses protein misfolding diseases. It explores recent developments in diagnostic techniques and discusses their pros and cons.

Chapter 4, titled "New Studies on the Gaits Displayed by Miocene, Pliocene, and Pleistocene Fossil Horse Trackways", presents a refined method for assessing the gaits of fossil equids through the study of Miocene, Pliocene, and Pleistocene fossil trackways. The results are utilized to explore the herding behaviors of prehistoric equids.

Chapter 5, titled "Role of Dopamine Receptors in Olfaction Learning Success", describes and discusses the biogenic amine neurotransmitters that contribute to olfaction success in honeybees.

Dr. Edward Narayan
School of Agriculture and Food Sustainability,
The University of Queensland,
Brisbane, Australia

Chapter 1

Ecology and Conservation of Mountain Ungulate in the Western and Trans-Himalayas, India

Khursheed Ahmad

Abstract

The Western and Trans-Himalayan region of India is home to several unique and threatened mountain ungulates including Kashmir red deer or Hangul, Kashmir Musk deer, Urial, Argali, Tibetan Antelope or Chiru, Tibetan Gazelle, Wild Yak, and Wild Ass that are endemic to this region. However, this ecologically significant and diverse biodiversity is threatened by climate change, habitat degradation, and fragmentation accompanied by overexploitation in the form of poaching. In locations where the ungulates are common, the situation inevitably leads to human-wildlife conflict. All these have caused many wildlife species to become ecologically isolated, reduced in numbers, and in the process of becoming locally extinct. Over the years, I have undertaken extensive surveys to assess the status of 20 ungulate species inhabiting the Himalayan region belonging to four families, namely *Bovidae*, *Cervidae*, *Equidae*, and *Moschidea* including the eight out of the 10 most highly endangered ungulates in India, which are unique to this region. The results of our findings on the current status, information on the lesser known aspects of ecology, and critical factors determining the population decline, knowledge gaps, conservation threats, and management suggestions are presented in this paper.

Keywords: Himalayas, ungulates, Hangul, Chiru, musk deer, argali, Urial, gazelle

1. Introduction

Himalayas are one of the 36 Biodiversity hotspots in the world. The Himalayan region spreading across 2400 km from Kashmir in the North West to Arunachal Pradesh in the east covers nearly 6.41% of the total area of India. The Himalayas are geographically divided into four biotic provinces or sub regions, namely the Northwest Himalayas, Western Himalayas, Central Himalayas, and Eastern Himalayas [1].

The Western Himalayas largely comprises the North Western Himalayas (30^0 18′ to 32^0 06′ north and 72^0 32′ to 79^0 04′ east), which ranges from Kashmir to river Sutlej in Himachal Pradesh [1] and the Western Himalayas (29^0 5 to 31^0 25 north and 77^0 45 to 81^0 east) comprising of the Garwal and Kumaon hills and eight hill districts of Uttarakhand between Kali and Sutlej rivers [1].

Much of the geographical area of North Western and Trans-Himalayan region of India encompasses largely the Jammu and Kashmir and Ladakh besides Lahul and

Spiti districts of Himachal Pradesh and is located at the intersection between the temperate Palaearctic and tropical Oriental Biogeographic regions of the World [1].

South to north the mountain ranges here are the Shivaliks, Pir Panjal, Great Himalaya, Zanskar, Ladakh, and Karakoram, and enormous biodiversity and endemism are seen in these ranges as a result of the extreme variations related to temperature and rainfall [1–4]. Between Pir Panjal and the Greater Himalayan mountain range lies the Kashmir valley, which with an area of ca. 15,520 sq.km, is the largest valley in the entire Himalayan range.

As the Western Himalayas merges with the Hindukush and then the mountains of Central Asia, the faunal diversity of the region is marked by the presence of Northern Palearctic elements [1, 2, 5]. The rich diversity of species inhabiting the north western and trans-himalayas region is shown by the mammals (110 species, 26% of diversity of India) over 500 species of birds (40% of avifauna of India), and 68 species of reptiles (13% of reptilian diversity of India) [4, 5]. Besides, the area exhibits enormous diversity in ungulates including unique species such as Kashmir red deer or Hangul (*Cervus hanglu hanglu*), Kashmir Musk deer (*Moschus cupreus*), Markhor (*Capra falcorni*), Asiatic Ibex (*Capra sibirica*), Himalayan Tahr (*Hemitragus jemlahicus*), Himalayan Serow (*Capricornis thar*) Himalayan Gray Goral (*Nemorhaedus bedfordi*), Urial or Shapu (*Ovis orientalis*), Greater Blue sheep (*Pseudois nayaur*), Argali (*Ovis ammon*), Tibetan Gazelle (*Procapra picticaudata*), Tibetan Antelope or Chiru (*Pantholops hodgsoni*), Wild Ass (*Equus kiang*), and Wild yak (*Bos mutus*) most of which having their origin in Central Asia & Middle East, have remarkably adapted to the region [1, 3, 4] although some of them share their ranges with the parts of the Central and eastern Himalayan region [4].

Of the 34 ungulate species found in India, 20 species belonging to four families, namely *Bovidae, Cervidae*, *Equidae*, and *Moschidea* occur in the Himalayas. Eight of the 10 most highly endangered species of ungulates in India with only single populations [6] are found only in this region. The endemic Kashmir red deer or Hangul and the Kashmir Musk deer inhabiting this region are highly endangered as they are confined to a restricted area in this Himalayan range [4]. The only global population of around 150–180 Hangul individuals is restricted to a confined area of Dachigam National Park and adjoining landscape in Kashmir Himalayas [7–9]. Immediate feasible conservation steps are needed to save these species. Although endemic and endangered sufficient basic information on these species is not available for planning and implementing suitable conservation measures for these species.

In this article, the information on the status distribution, ecology, and conservation of key mountain ungulates including eight of the 10 most highly endangered species of ungulates in India found in the region is presented. The chapter has separate sections for each group of species, namely section for mountain deer, Antelopes and Gazelles, Goat antelopes, Wild Goat and sheep, and section for other mountain ungulates, which include Wild yak and the Tibetan Wild Ass—the only unique member of the Odd toed ungulates of family *Equidae*.

2. Ecology and conservation of unique mountain deer of the region

2.1 Kashmir red deer or Hangul (*Cervus hanglu hanglu* Wagner 1979)

The Kashmir red deer or Hangul (*Cervus hanglu hanglu*), in the State Animal of Jammu & Kashmir, is a highly threatened species endemic to a much restricted

area in the Greater Himalayan mountain range of the Kashmir Valley [7, 10–12]. The Hangul, which was earlier considered as one of the six eastern most subspecies of the European red deer (*Cervus elaphus*), is one of the three subspecies of the Central Asian clad of Red deer recently recognized by IUCN as an effective taxon and given a separate species status as Tarim Red deer (*Cervus hanglu*) [11–13]. The Hangul is classified as critically endangered by IUCN owing to small population, highly restricted range distribution globally confined to small pockets in the Kashmir Himalayas. The conservation of this species is subjected to strong demographic stochasticity and loss of genetic diversity. The deer were once widely distributed in the mountains of Kashmir along the Zanskar Mountain range from Shalurah and Karen in the Kishenganga catchment over to Dorus in Lolab Valley and the Erin catchments in Bandipora in the north to Bringi valley and Marwah/Wadwan in Kishtwar High Altitude National Park (NP) in the lower Chenab Valley in Kashmir Himalayas. It was also reported in the past in the GamagulSiya-Behi Sanctuary in the adjoining Himachal Pradesh [14, 15]. At present, the only genetically viable global population of ≤200 Hangul is restricted to a small area, which includes the Dachigam National Park (141 sq. km) and adjoining relic range areas across the Greater Himalayan mountain range in Kashmir totaling to around 808 sq. km. There is no animal is in captivity [5, 7, 9, 10, 16–18].

The Hangul is a mixed feeder, but it ingests disproportionate amounts of browse in almost all seasons, and also bark-strips woody species such as *Pinus wallichiana*, *Robinia pseudoacacia*, *Parrotiopsis jacquimontiana*, *Lonicera quinquelocularis,* and *Prunus ceresifera,* mostly during spring and winter [8]. Our studies have indicated that the Hangul feeding habits varied according to resource availability in different seasons. In spring, the Hangul food consisted mainly of dicotyledonous shrubs, trees, and herbs together with the monocotyledon grasses and herbs, which included *Carex cernua*, *Panicum crusgalli*, *Poa anua,* and *Hamerocallis fulva,* among the monocots, and *Dipsacus mits*, *Inula royeleana*, *Berberis lycium*, *Quercus robber,* and *Jasminum humile,* among dicotyledonous plants [8]. Hangul in summer consumed *Poa anua*, *P. crusgalli* (monocots) and *Verbascum thapsus*, *Fagopyrum cymosum*, *Jasminum humile,* and *Prunus armenica,* among dicots. In autumn, maximum Hangul was observed feeding on *Indigofera heterantha*, *Isodon plectranthus*, *Lonicera quinquelocularis*, *smilax vaginata*, *V. thapsus*, *Fagopyrum cymosum*, *Geranium pratines* (all dicots) besides debarking on *Prunus cerasifera* and *Parrotiopsis jacquimontiana*. The winter diet, however, mainly constituted browse (trees and shrubs) although during significant number of sightings, Hangul was observed debarking on trees. Hangul consumed *Salix alba, Quercus robber, Aesculus indica, Prunus pyrus, Parrotiopsis jacquimontiana, Lonicera quinquelocularis, Berberis lycium,* besides *Carex cernua* (in late winter), among monocots [8].

Our studies have indicated that the Hangul habitat use varied between sexes and across seasons. The female Hangul habitat use was consistent across seasons, but male Hangul showed differences in seasonal use of habitats. Hangul showed strong preferences for Riverine habitats in the valleys and Grassland/Scrub habitats in the mountain slopes of the Dachigam National Park. The deer uses primarily the riverine forest habitats including the mixed oak and mixed Morus habitats during winter months as these habitats provided sufficient food, shelter, and cover to avoid chilly winds [8]. Whereas during summers, the Hangul tend to inhabit largely coniferous forests associated with rugged, broken terrain, or foothill ranges, which provide good shelter from summer heat and nutritious diet. The deer also shows preference for mid-altitudes between 1700 and 2300 m and 1900–2300 m, and South-facing slopes (North, East, and Northeast and Northwest aspects) were generally favored by both male

and female Hangul in the Dachigam National Park [8]. The deer also showed greater use of lower and middle altitudes (between 1700 and 1900 m and 1900–2300 m). South-facing slopes (North, East, Northeast, and Northwest aspects) were generally favored by both male and female Hangul in Dachigam National Park. The use of slope by Hangul in Dachigam National Park varied between the seasons. In spring, summer, and winter, Hangul generally used flat slopes, but in autumn the deer used very steep slopes in the Dachigam National Park [8].

The deer population has shown wide fluctuations over the years and has declined drastically from 5000 deer in 1947 [14, 15, 19] to around ≤200 Hangul at present [9]. Our studies so far have indicated that besides other causes, the major factors affecting the long-term survival of the Hangul deer are declining population trends and distributional range, very low adult sex ratio and fawn-to-female ratio [7, 8, 17, 18] loss of high-altitude summer habitat to graziers [9, 20] and the problem of survival of the young and inadequate recruitment of calf to adulthood due to factors such as considerable predation by common Leopard, dogs, and meso-carnivores (Fox and Jackal) [7–9, 18]. The sex ratio in the deer population is female-biased with 17.76 male: 100 females and the spring calf-to-female ratio very low with 13.70 calves: 100 females (SE = 2.49). The spring calf-to-female ratio showed significant decline (t = 3.4, p = 0.01) from 23:100 in 2004 to its lowest level of 9:100 in 2006 [7, 10] before showing some recovery to 13.70–15.00 calves: 100 between 2017 and 2020 [4, 9, 21]. The preliminary mitochondrial DNA and nuclear microsatellites also have indicated a relatively low genetic diversity in Hangul as compared with other red deer species predisposing them to inbreeding depression in lieu of their small population size [7, 8, 22].

A population viability model with demographic parameters for Hangul in Dachigam NP indicated that this population can easily shift toward extinction [9, 21]. We strongly recommend a set of management actions to reduce the risk of extinction faced by the small population of this threatened deer. The initiation of the conservation breeding and reintroduction program to augment the wild deer population in its past range in the Kashmir Himalayas and a robust science-based Hangul population monitoring and surveillance program are the vital steps in this direction.

2.2 Kashmir musk deer (*M. cupreus* Grubb, 1982)

Musk deer (*Moschus* **spp),** which have been classified into seven species [23] with six species listed as endangered [13], are endemic to the mountains of south Asia. Of these six endangered species of Musk deer, five species, namely the Kashmir musk deer *M. cupreus*, Himalayan musk deer *Moschus leucogaster*, Alpine musk deer *Moschus chrysogaster*, Black musk deer *Moschus fuscus,* and the Dwarf Musk deer *Moschus berevoskii,* inhabit different zones of the Indian Himalayas [24, 25] with the first three species having isolated distributional ranges along the mountain ranges in the northwest Himalayan region.

The Kashmir musk deer has historically been reported and described from the Kashmir region of the Western Himalayas from elevations between 2000 and 4200 asl [4, 26, 27] although some recent reports of presence of isolated populations from Nuristan, northeast Afghanistan [25], which is the western limit of the species and genetic analysis based on a few tissue samples [28] and species distribution modeling study [29–31], have indicated the occurrence of Kashmir musk deer in the Mustang area of central Nepal, which forms the eastern limit of the species. However, the reported occurrence of the species beyond the Kashmir Himalayas may not be true and warrants detailed investigation.

In Kashmir, the Kashmir musk deer occurrence is confirmed from isolated habitats all along Greater Himalayan and Pir Panjal mountain ranges above 2500 m asl. The fairly significant population has been observed in the protected areas particularly the Kishtwar National Park, Rajparyan wildlife sanctuary, Overa-Aru wildlife sanctuary in the southeast, and Baltal-Thajwas wildlife sanctuary and Gurez-Tulel landscape in the northeast along Greater Himalayan and Zanskar range, besides Hirpora wildlife sanctuary in the southwest and Kazinag National Park including Limber-Lachipora landscapes in the northwest along the Pir Panjal mountain range, Dachigam National Park, and adjoining landscapes [4].

Kashmir musk deer is the least studied among all species of musk deer of the Himalaya. This is due to its restricted distribution to an area that has been politically sensitive as a result of extended periods of armed conflict making the area extremely unsuitable for field research [3, 4, 27]. There is as such very little information available on the ecology and biology of the Kashmir musk deer. However, our decade's long field observations in its distributional range areas indicate that the populations of Kashmir Musk deer have declined in the recent years owing to habitat loss and poaching in some of its distribution areas in the Pir Panjal range areas and in Gurez-Tulel area bordering Pakistan adjoining Zanskar mountain range in Kashmir [4]. Globally also, the populations of musk deer in their distributional ranges are reported to have dramatically dwindled to half of the original size in three generations (approximately 21 years) primarily because of poaching and habitat degradation [32–34]. There is, however, lack of information about the status, distribution, effective population size, exact number, and genetic structure of Kashmir Musk deer in India, which are a must for planning a conservation strategy of any endangered species. The information on the population status, distribution, ecology, and biology and threats to the populations of Kashmir musk deer endemic to Kashmir Himalayas is limited or not available so far [3, 4]. There are no population estimation records available for the species in its endemic distributional range in Kashmir. Owing to their small and declining population size with restricted geographic range, the species require immediate conservation action before their extinction in the wild. There is a dire need for intensive scientific studies to understand the ecology and biology of the species including comparative ecology with the Himalayan Musk deer.

2.3 Himalayan musk deer (*M. leucogaster* Hodgson, 1839)

The Himalayan Musk deer were once continuously distributed all along the southern side of the Greater Himalaya in India from Central Kashmir through Himachal Pradesh up to Sikkim, Bhutan, Nepal, and marginally in China, between 3000 and 4300 m and tree line [26, 35, 36]. However, as a result of human habitations, habitat alterations, and poaching, they are now restricted to a few isolated pockets throughout its former range [30, 33, 35, 37]. In Jammu and Kashmir, the Himalayan musk deer shares range and habitats with Kashmir musk deer in some of its range areas in Kishtwar NP and Bani WLS bordering Himachal Pradesh.

In general, Himalayan Musk deer are solitary and shy animals with crepuscular and largely nocturnal activities known to inhabit mature conifer and broadleaved forests preferably prefer oak forest, rhododendron forest, blue pine, *Betula*, *Fir*, and juniper forests and grassland habitat [32, 38–40]. The deer are considered predominantly a browser, feeding mainly on shrubs, forbs, leaves, moss, lichens, shoots, grasses, and twigs [32, 41]. The Musk deer are "nibblers" rather than browser, as they selectively feed on young leaves, buds, fruits, and flowers of dicotyledonous

plants [35]. Lichens are reported to constitute the bulk of the musk deer's winter diet, mostly [32]. In Nepal, musk deer have been observed climbing trees to feed on lichen and to escape from predators [38].

Although degradation of Musk deer habitats all across its distributional range is a concern, poaching and snaring of musk deer for trade fuelled by high demand for use in traditional Chinese medicines and perfumes in China, India, and other countries since the fifth century and the high price paid for musk pod pose the biggest threat to the long-term survival of Musk deer [42, 43]. Snaring adopted by the poachers to kill the musk deer not only kills the adult males, which only carry the musk pods but also the young and the females. The estimated number of musk deer killed in the Himalayas is estimated to vary between 5350 and 16,000 every year during 1970s and 1980s [35].

2.4 The alpine musk deer (*M. chrysogaster* Hodgson 1839)

This subspecies of musk deer of alpine scrub and meadows is largely distributed across the alpine zones of Central and Eastern Himalayas in Aurunachal Pradesh and Sikkim. In the western Himalayas, Alpine musk deer has some patchy distribution to confined areas in the Uttarakhand [26, 36].

Musk deer is an endangered animal under the IUCN category and is listed in CITES Appendix 1 for Afghanistan, Nepal, India, and Pakistan and in Appendix II for Bhutan and China [13, 30, 44, 45]. Although number of studies and conservation efforts have been undertaken for conservation of musk deer populations and sustainable utilization of musk to meet the growing demand of musk trade in China and some parts of India, concerted efforts are still needed to enhance our knowledge and understanding on the population status, distribution, and ecology and biology of the musk deer for its effective management and long-term conservation planning in its habitats. Increased protection to musk deer and its habitat, creating general awareness about the musk deer, and wildlife research and management are absolute necessities for the conservation of this species.

3. Antelopes and gazelles

3.1 Tibetan antelope or Chiru (*Pantholops hodgsoni* Abel)

Tibetan Antelope or Chiru is endemic to the Tibetan Plateau at elevations of 3250–5500 m [46, 47] and ranges across the whole Qinghai-Tibet Plateau, China, and a small area of northwest Nepal [48]. At present, Chiru are restricted mainly in the remote Chang-Thang area of north-western Tibet [49] with a small population occurring seasonally in extreme north western parts of Tibet in India in Daulet Beg Oldi (DBO) in Karakoram (Nubra) wildlife sanctuary and Changchenmo Valley of eastern Ladakh [48, 50]. However, most of the Chiru that come to ChangChenmo Valley are males, and the females prefer the neighboring Lingti Tsiang plains in the Aksai Chin region, where they often fawn, and a small sedentary female Chiru population inhabits Daulat Beig Area (DBO) of Ladakh region in India [49–52]. The estimated populations of Chiru in the India Tibetan plateau in Daulat Beg Oldi and Changchenmo wildlife sanctuary range between 250 and 270 animals [50, 53–55].

It was till recently not clear whether the population of Chiru, which seasonally migrate to India from Chinese province of Tibetan (Xinjiang) [56], is truly

migratory like the other populations of Quinghai Tibetan Plateau (QTP) [57–59] or is resident. It is reported that individual female Chiru travels distances of 300–400 km in late spring and early summer [60]. During our recent studies between 2012 and 2015, we confirmed that a small population of around 15–20 Chiru individuals to have become resident and are staying in Chang Chenmo Valley in eastern Ladakh during winters as well resulting in the year-round distribution of Tibetan antelope within eastern Ladakh in India [50, 53–55]. We also documented for the first time the genetic variation of the Indian population of the Tibetan antelope from other populations of China and results indicated a separate resident population of Chiru in Indian Changthang region and the presence of relatively low genetic diversity in the surviving Tibetan antelope population in India [50, 53, 55].

The population decline due to poaching and habitat degradation for Tibetan antelopes or Chiru is of grave concern. The Chiru are poached for their wool, known as shahtoosh-King of wools, which has been posing great threat for long-term survival of the species. Shahtoosh is different from other wools as it cannot be sheared or combed because the fibers are very short and attached to the bases of guard hairs; in turn, it can only be obtained after sacrificing the animal. One individual yields about 125–150 g of shahtoosh, and weaving one shawl requires wool from four to five individuals [49, 58, 61]. The recent estimates have indicated that every year, more than 20,000 individuals are poached for their fine wool to make shahtoosh shawls and scarves [57, 62–64]. During our studies in Changchenmo along the China boarder (LAC) despite the area being under high security surveillance, we collected two heads of poached Chiru and observed that two indigenous circular foot traps placed over a hollow tin bucket, concealed, and tied to a stack were also encountered on a regular Chiru trail [54, 55] The drastically declining population of Chiru during the recent years cannot long endure the additional stress of poaching, habitat disturbances, and any chances of disease. As such the monitoring of economic circumstances may be as important to Tibetan antelope or Chiru conservation as regular scientific-based population monitoring, surveillance, and management.

3.2 Tibetan gazelle (*P. picticaudata* Hodgson 1846)

The Tibetan Gazelle, a species endemic to the Tibetan Plateau, with small population occurring in confined areas in the Hanley plains in Changthang area of Laddakh in the Indian trans-himalayas. In the Ladakh region, its range had declined from ca. 20,000 km^2 in the early 1900s to ca.1000 km^2 in the late 1980s. The recent range-wise surveys carried out during 1999–2003 for assessment of the Gazelle's conservation status in Ladakh indicate that the present population of Tibetan Gazelle in Ladakh is ca. 50, restricted to a range of about 100 km^2 [65–68]. Apart from this single survey conducted during 1993–2003, there have been no intensive studies undertaken on the species in Indian. Habitat fragmentation and livestock grazing are the major threat to long-term conservation of the species in its distributional range in Hanley plains in Indian Changthang.

There is a dire need for undertaking studies to understand the biology and ecology of the species for effective management and conservation planning of the species and its habitats in its restricted range areas in Indian Changthang region. Besides, the reassessment of its IUCN Red List Status is imperative for long-term conservation of the species.

4. Goat: Antelopes

4.1 Himalayan gray goral (*Nemorhaedus bedfordi* Lydekker 1905)

The Himalayan gray Goral is one of the three subspecies of Goral [13, 69, 70] endemic to the Kashmir and Western Himalayas largely ranging from Pakistan to north India, Nepal, Bhutan, up to Mishmi hills of Assam [4, 70–73]. Although, recent genetic study while confirming the classification of Groves and Grub (1985) has confirmed existence of three species of Goral and suggested Himalayan Gray Goral *Nemorhaedus bedfordi* as subspecies of Himalayan Goral *Nemorhaedus goral* [74].

In India, Himalayan gray Goral is distributed largely in Jammu and Kashmir and Himachal Pradesh, Uttrakhand, Sikkim, and Arunachal Pradesh [75]. It inhabits steep open and rugged grassy hill or rocky and scrub habitats in the southerly aspects at elevations of 900–300 m and above up to 4200 m asl. [39, 76] usually in small groups of 4–8 individuals.

In Jammu and Kashmir, it occurs in Kazinag National Park and Nagnari Conservation Reserve while as Tatakuti-kalamuund Wildlife Sanctuary and Khara Gali Conservation Reserve in Pirpanjal range of the Himalaya are thought to be the potential goral areas [36, 77–80]. During our surveys, we recorded occurrence of Goral in confined areas in Greater Himalayas and Pir Panjal mountain ranges in Kashmir and Chenab Valley [81].

In Jammu and Kashmir, it occurs in Kazinag National Park and Nagnari Conservation Reserve while as Tatakuti-kalamuund Wildlife Sanctuary and Khara Gali Conservation Reserve in Pirpanjal range of the Himalaya are thought to be the potential goral areas [77, 79, 80].

Increasing human settlements result in habitat loss and increased hunting pressure Deforestation, grass extraction, timber and fuel wood, collection, illegal poaching, and competition with livestock are crucial threats to the survival of wild ungulates [39, 41, 82]. Anthropogenic pressures and disturbances especially movement of local people and operations by security forces in upper reaches are a few of the major threats to Himalayan goral population, which need to be evaluated if its conservation is a priority.

Himalayan Gray Goral is categorized as near threatened (IUCN 2017) and listed as Appendix 1 species by CITES. The effective management of species needs an extravagant understanding of its biology, but very few have addressed the goral at global level [83–89] with detailed assessment of the ecology and biology of the population surviving in the Greater Himalayas and Pir Panjal mountain ranges of Kashmir required for long-term conservation planning.

4.2 Himalayan Serow (C. thar Hodgson, 1831)

The Himalayan Serow is one of the four races of the widely distributed Serow in India [76]. Recent genetic study has indicated four species of Serow and suggested grouping together of C. thar and other two species *C. milnedwardsii* and *C. maritimus* into *Capricornis sumatraensis* [74].

Himalayan Serow is distributed in the southern Himalayas from Jammu & Kashmir in the west to Arunachal Pradesh in the east. In western Himalayas, the Himalayan Serow is widely distributed largely all along the Greater Himalayan range [36]. In Jammu & Kashmir, we have recorded Himalayan Serow widely distributed along the Great Himalayan mountain range largely from Jammu, Chinab Valley,

Kishtwar National Park and adjoining landscape, Zabarwan Hills, Dachigam National Park [4], and recently reported from Bani WLS [81].

In its distribution range, the Himalayan Serow inhabits the boulder strewn thickly wooded gorges at elevations between 1800 and 3000 m. The Serow are very active during morning hours in the open hill slopes, generally more or less solitary but occasionally in groups of 4–6 individuals seen foraging together. During our survey, we have recorded a herd of seven serow foraging on the open grassy slopes of the Brain-Nishat conservation reserve in the Zabarwan hills in Srinagar during spring season in 2000 and 2001 [4, 81]. This is the least studied species in its distributional range in the Himalayas and calls for systematic surveys and studies to understand ecology and biology of the species for conservation planning.

5. Unique wild goats and sheep of the region

5.1 The Markhor (*Capra falconeri* Wagner)

The Markhor *C. falconeri,* the large goat of the world, is native to the Himalayas and Central Asia occurring from the Kashmir Valley westwards to the Hindu Kush [36, 45, 48, 76, 89, 90] through Afghanistan in the west [91] northern and central Pakistan, southern Tajikistan, and southern Uzbekistan [24]. In India, the Markhor is restricted to confined areas in the parts of Pir Panjal mountain range in the southwestern Kashmir in the Western Himalayas [77, 79, 90, 92]. The Pir Panjal Markhor or Kashmir Markhor (*C. falconeri cashmiriensis*) as it is called is reported to occur all along the Pir Panjal range in Jammu & Kashmir from the Banihal pass in the south through Poonch, Hirpora (Shopian), Gulmarg (Nilkanth area), Boniyar (across LOC), Bonyar, Kaji Nag, Shamsbari south, Shamsbari (across LOC) and Shamsbari north [48, 93], and Baltistan, Gilgit, and Chitral on the other side of the Kashmir in Pakistan [36]. However, recent studies and surveys have indicated that the Pir Panjal Markhor now has a restricted distribution in Kazinag National Park and Hirpora Wildlife Sanctuary in Kashmir with an estimated population of 280–330 individuals (Anonymous 2005) although some confirmed reports of its occurrence were obtained from the Boniyar and Poonch survey blocks. In most of the other range areas such as entire Shamasbari and Baderwah-Kishtwar blocks, the Markhor populations are reported either extinct or are near extinction.

The Markhor in the Pir Panjal range inhabits the dense pine and birch forest habitats interspersed with grassy glades, which offer a preferred grazing ground for the animal. The food preferences of Markhor change according to season and availability [48]. It generally feeds on grass, leaves, and other available vegetative matter. However, during spring and summer, it consumes primarily grasses and forbs, while in the winter, it feeds primarily on browse for nourishment [71, 94].

Though the Markhor is protected as Schedule 1 species under Indian Wildlife Protection Act 1972 (amended 2006) and its status put down recently from endangered to near threatened by IUCN [94], the threat against its survival remains very much in place. Poaching, overgrazing, and constant conflicts at the border besides large-scale developmental activities including limestone and gypsum mining in and around the prime habitats seem to be major threats to Markhor conservation in Jammu & Kashmir. Apart from a single intensive study by Ahmad [90] and a few brief surveys by Ahmad and coworkers [77, 79, 80, 90], no detailed studies have been undertaken on the species. More detailed ecological studies on the Markhor

including understanding the movement and ranging pattern of the species across the Pir Panjal landscape, strengthening the protection and habitat restoration measures, participatory management of Markhor areas with the Indian Army, nomadic herders, and Local communities, capacity building in terms of infrastructure, manpower, and training; of the implementing agencies such as forest and Wildlife departments are some of the measures need to be taken immediately to conserve this largest goat of the world we are bestowed with. Need to strengthen the research and awareness measures to better understand measures required to be undertaken for effective management and long-term conservation and survival.

5.2 Himalayan Tahr (*H. jemlahicus* smith, 1826)

Himalay Tahr, one of the least studies species, is considered to inhabit most inaccessible habitats Fragmented distribution in western and central Himalayas from Jammu and Kashmir (rare west of Doda) to Sikkim near-threatened mountain goat.

Found on the southern temperate and sub alpine forested slopes along greater Himalayas between 1500 and 5300 m preferably at higher elevations between 2000 and 4400 m best known in Kedarnath WLS in Uttarakhand [30, 41] and Kishtwar National Park in Jammu & Kashmir [4] with a small population reported from Bani WLS adjoining Himachal Pradesh [81].

There is very limited scientific information available on the species. There is urgent need for initiation of population assessment and occurrence surveys and intensive studies to enhance our knowledge and understanding on the ecology and biology of the species for effective management and conservation planning.

5.3 Argali (*O. ammon hodgsoni* Blyth)

Argali or Great Tibetan Sheep, locally known as Nayan, is the largest but the rarest wild sheep found in the world [76]. It is distributed across the Tibetan Plateau from eastern Ladakh eastwards to Sikkim with some populations crossing over the adjacent mountains into Spiti Valley of Himachal Pradesh, Kumaon hills, Nepal, and Bhutan [76]. In India, the main population of around 300–360 survives in the Ladakh mainly in the eastern part of the Indian Changthang region in Gya Miru, Changchenmo, and Tsokar with a smaller population in Sikkim and extremely rare in Lahul and Spiti Valley of Himachal Pradesh [36, 95–97].

It is one among the two Argali subspecies categorized as Near Threatened by the IUCN and listed as Appendix 1 species by CITES. The preference for open areas, generally closer to human settlements, has made it an easy hunt for nomadic herders, army personnel, and some government officers who hunted the species for meat, besides trophy hunting by hunters [96, 97]. Competition from Pashmina goats seems to be current threat, hindering the recovery of Argali in Ladakh [97].

Despite its restricted range distribution confined to a small area of around 10,988 km^2 in Changthang and eastern Ladakh and small population with earlier records of around 200 individuals [56], Argali is one of the least studied species in the region [95]. During our studies and surveys from 2012 to 2015 apart from some sightings of Argali recorded around Marsmicla north east of Pangong, we could record a significant population of Argali (240 individuals in 21 sightings) with a mean group size of 11.43 ± 9.17 Argali largely using sandy plateau habitats in the Changchenmo Valley in the eastern Ladakh [54, 55]. Though some isolated population of Argali is reported from Hemis National Park, but during several surveys ranging including one

15-day survey in the Hemis NP, I have not been able to locate any Argali individual in the area. Range-wise population status survey and detailed studies in its restricted range area in the region are required to understand its current population status in India and lesser known aspects of ecology and biology prerequisite for effective management and conservation planning of the species and its habitats.

5.4 Urial or Shapu (*O. orientalis vignei* Blyth 1984)

The Ladakh Urial, a smallest of all wild sheep, is endemic to trans-himalayas mainly inhabiting the gentler grassy hills and open arid alpine steppe habitats of Ladakh in India to northern Tibet besides Gilgit and Astor, Punjab, Sind, and Baluchistan in Pakistan and south Persia [64, 76]. In India, its restricted distribution to the confined areas in Indus and Shayok valleys in Ladakh besides two isolated populations of around 100 Urial reported from Kargil around Junkar Lake and around Chicktan areas [36, 95] has led to its vulnerable status in the region [56, 70, 98].

The population of Urial has declined drastically largely due to the proximity of its distribution habitats to the highway and human habitation resulting in loss of habitats to humans and bringing the species into direct conflict and easy access to poaching [95]. The population was estimated to be about 2000 individuals [99, 100] and indicated 30–40% increment from 700 individuals reported two decades earlier [98] and 1000 Urial reported from Indus and Nubra valley in 1991 [56]. But a recent study puts the number again below 800 individuals [101], which is perhaps the lowest so far. The recent surveys have estimated densities of 1.27 (1.27–1.39) urial km^{2}and 0.96 (0.96–1.10) urial km^2 across the two landscapes covering 18% of surveyed area [102]. Competition with livestock, hunting by security agencies and locals, and depredation by free-ranging dogs have been the major threats [103]. During our recent surveys in 2001, we recorded around 100 urial in three different sightings along main Srinagar-Leh highway near Saspool, Nemu, and in Markhah Valley in the Hemis National Park [81].

Apart from a short study by Raghavan and Bhatnagar [103, 104], little is known about the species, and there is need for detailed systemic scientific studies to understand the ecology and biology of the Urial for the species long-term conservation planning in its suitable habitats in its narrow distribution range in Ladakh.

5.5 Asiatic ibex (*Capra siberica* Pallas 1776)

One of the large mountain goats distinct from other *caprids* by its characteristic horn and beard [36, 76]. The Ibex is distributed widely in the mountain ranges of Central Asia from Altais in Afghanistan to the western Himalayas and upto Kumaon in Uttarakhand with eastern limits set by upper reaches of the Sutlej river east of which it does not occur [76], and one reason that could determine this occurrence is the high precipitation east of the Gorge. There could be 15,000 Himalayan ibex, which is an important prey for snow leopard [105].

The Ibex inhabits the higher elevations above the tree line usually preferring rugged and rocky precipitous terrain and dry grassland steppes between 3400 and 4400 m in the Himalayas and 4000–5500 m in the trans-himalayas [76, 106]. It usually grazes on the thickets along the rocky hills and unlike most other caprids, it is known to dig craters through snow to access forage in winters [6, 28, 76]. The Ibex and Blue sheep are the main prey for the snow leopard, and they share similar habitats at

many places such as Nubra Valley and either side of the Zanskar river in Kargil, with Ibex using steeper slopes at higher elevations closer to Blue sheep, which prefer more open pastures at lower elevations [56, 106, 107]. The presence of Ibex and blue sheep in an area is usually thought as indicator of occurrence of snow leopard in the area.

Although earlier Ibex used to occur in large densities throughout its wide distributional range in Ladakh, the population was reduced due to large-scale hunting in the past and competition with livestock during summers. The earlier estimates of Ibex occurring in low densities ranging from 0.4 to 1.5 Ibex/Km^2 throughout its range in Ladakh and 2.3 Ibex/ Km^2 in Pin Valley National Park, Himachal Pradesh [6, 106] compared to a density of 6 Ibex/Km^2 reported from former USSR Russia [48, 95].

Apart from pioneering studies by WII in Spiti Valley [106] and some small studies in Hemis National Park, no detailed studies have been undertaken on the species.

5.5.1 Great blue sheep (P. nayaur *Hodgson*)

The Blue sheep or the Bharal, it is usually called, is intermediate between sheep and goat. Its horns are rounded and smooth and curved backwards over the neck and its lacks facial glands [76]. Unlike goat in Bharal, ram is not bearded, and it has glands between the hooves in all four feet, and it does not have "goaty" odor [76]. Bharal is typically a Tibetan animal also found in Ladakh, Kumaon Himalayas, Nepal, Sikkim, and Bhutan [76]. It has a wide distribution in almost all the Asian mountain ranges in China [49], Nepal [48, 108], Bhutan, and parts of Pakistan [48]. In India, Bharal is one of the most common ungulates found in the Trans-Himalayan region in Ladakh [54, 55, 95, 99, 109].

The Bharal usually inhabits grassland habitats close to cliffs between tree line and snow line at elevations between 3300 m and 5500 m. Bharal are a mixed feeder both grazer and browser foraging largely on grass, moss, and dwarf shrubs. In Ladakh, the Bharal has a wide and continuous distribution ranging from Kargil and Zanskar in the east to Changthang area in the west up to upper catchment of the Changchenmo valley in the Far East [54, 55, 71, 95, 110]. It is, however, absent from the southern slopes of Ladakh range (north of Indus) except at few localities [52, 95]. It is reported to occur in low densities between 0.5 and 2.5 Bharal/km^2. They live in large herds usually in summers in the high-altitude summer pastures where they have been observed in groups of up to as many as 200 individuals with densities of 20 Bharal/Km^2 [52, 95, 110]. During our surveys in the Changchenmo Valley, we have recorded 74 Bharal in the seven sightings with an encounter rate of 0.49 ± 0.27. The average group size was 10.57 ± 8.34, and the largest group recorded comprised around 70 individuals [54, 55].

Excessive overgrazing by livestock and poaching coupled with predation by dogs are some of the major challenges for the Bharal populations in the landscape. Blue sheep and Ibex are the major prey for the snow leopard in its entire distribution range and as such the conservation and management of bharal populations are essential to ensure sustenance of the predation pressure and long-term conservation of large predators and associated prey in the landscapes.

6. Other unique mountain ungulates of the region

6.1 The wild yak (*Bos mustus* Przewalski 1883)

The wild yak, the only wild oxen of the region, is endemic to the Tibetan Plateau and part of the Kansu Province in China. In India, the wild yak is restricted to only

Changchenmo Valley in the eastern Ladakh [76] although there are some recent unconfirmed new records from Sikim and other Trans-Himalayan areas of India [36].

Wild yak is one of the highest dwelling animals in the world inhabiting the habitats with the harsh coldest and dray desert environmental conditions between elevations ranging from 14,000 to 20,000 ft. (4270–6100 m) asl. Wild yak is considered behaviorally close to American Bison (Menon 2014). Despite its restricted distribution to confined area of Ladakh in India, the wild yak is again one of the least studied species. During our studies on Chiru in Changchenmo from 2012 to 2014, we recorded a total of 19 sightings of 85 individuals of wild yak in a mean group size of 4.47 ± 3.89 individuals [54, 55]. The Wild Yak were largely seen either solitary or in a group of 2–3 individuals at higher elevations above 5000 m asl. Along south-east of Hot Spring and K. Hill besides Kugrang nullah during summer but used to congregate in large groups in areas along river basin in and around hot spring in association with Chiru and Kiang from late autumn till spring [54, 55].

An extensive in-depth study to understand the ecology and biology of the animal is imperative for effective management and long-term conservation of the species and its habitats in its limited distribution range in ChangChenmo Valley of eastern Ladakh in India bordering China.

6.2 Tibetan wild ass (*Equus kiang kiang* Moorcraft 1841)

Tibetan Wild Ass is endemic to the Tibetan Plateau and Indian trans-himalayas in eastern Ladakh confined mainly in Changchenmo and Hanle Basins [36, 54, 55, 76].

It is an animal of high open hills and valleys of cold deserts of trans-himalayas. There is very limited scientific information available on the species particularly from its limited distributional range in the Indian trans-himalayas.

We carried out range-wise surveys in the eastern Ladakh in the Changchinmo valley and adjoining Neuma Valley from Upshy till Chushul via Tsomorari, Mahe, loma, and Hanley in the Changthang cold desert sanctuary, Leh, Ladakh in 2004, 2006, 2007, 2008, 2012–2015. In Neuma valley of Changthang WLS, in July 2007, a total of 89 Wild Ass or Kiang were sighted between Tsomorari and Chushul. Whereas in May 2008, a total of 67 kiang were sighted in the same stretch, with an encounter rate of 0.74–0.92 Kiang/km. In the Changchinmo valley, however, the Kiang occurs in significant densities with encounter rates that showed an increase in 10 years from 1.88 Kiang/km walk recorded in the surveys in 2004 to as high as 4.12 kiang/km recorded in 2014 [54, 55]. A maximum of 395 Kiang were sighted in the area in one season in 2014 in 162 transect walks carried out, with the group size varying from solitary animal to a group of 76 sighted. In the 81 Km long drive transect between Phobrang and Hotspring post of the Changchinmo valley of Changthang, however, a maximum of 95 Wild Ass or Kiang were sighted in 2014 with an encounter rate of 1.17 Kiang/km walk.

Detailed ecological studies are recommended to be initiated to fully understand the lesser known aspects of ecology and biology of this endangered and the only member of the odd-toed (*Persiodactyla*) ungulate of family *Equidae* found in the Indian trans-himalayas.

7. Recommendations and conclusion

Striking a balance between biodiversity conservation and sustainable development poses major challenges at the global level during twenty-first century. In the

perspective of limited knowledge and risk of local extinction, conservation of a species remains a challenge. Basic ecological information about a species assists in understanding their survival requirements and to provide a basis for further management policies.

The Himalayan ecosystems face great conservation challenges due to increasing threats of ill-planned developmental activities, uncontrolled grazing by domestic livestock, and unlimited resource use leading to the degradation of its wildlife habitats and in this changing environment, the inhabiting ungulates often modify their activity pattern in response to habitat differences, seasons, and disturbance factors. Of the 31 caprine species found worldwide, 12 have been reported from the Himalayas and its allied mountain ranges, the richest in any part of the world. However, scientific information on a number of them is meager. Barring a few ecological studies, which have been carried out in the recent past, most of the information is based on preliminary surveys and short-term studies.

This region despite inhabiting more number of threatened species than other regions in India has remained little explored. Many of the 20 ungulates unique to the western and Trans-Himalayan region of India are highly threatened and endemic to this region. These species although having their origin in Central Asia & Middle East display greater adaptive variations in this region than in any other part of the world. The Kashmir red deer or Hangul, Tibetan Antelope or Chiru, and Musk deer have been of great social, economic, and cultural value for the people of the region. However, the poaching, habitat loss, habitat degradation and fragmentation, and overexploitation and hunting/poaching of these wild bioresources coupled with human-wildlife conflicts have caused many wildlife species to become ecologically isolated, drastically declined, and locally extinct or at the brink of extinction, which is the case with these threatened Himalayan ungulates as well. Around 87% of the mountain ungulates are protected as Schedule 1 species under the Indian Wildlife Protection Act 1972 and twelve [12] of the 20 mountain ungulates unique to this region are listed under different threat categories by the IUCN.

Since the ungulates as major prey for mammalian predators, they are indicators of health of the habitat. However, there has been drastic decline in the populations and reduction in the distribution ranges of many of the mountain ungulates particularly the eight most highly endangered species occurring in the Indian trans-himalayas with only single populations. As in other parts of the world and in the country, the drastic decrease in the populations of major ungulates in the region has created an imbalance in the ecological pyramid. The decline in the prey populations particularly ungulates in the Protected Areas (PAs) and reserve forests has forced the carnivorous species to stray out to prey on livestock and even injuring or killing to varying degrees resulting in a more frequent human-wildlife interfaces and conflict situations across the region.

The conservation and management of the ungulate populations are vital for long-term conservation of large carnivores and in reducing the large carnivore depredation of livestock and damage to humans, which in turn can go long way in mitigating the growing human-wildlife interfaces and conflicts in the region. There is need for furthering our understanding about the critical ecological factors that are pushing unique Himalayan wild ungulates particularly the most threatened species with single population unique to this region, toward extinction and in providing several science-based solutions to reverse the declining populations of threatened wild ungulates to ensure recovery of their populations in the wild including strengthening the

- Lack of comprehensive database of species and ecosystems including lack of baseline information on aspects of ecology and biology of species.

- Minimal comprehensive systematic survey and studies to understand population trends of flagship/endemic or threatened species

- Need for extensive and in-depth assessment of flagship species in the critical landscape.

- Lack of information on the status of significant disease prevalent in the wildlife under free range and disease transmissions from livestock to wild and humans. There is as such need for surveillance and monitoring of wildlife diseases, disease
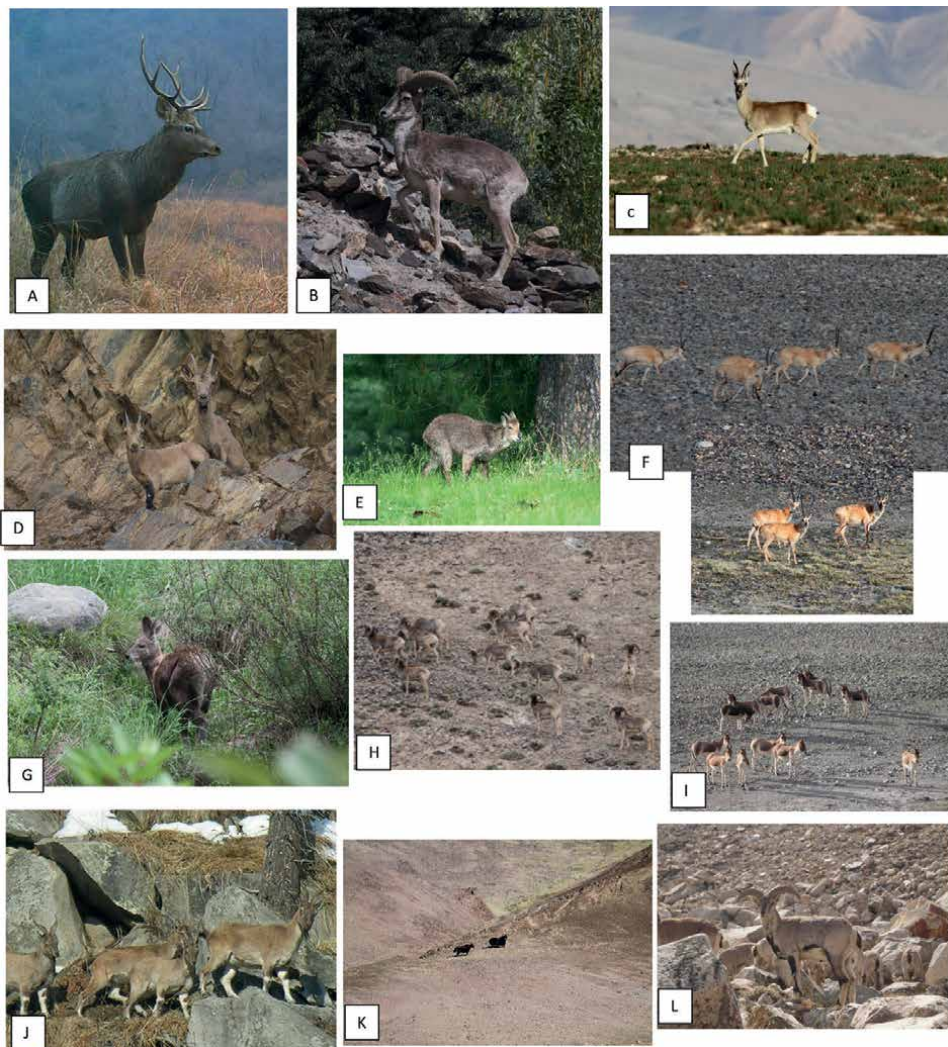
Figure 1.
A) Kashmir red deer or Hangul B) Urial C) Tibetan Gazelle D) Asiatic Ibex E) Himalayan Grey Goral F) Tibetan Antelope or Chiru G) Kashmir Musk deer H) Argali I) Tibetan Wild Ass or Kiang J) Markhor K) Wild Yak L) Blue Sheep.

transmission and outbreak in the wild particularly in the mountain ungulates, which share resources with livestock, and their treatment has become relevant.

- Since livestock has outnumbered wild ungulates in the landscape, creating overlap of diet and forage competition, there is need for understanding the wildlife-livestock interaction in the Himalayan ecosystems particularly at highland pastures.

- There is also need for studies to assess the biomass productivity of pastures and pasture development and enrichment through improved fodder varieties to ensure coexistence of mountain ungulates and livestock (**Figure 1**).

Author details

Khursheed Ahmad
Division of Wildlife Sciences, Sher-e-Kashmir University of Agricultural Sciences & Technology of Kashmir (SKUAST-Kashmir) Shalimar, Srinagar, Jammu and Kashmir, India

*Address all correspondence to: khursheed47@gmail.com

IntechOpen

References

[1] Rodgers WA, Panwar HS. Planing a Wildlife Protected Area Network in India. Vol. 1. Dehradun: Wildlife Institute of India; 1988

[2] Mehta HS, Julka JM. Mountains: Northwest Himalaya. In: Ecosystems of India. Kolkata: Zoological Survey of India; 2002. pp. 51-72

[3] Ahmad K, Trag AR, Wani AR, Rahman M. Endangered wildlife & biodiversity of Jammu & Kashmir-Conservation gaps, priorities and way forward. In: Lead Paper "International Conference on Wildlife & Biodiversity Conservation Vis-à-Climate Change". Srinagar (J & K) India: SKICC; 2010 on June 3-5

[4] Ahmad K, Bhat BA, Ahmad R, Suhail I. Wild mammalian diversity in Jammu and Kashmir. In: Dar GH, Khuroo AA, editors. Biodiversity of the Himalaya: Jammu and Kashmir State, Topics in Biodiversity and Conservation. Vol. 18. Singapore: Springer Nature Singapore Pte Ltd; 2020. pp. 933-951. DOI: 10.1007/978-981-32-9174-4_36

[5] Suhail I, Ahmad R, Ahmad K. Avian diversity of Jammu & Kashmir State. In: Dar GH, Khuroo AA, editors. Biodiversity of Himalaya: Jammu & Kashmir State, Topics in Biodiversity and Conservation 18. Singapore: Springer Nature Singapore Pte, Ltd; 2020. pp. 897-931

[6] Sankar K. Ungulate conservation in India. In: Reddy MV, editor. Wildlife Biodiversity Conservation. New Delhi, India: Daya Publishing House; 2008. pp. 37-50

[7] Ahmad K, Sathyakumar S, Qureshi Q. Conservation status of the last surviving wild population of Hangul or Kashmir Red Deer Cervus elaphus

hanglu in Kashmir, India. Journal of the Bombay Natural History Society. 2009;**106**(3):245-255

[8] Ahmad KQ, Qureshi GA, Nigam P. Habitat use patterns and food habits of the Kashmir red deer or Hangul (Cervus elaphus hanglu) in Dachigam National Park, Kashmir, India. Ethology Ecology & Evolution. 2015;**28**:85-101. DOI: 10.1080/03949370.2015.1018955

[9] Ahmad K, Nigam P, Naqaah RY. Long Term Conservation Plan for Hangul Part II: Hangul Movement Pattern Study Using GPS-Satellite Telemetry" Final Technical Report SKUAST-Kashmir, MOEF & CC (Wildlife Division). New Delhi: Govt. of India; 2021. pp. 1-15

[10] Qureshi Q, Shah N, Wadoo AR, Naqash RY, Bacha MS, Kitchloo NA, et al. Status and distribution of Hangul Cervus elaphus hanglu Wagner in Kashmir. Journal of the Bombay Natural History Society. 2009;**106**(1):63-71

[11] Brook SM, Donnithorne-Tait D, Lorenzini R, Lovari S, Masseti M, Pereladova O, et al. Cervus hanglu (amended version of 2017 assessment). The IUCN Red List of Threatened Species 2017: e.T4261A120733024. ICUN; 2017

[12] Brook SM, Thakur M, Ranjitsinh MK, Donnithorne-Tait D, Ahmad K. Cervus hanglu ssp. hanglu. The IUCN Red List of Threatened Species 2017: e.T113259123A113281791. ICUN; 2017

[13] IUCN. The IUCN Red List of Threatened Species. Version 2017-1. IUCN; www.iucnredlist.org. Gland, Switzerland

[14] Gee E. Report on the status of the Kashmir stag: October 1965. Journal of

the Bombay Natural History Society. 1966;**62**(3):1-15

[15] Holloway CW, Wani AR. Management plan for Dachigam sanctuary. Cyclostyled (Mimeo). 1970;**10**(6):373-382

[16] Ahmad K. Aspects of Ecology of Hangul (Cervus elaphus hanglu) in Dachigam National Park, Kashmir, India [Thesis]. DehraDun, Uttarakhand, India: Forest Research Institute (Deemed University); 2006. pp. 220

[17] Ahmad K, Qureshi Q, Nigam P, Suhail I. Status and conservation of Hangul (Cervus elaphus hanglu) in its relic range areas outside Dachigam National Park, Kashmir. Indian Forester. 2013;**139**(10):883-887

[18] Khursheed A, Nigam P. Kashmir red deer or Hangul Cervus elaphus hanglu at the brink of extinction-conservation action, the need of an hour. IUCN-DSG Newsletter. 2014;**26**(April 2014):37-47

[19] Schaller GB. Observation on Hangul or Kashmir stag (Cervus elephus hanglu). Journal of the Bombay Natural History Society. 1969;**66**(1):1-7

[20] Johnsingh AJT, Ahmad K. Hangul losing its ranging grounds to livestock in Kashmir. Maharashtra, India: Saevus Magazine. 2014

[21] Ahmad K, Pereladova O, Nigam P, Qureshi Q, Naqash RY. Hangul deer/ Tarim red deer Cervus hanglu (Wagner 1844). In: Melletti M, Focardi S, editors. Deer of the World: Ecology, Conservation and Management. Singapore: Springer Nature Singapore Pte, Ltd; 2022

[22] Kumar VP, Thakur M, Rajpoot A, Joshi BD, Nigam P, Ahmad K, et al. Resolving the phylogenetic status and taxonomic relationships of the Hangul

(Cervus elaphus hanglu) in the family Cervidae. Mitochondrial DNA Part A DNA Mapping Sequencing and Analysis. 2016;**28**(6):835-842. Available from: http://www.tandfonline.com/loi/imdn 21

[23] Groves C, Grubb P. Ungulate taxonomy. Baltimore, MD, Switzerland: The Johns Hopkins University Press; 2011

[24] Grubb P. Artiodactyla. In: Wilson DE, Reeder DM, editors. Order Artiodactyla, Mammal Species of the World. A Taxonomic and Geographic Reference. 3rd ed. Baltimore, USA: Johns Hopkins University Press; 2005. pp. 637-722

[25] Ostrowski S, Rahmani H, Ali JM, Ali R, Zahler P. Musk deer Moschus cupreus persist in the eastern forests of Afghanistan. Oryx. 2016;**50**(2):323-328

[26] Sathyakumar S, Rawat GS, Johnsingh AJT. Order Artiodactyla Family Moschidae evolution, taxonomy and distribution. In: Mammals of South Asia. Dehradun, India. 2015. pp. 159-175

[27] Singh PB, Mainali K, Jiang Z, Thapa A, Subedi N, Awan MN, et al. Projected distribution and climate refugia of endangered Kashmir musk deer Moschus cupreus in greater Himalaya, South Asia. Scientific Reports. 2020;**10**:1511

[28] Kumar A, Singh B, Sahoo S, Gautam KB, Gupta SK. Genetic evidence indicates the occurrence of the endangered Kashmir musk deer Moschus cupreus in Uttarakhand, India. Oryx. 2022;**56**(3):367-372

[29] Singh PB, Khatiwada JR, Saud P, Jiang Z. mtDNA analysis confirms the endangered Kashmir musk deer extends its range to Nepal. Scientific Reports. 2019;**9**:4895

[30] Shrestha B, Khatiwada J, Tanet D. mtDNA confirms the presence of Moschus leucogaster (Ruminantia, Moschidae) in Gaurishankar conservation area. Nepal. Arxius de. Miscel·lània/Zoològica. 2019;**17**:209-218

[31] Guo K, Li F, Zhang Q, Chen S. Complete mitochondrial genome of the Himalayan musk deer, Moschus leucogaster, with phylogenetic implication. Conservation Genetics Resources. 2018;**39**:1-4

[32] Green MJB. The distribution, status and conservation of the Himalayan musk deer Moschus chrysogaster. Biological Conservation. 1986;**35**(4):347-375

[33] Timmins RJ, Duckworth JW. Moschus leucogaster. The IUCN Red List of Threatened Species 2015: e.T13901A61977764. 2015. Brussels, Belgium

[34] Homes V, editor. No Licence to kill: The population and harvest of musk deer and trade in musk in the Russian Federation and Mongolia. This report was published with the kind support of Defra (Department for Environment, Food and Rural Affairs, UK). In: WWF-UK, WWF Germany and WWF Italy, with Additional Support from the Rufford Maurice Laing Foundation. Traffic Europe, Brussels, Belgium; 2004

[35] Green MJ. Aspects of the Ecology of the Himalayan Musk Deer [Thesis]. England: Cambridge University; 1985. p. 292

[36] Menon V. Indian Mammals- a Field Guide. Gurgaon, India: Hachette Book Publishing, Pvt, Ltd. www.hachetteindia. com 2014. p. 528

[37] Wilson DEM, Russell A. Handbook of the Mammals of the World. Hoofed Mammals. Vol. 2. Barcelona, Spain: Lynx Editions; 2011

[38] Kattel B. Ecology of the Himalayan Musk Deer in Sagarmatha National Park, Nepal [thesis]. USA: Colorado State University; 1993

[39] Sathyakumar S. Habitat Ecology of Ungulates in Kedarnath Musk Deer Sanctuary [Thesis]. Rajkot: Saurashtra University; 1994. p. 244

[40] Ilyas O. Status, habitat use and conservation of alpine musk deer (Moschus chrysogaster) in Uttarakhand Himalayas, India. Journal of Applied Animal Research. 2014;**43**(1):83-91

[41] Sathyakumar S, Prasad SN, Rawat GS, Johnsingh AJT. Conservation status of Himalayan musk deer in Kedarnath wildlife sanctuary, Western Himalaya. In: Pangtey YPS, Rawal RS, editors. High Altitudes of the Himalaya. Nainital, India: Gyanodaya Prakashan; 1993. pp. 240-245

[42] Singh PB, Shrestha BB, Thapa A, Saud P, Jiang Z. Selection of latrine sites by Himalayan musk deer (Moschus leucogaster) in Neshyang Valley, Annapurna conservation area, Nepal. Journal of Applied Animal Research. 2018;**46**:920-926

[43] Jones, P.R., and Wu, J.Y. (2001) "Musk deer farming as a conservation tool in China"

[44] Jnawali SR et al. The status of Nepal mammals. In: The National red List Series. Kathmandu, Nepal: Department of National Parks and Wildlife Conservation; 2011. p. 276

[45] IUCN. 2008 IUCN Red List of Threatened Species. Gland, Switzerland: IUCN; 2008

[46] Bower H. Diary of a Journey across Tibet. London, United Kingdom: Rivington, Percival and Company; 1894

[47] Blanford WT. The fauna of British India, including Ceylon and Burma. In: Mammalia. London, United Kingdom: Taylor and Francis; 1888

[48] Schaller GB. Mountain Monarchs: Wild Sheep and Goats of the Himalaya. Chicago, Illinois: University of Chicago Press; 1977

[49] Schaller GB. Wildlife of the Tibetan Steppe. Chicago, Illinois: University of Chicago Press; 1998

[50] Ahmad K, Ahmed R, Nigam P, Thapa J. Analysis of temporal population trend and conservation of Tibetan antelope in Chang Chenmo Valley and Daulat beg Oldi, Changthang, Ladakh, India. Antelope Specialist Group Newsletter GNUSLETTER. 2017;**34**(2):16-20

[51] Schaller GB, Ren JR, Qiu MJ. Observations on the Tibetan antelope (Pantholops hodgsonii). Applied Animal Behavior Science. 1991;**29**:361-378

[52] Mishra C, Wieren SE, Van KP, et al. Competition between domestic livestock and wild bharal Pseudois nayaur in the Indian trans-Himalaya. Journal of Applied Ecology. 2004;**41**:344-354

[53] Ahmad K, Kumar VP, Joshi BD, Raza M, Nigam P, Khan AA, et al. Genetic diversity of the Tibetan antelope (Pantholops hodgsonii) population of Ladakh, India, its relationship with other populations and conservation implications. BMC Research Notes. 2016;**9**:477. DOI: 10.1186/s13104-016-2271-4

[54] Ahmad K, Nigam P. Ecological and Socio-Economic Study on the Tibetan Antelope or Chiru (Pantholops hodgsonii) in Chang Chenmo Wildlife Sanctuary, Leh, Ladakh [Thesis]. Shuhama, Alusteng, Srinagar,

J&K: Department of Science and Technology, Govt. of India, Sher-e-Kashmir University of Agricultural Sciences & Technology of Kashmir; 2015. p. 59

[55] Ahmad, K. and Nigam P. (In prep.) Population and Habitat Use Patterns of Tibetan Antelope (Panthologos Hogsonii) and Other Ungulates for Conservation Planning in Changchenmo Valley, Changthang, Ladakh, India.

[56] Fox JL, Nurbu C, Chundawat RS. The mountain ungulates of Ladakh. India Biological Conservation. 1991;**58**(2):167-190

[57] Schaller GB, Kang A, Cai IX, Liu DY. Migratory and calving behavior of Tibetan antelope population. Acta Theriologica Sinica. 2006;**26**:105-113

[58] Schaller GB. Wildlife conservation in the Chang tang reserve, Tibet. In: Lu Z, Springer J, editors. Tibet's Biodiversity, Conservation and Management. Beijing: China Forestry Publishing House; 2000. pp. 21-28

[59] Du YR, Gu SC, Wang ZF, Ci HX, Cai ZY, Zhanag Q, et al. Demographic history of the Tibetan antelope Pantholops hodgsoni (chiru). Journal of Systematics and Evolution. 2010;**48**(6):490-496. DOI: 10.1111/j.1759-6831.2010.00095.x

[60] Leslie DM, Schaller GB. Pantholops hodgsonii (Artiodactyla: Bovidae). Mammalian Species. 2008;**817**(2008):1-13

[61] Wright B, Kumar A. Fashioned for Extinction: An Expose of the Shahtoosh Trade. New Delhi, India: Wildlife Protection Society of India; 1997

[62] Network T. Fashion statement spells death for Tibetan antelope. New Delhi,

India: World wide Fund for Nature and the world conservation union; 1999

[63] Ru H, Xu J, Jiang S. Experimental observation and analysis of traffic impact on Tibetan antelopes on the Qinghai-Tibet highway. Advances in Civil Engineering. 2022;**2022**:1226781. DOI: 10.1155/2022/1226781

[64] Mallon DP. Pantholops hodgsonii. The IUCN Red List of Threatened Species 2008: e.T15967A5335049. 2008

[65] Bhatnagar YV, Namgail T, Bagchi S, Mishra C. Conserving the Tibetan Gazelle, CERC Technical Report No. 14. Mysore: Nature Conservation Foundation; 2006b

[66] Mallon, D. and Y. Bhatnagar (2007) "Procapra picticaudata," in 2007 IUCN Red List of Threatened Species, op. cit

[67] Namgail T, Bagchi S, Mishra C, Bhatnagar YV. Distributional correlates of the Tibetan gazelle Procapra picticaudata in Ladakh, northern India: Towards a recovery programme. Oryx. 2008;**42**(1):107-112

[68] Bhatnagar YV, Seth CM, Takpa J, Ul-Haq S, Namgail T, Bagchi S, et al. A strategy for conservation of Tibetan gazelle Procapra picticaudata in Ladakh. Conservation and Society. 2007;**5**(2):262-276

[69] Groves CP, Grubb P. Reclassification of the serows and goral (Naemorhedus: Bovidae). In: Lovari S, editor. The Biology and Management of Mountain Ungulates. USA: Croom Helm; 1985. pp. 71-76

[70] IUCN. IUCN Red List of Threatened Species/Caprinae Specialist Group Report. Gland, Switzerland; 2017

[71] Roberts TJ. Mammals of Pakistan. Revised ed. Karachi, Pakistan: Oxford University Press; 1997. p. 525

[72] Wilson DE, Reeder ME. Mammal Species of the World. Second ed. Washington: Smithsonian Institution Press; 1993

[73] Wilson DE, Reeder DM. Mammal Species of the World. Baltimore, MD: John Hopkins University Press; 2005

[74] Mori E, Nerva L, Lovari S. Reclassification of the serows and gorals: The end of a never ending story? Mammal Review. 2019;**49**:256-262

[75] Duckworth JW, MacKinnon J. Naemorhedus goral. The IUCN Red List of Threatened Species. Gland, Switzerland: ICUN; 2008. Available from: https://www.iucnredlist.org

[76] Prater SH. The Book of Indian Animals. Bombay, India: Bombay Natural History Society; 1980

[77] Bhatnagar YV, Ahmad R, Subba Kyarong S, Ranjitsinh MK, Seth CM, Lone AI, et al. Endangered markhor (Capra falconeri) in India: Through war and insurgency. Oryx. 2009;**43**(3):407-411

[78] Bhattacharya T, Bashir T, Poudyal K, Sathyakumar S, Saha GK. Distribution, occupancy and activity patterns of goral (Nemorhaedus goral) and serow (Capricornis thar) in Khangchendzonga biosphere reserve, Sikkim, India. Mammal Study. 2012;**37**:173-181

[79] Ranjitsinh MK, Seth CM, Ahmad R, Bhatnagar VY, Kyarong S. Goats on the Border: A Rapid Assessment of the Pir Panjal Markhor in Jammu and Kashmir: Distribution, Status and Threats. New Delhi, India: Wildlife Trust of India; 2005

[80] Ahmad R, Pacchnanda U, Suhail I, Haq S, Querishi S, Puri M, et al. The Lost Markhor of Pirpanjal: Assessing the Distribution of Markhor (Capra falconeri)

and Other Important Fauna along the Southern Slopes of Pirpanjal with Special Reference to Resource Competition with Local Grazier Communities in Hirpora WLS, Jammu and Kashmir. Noida, UP: Wildlife Trust of India; 2011

[81] Ahmad K. Ungulate Survey and Distribution. Srinagar, Kashmir, India: Pers. Communication; 2022

[82] Ilyas O, Khan JA, Khan A. Status, distribution and conservation of deer populations of oak forests in Kumaon Himalayas, India. In: Proceeding of 4th International Deer Biology Congress. Kaposvar, Hungary; 1998

[83] Ilyas O, Khan JA, Khan A. Status, abundance and factors governing distribution of ungulates in Kumaon Himalayas, U.P., India. International Journal of Ecology and Environmental Sciences. 2003;**29**:2-8

[84] Green MJB. Ecological separation in Himalayan ungulates. Journal of Zoology. 1987;**1**:693-719

[85] Pendharkar AP, Goyal SP. Group size and composition of the gray goral in Simbalbara sanctuary and Darpur reserved Forest. India Journal of Mammals. 1995;**76**(3):906-911

[86] Mishra C, Johnsingh AJT. On habitat selection by the goral (Naemorhedus goral bedfordi). Journal of Zoology. 1996;**240**:573-580

[87] Abbas F. A Study on Ecobiology of Gray Goral (Naemorhedus goral) with Reference to Pakistan [Thesis]. Lahore, Pakistan: University of the Punjab; 2006. p. 179

[88] Ashraf N, Anwar M, Hussain I, Mirza SN, Latham MC, Latham ADM. Habitat use of Himalayan grey goral in relation to livestock grazing in Machiara

National Park, Pakistan. Mammalia. 2016;**80**(1):59-70

[89] Habibi K. Afghanistan. In: Shackleton DM, editor. Wild Sheep and Goats, and their Relatives: Status Survey and Conservation Action Plan for Caprinae. Gland, Switzerland and Cambridge, UK: IUCN; 1997. pp. 204-211

[90] Ahmad R. An Investigation into the Interactions among Wild Ungulates and Livestock in the Temperate Forests of Kajinag [Thesis]. Jaipur, India: Manipal University; 2014

[91] Fox JL, Johnsingh AJT. India. In: Shackleton DM, editor. Wild Sheep and Goats, and their Relatives: Status Survey and Conservation Action Plan for Caprinae. Gland, Switzerland and Cambridge, UK: IUCN; 1997. pp. 215-231

[92] Ahmad R, Mishra C, Singh NJ, Kaul R, Bhatnagar Y. Forage and security trade-offs by Markhor Capra falconeri mothers. Current Science. 2016;**110**:1550-1559

[93] Burrard G. Big Game Hunting in the Himalayas and Tibet. London, UK: H. Jenkins; 1925

[94] IUCN. IUCN Red List of Threatened Species Capra falconeri (Markhor). Gland, Switzerland; 2015

[95] Chundawat RS, Qureshi Q. Planning Wildlife Conservation in Leh and Kargil Districts of Ladakh, Jammu and Kashmir. Dehradun, India: Report submitted to the Wildlife Institute of India; 1999

[96] Namgail T, Fox JL, Bhatnagar YV. Habitat shift and time budget of the Tibetan argali: The influence of livestock grazing. Ecological Research. 2007a;**22**:25-31

[97] Namgail T, Bhatnagar YV, Mishra C, Bagchi S. Pastoral nomads of the Indian

Changthang: Production system, landuse and socio -economic changes. Human Ecology. 2007;**35**:497-504

[98] Mallon D. The status of Ladakh urial Ovis orientalis vignei in Ladakh. India Biological Conservation. 1983;**27**(4):373-381

[99] Namgail T, van Wieren SE, Mishra C, Prins HHT. Coexistence of Ladakh Urial and Blue Sheep at Multi-Spatial Scales in the Trans-Himalayan Mountains. Geography of Mammalian Herbivores in the Indian Trans-Himalaya: Patterns and Processes. Wageningen: Wageningen University; 2009. pp. 81-94

[100] Namgial T, Van Wieren SE, Mishra C, Prins HHT. Multi-spatial co-distribution of the endangered Ladakh urial and blue sheep in the arid trans-Himalayan mountains. Journal of Arid Environments. 2010;**74**(10):1162-1169

[101] Ghoshal A, Bhatnagar YV, Pandav B, Sharma K, Mishra C, Raghunath R, et al. Assessing changes in distribution of the endangered snow leopard Panthera uncia and its wild prey over 2 decades in the Indian Himalaya through interview-based occupancy surveys. Oryx. 2019;**53**(4):620-632

[102] Khara A, Khanyari M, Ghoshal A, Rathore D, Pawar UR, Bhatnagar YV, et al. The forgotten mountain monarch? Understanding conservation status of the vulnerable Ladakh urial in India. European Journal of Wildlife Research. 2021, 2021;**67**:62. DOI: 10.1007/s10344-021-01492-4

[103] Raghavan B, Bhatnagar YV, Qureshi Q. LADAKH URIAL (Ovis vignei vignei). 2006. Available from: snowleopardnetwork.org

[104] Raghavan B. Interactions between Livestock and Ladakh Urial (Ovis vignei

vignei). Final Report. Dehradun: Wildlife Institute of India; 2003

[105] Johnsigh AJT. Personal communication. Bangaluru, India; 2022

[106] Bhatnagar YV. Ranging and Habitat Utilization by the Himalayan Ibex (Capra ibex Sibirica) in Pin Valley National Park. Bangaluru, India: Saurashtra University, Rajkot; 1997

[107] Bhatnagar YV, Wangchuk R. Status survey of large mammals in eastern Ladakh and Nubra. Conservation Biodiversity in the Trans-Himalaya: New Initiatives for Field Conservation in Ladakh. Conservation Society; 2001;**6**(3):108-125

[108] Aryal A, Coogan SCP, Ji W, et al. Foods, macronutrients and fibre in the diet of blue sheep (Psuedois nayaur) in the Annapurna conservation area of Nepal. Ecology and Evolution. 2015;**5**:4006-4017. DOI: 10.1002/ece3.1661

[109] Joshi BD, Kumar V, De R, Sharma R, Bhattacharya A, Dolker S, et al. Mitochondrial cytochrome b indicates the presence of two paraphyletic diverged lineages of the blue sheep Pseudois nayaur across the Indian Himalaya: Conservation implications. Molecular Biology Reports. 2022;**49**:11177-11186. DOI: 10.1007/s11033-022-07832-

[110] Bhattacharya A, Chatterjee N, Rawat GS, Habib B. Blue sheep resource selection in alpine grasslands of a western himalayan landscape – A point process approach. Zoological Studies. 2020;**59**:e11. DOI: 10.6620/ZS.2020.59-11

Chapter 2

Alimentary System of Native Goat Breeds of Pakistan

Arbab Sikandar and Amar Nasir

Abstract

Goat in Pakistan has been raised both for getting meat and milk with a total production of 748 tons of mutton and 965 tons of milk. In Pakistan, goat meat is the most preferred protein source among muttons. Goats possess a healthy alimentary canal and are mostly offered low-cost grazing land-grown roughage. A chain of tubular organs/tissues and allied glands are observed in the goat alimentary system. A healthy digestive system transforms the available nutrients after digestion and absorption into better growth performance. Only few reports available in literature focusing different local raising goat breeds, its feeding behavior, and the morphological structures of their guts. In this chapter, we tried to draw attention to the embryological development of the goat, the nutrition, and the gross/microscopic anatomy and physiology of gut, which is comprised of oral cavity, pharynx, esophagus, stomach, intestines, liver, and pancreas. The histology of the mucosal structures is focused for better understanding because this tunic is in contact with the ingested food particles and is playing a key role in the process of digestion and absorption. Furthermore, health and clinical issues that can occur with goat alimentary systems are also highlighted in this chapter.

Keywords: microscopic anatomy, physiology, management, gastrointestinal system, small ruminants

1. Introduction

Pakistan has 35 goat breeds (mostly of medium size) with a total population of 78.2 million. Goats belong to Bovidae family and their scientific name is *Capra hircus* are the most crucial contributor to the national GDP in the form of milk, meat, and skin production and also this small ruminant is a livelihood source for people of wide geographical areas of Pakistan [1, 2]. Skin/hides are also very valuable for the leather industry but are unfortunately a neglected by-product of goat slaughtering [3]. According to the country's economic survey, Pakistan has produced 30,946 million goat skins annually. This foremost economic movement adopted of rearing goats chiefly by the people living in rural areas of the arid and semiarid areas of the country. The families rearing the animals in captives in their households are mainly illiterate or have primary level schooling with a below poverty level lifestyle. This mean has a considerable positive influence in reducing poverty and creating employment in the country and it is believed that small ruminant livestock farming is pondered as an

economic and social growth engine, particularly in the rural areas. This animal reaches puberty age within 5–9 months, its length of the Estrus cycle is almost 21 days but is influenced by buck where the total duration of Estrus is 24 to 40 hours. The government of Pakistan has recently approved several projects to boost the existing growth practices of animal husbandry and created new plans by offering free animals to the poor and deserving families of the country [3, 4]. This offering of "poor man cow" put some bright insights into the life standards of the landless farmers/laborers [5]. Dairy goat owners in Pakistan often confront several challenges like adaptation issues to the new environment when there is sparse provision of quality feeds especially during harsh environment, nevertheless, there is growing demand of goat milk locally which is assumed to be comparable to the human milk maintained confident expectations for the raising of dairy goats in Pakistan [6–8]. Most of them shifted from the begging profession toward self-sustained rearing animals as their primary occupation [9]. The animals are mostly kept in open houses and are being reared on browsing by the family members while some of the households' exercise to offer the available grains as supplements. Some of the families are now traditional of having large-size flocks and they carry their animals from area to area to graze their animals [10]. The whole family is shifting from one area to another along with the animals on the availability of grazing pastures and seasons. Use local remedies to treat the animals of suffered in the harsh seasons as they adopt partial standard management practices.

It has been observed that flock and family size is contributing depressingly while training and education of the family putting in positively to implementation index of fruitful management practices. Due to low literacy, lack of technology, the pitiable/high-cost veterinary services and extension infrastructure, un-accessibility of grazing land, the obtaining of value animals are the vital constraint. The prim indicator of the farm is mortality rate and it is observed that the mortality animal is predominantly due to diseases affecting the alimentary system where goats with kids and adults are nearly likewise affected [11, 12]. It is suggested that a state-level knowledge and inspiration of the people toward management development may also be accorded to the people. Lack of awareness about better management may possibly be attributed to the reality that the majority are illiterates and they do not have access to the latest information in the print media and also scientific lectures impart less on them. It is anticipated that government should arrange awareness *via* audio-visual aids and frequent visits of the veterinary experts, aligning marketing system and support system that will further improve the animal production practices and the farmer will get good rewards for their hard work [13].

The ruminants in Pakistan are alienated into browsers and grazers. It has been reported that the browsers have considerable foregut functions, whereas the grazers mainly depend on abomasum, caecum, and intestines. Due to this anatomical difference, grazers can digest high-quality feed, whereas browsers can digest the fibrous parts of the plant. The digestive system is composed of many tubes-like organs and the associated glands [14]. Its prime role is to cut down the ingested food into smaller parts which can be absorbed into the circulation and used for the maintenance of the organism [15]. Considerable unique morphological structures of the tubular system, including oral cavity, stomach, and intestine, play important roles in digestive physiology. For example, the teeth of goats are made to grind roughages, and the stomach particularly the fore-stomach makes possible the microbial digestion of rough fibrous food [16]. There are numerous accessory/supportive glands, such as salivary gland, liver, and pancreas, located aside from the GIT tube but are connected with the duct system. Their ducts go through the walls of tube-like organ and pour their secretary

products into lumina. The morphological study is of utmost necessary to precisely understand the function, nutrition, and pathology of the alimentary system; therefore, the current report is aimed to enlighten the anatomy and histology of the GIT since it is intricately involved with the conversion of food by enzymatic digestion into useful products in form of milk, meat, and skin [17, 18].

2. Key goat breeds and their geographical location in Pakistan

The goat breeds of Pakistan are found in various geographical and climatic environments ranging from cold mountains to hot plains [1]. Beetal bread is the most popular goat breed in Punjab region of Pakistan as its meat, milk, and skin is liked by the community (**Figure 1**). Kamori breed is an inhabitant of the Sind region and is another loved breed of the area particularly for getting milk. Dera Din Panah and crossbreeds are reared for milk and meat in Punjab [19–21]. Barbari breed is raised for milk and meat in Sindh and Punjab [22]. Bugri, Chappar, Jattan and Kamuri, Pateri, Sindh Desi, Tapri, and Tharri breeds are raised in the Sindh province of Pakistan [23]. Gaddi, Damani, and Kaghani breed are present in KPK and mostly used for meat purpose [24, 25]. Gulabi, a giant goat breed is preferred for meat and milk. Teddy breed is raised for mutton in Punjab and Azad Kashmir [26]. The home tract of Nachi goat breed encompasses Bahawalpur and Multan districts living in hot climatic conditions

Figure 1.
Local goat breeds kept in the research center, Ravi campus, UVAS, Pattoki.

[25]. Khurasani and Lehri breeds are present in Balochistan region of Pakistan [23, 27]. Jattal, Beiari, Buchi, Jarakheil, Labri, Pamiri, Shurri, and Baltistani goat breed are kept in cold environment of the mountainous areas of Kashmir, Mirpur, Kotli, and northern areas of Pakistan [21–23, 25, 28, 29].

3. Nutrition of goats

In juvenile ruminants, the initial three gastric compartments are underdeveloped [30] and the animal in this stage acts as monogastric where effective utilization of colostrum and milk occurs in the gut. The animal later consumes a high fibrous diet and there is an establishment of microbial population in the stomach compartment stimulating the rumen development. In some areas, the fattening protocol is adopted for the goats and fed excessive concentrates to attain earlier growth and higher quality of the carcass. *Zea mays (*maize), *Sesbania bispinosa (*janter), *Trifolium alexandrinum (*barseem), *Pennisetum Glaucum* (bajra), and *Cicer arietinum* (channa), etc. are being offered to the animals in most of the areas [31, 32]. Goat comes under the heading of browsers and is the one that put up good use of pasture land [33]. Most of the grasses that rise subsequent to the natural rain are being offered to the animals. Furthermore, soft branches of barked plants viz. Ziziphus sp. (Ber), *Acacia sp*. (Kekar), *Prosopis spicigera* (Jandi), *Dalbergia sissoo (*Sheesham*), Cymbopogon jawarancusa* (Khawai), *Aristida depressa* (Lamb), *Cenchrus pennisetiformis* (Dhaman), *Panicum antidotale* (Murat), *Haloxylon recurvum* (Lana), *Cymbopogon martinii* (Katran), *Euphorbia prostrate* (Khiri), *Leptadenia pyrotechnica* (Khip), *Capparis deciduas* (Dele), *Eleusine flagillif era* (Ghandeel), Neslia sp. (Phel), *Crotalaria burhia* (Chag), Callotropis sp. (Ak), *Salvadora oleoides* (Jal) *and Lasiurus hirsutus* (Gorkha)*, and their* fallen leaves are being offered to the animals [34–38]. Although all the ruminants have this ability, the low-quality forages are transformed by them into products of great nutritious importance and this is due to their digestive system structure. This particular ability of grazing is related to the unique morphology of the goat gut.
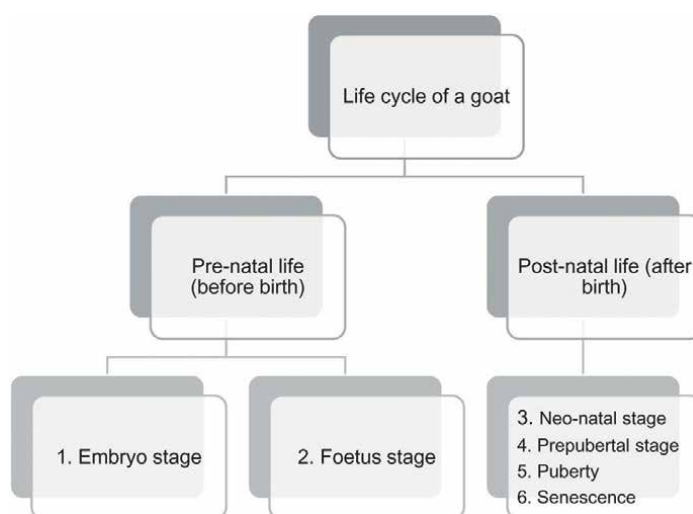

Figure 2.
Embryological development of goat.

4. Embryological development and baseline morphometrics of the alimentary system

During embryogenesis, the gut portion of the animal is derived from the endodermal germ layer, which lies ventrally to the embryo and forms the top surface of the yolk sac. With the passage of time, a greater part of this germ layer is integrated inward into the embryo to develop a gut tube, which is comprised of the foregut, midgut, and hindgut. The midgut is shared with the yolk sac through a narrow and longer vitelline duct. The foregut at the cranial end is enclosed by the oropharyngeal membrane, which later developed a passageway between the oral cavity and the primitive gut [39, 40]. The lateral plate mesoderm of the embryo is participating in the body cavity formation. The hindgut terminates at the cloacal region and forms an anal opening [41]. The whole developmental cycle of the goat is mentioned in **Figure 2**.

Goat lifecycle is completed according to the following stages:

1. Embryo stage: It is a developmental period between fertilization of ova to the endometrial attachment of the conceptus in the female reproductive tract. This process begins with fertilization leads to cleavage, followed by compaction, differentiation of cells, cavity formation, zona hatching, and then implantation with the endometrial lining [40, 41].

2. Fetus: It is a period of development between attachments of conceptus to the uterus to birth and is characterized by the development and growth of body system. This ranges from cell mass differentiation of hypoblast, epiblast, and trophoblast leads to bilaminar disc formation, development of ectoderm, mesoderm, and the innermost endoderm, which later produce the gut tissue, liver, and pancreas, and then the formation of embryo, chorion, amnion and development of Cotyledonary (epitheliochorial) placenta formation and histogenesis occurs [41, 42].

3. Neonatal stage: It is an early period of an individual (from birth to physiological independence).

4. Prepubertal stage: It is period up to which animal becomes sexually mature.

5. Puberty: It is the period of animal life when it attains sexual maturity to produce young ones [43].

6. Adult: It is the prime and transition stage of animal reproduction.

7. Senescence: It is the old age of animal when there is a cessation of reproduction and the overall decline of body system leading to death [44].

5. Digestive system of the goat

The organs present in this system are responsible to get the food, chemically and mechanically breaking it down into smaller pieces and then absorbing them so that it can be used to get energy and body growth and renewal of cells and tissues. Later, it has to remove the unabsorbed portion of the food. This system extends from mouth to anus, including other accessory gland and organs (**Figure 3**). The anal canal is a
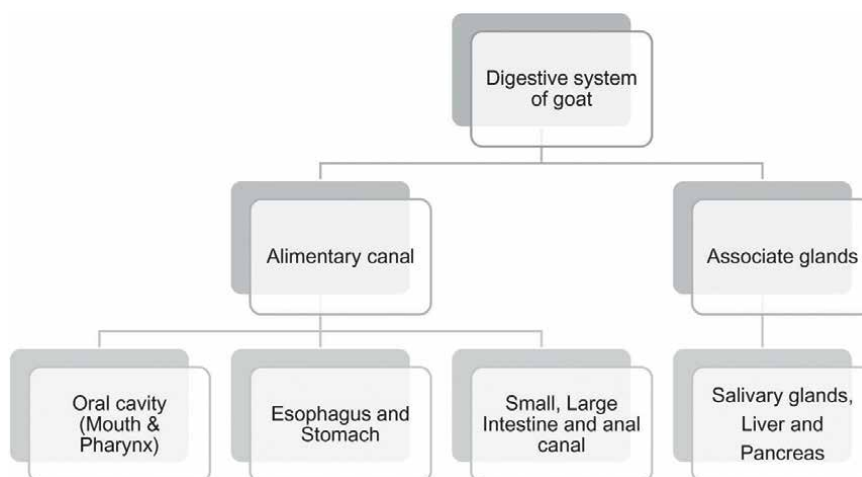
Figure 3.
The alimentary system of goat (flow diagram).

short tube and is the terminal portion of the elementary canal. This is controlled by internal consists of smooth muscle and external anal sphincters consists of striated muscles [45].

6. Oral cavity

The oral cavity plays an important role in procuring and mastication of food particles. The oral cavity includes tongue, lips, teeth gum, cheeks, palate (hard and soft), and the vestibular space. The tongue is the mobile muscular tissue covered dorso-ventrally by stratified squamous epithelium and has three parts: root, body, and apex. Within the oral cavity, the tongue is supported by the hyoid bone caudally, mandible rostrally, and ventrally, and is attached dorsally through frenulum linguae. A large number of papillae are present on its dorsal surface and the filiform (mechanical papillae) are most numerous. Other (gustatory papillae) including fungiform are scattered on the tips, circum vallate is located on the anterior root dorsally, and foliate on the sides of the tongue. The tongue executes functions like reception of dry leaves, mastication, and deglutition of food and the muscles of the intrinsic and extrinsic groups facilitate fodder movement inside the oral cavity [15, 46]. The group of muscles, including masseter muscle, internal pterygoid muscle, medial pterygoid muscle, and temporal muscles, are responsible for mastication.

7. Salivary glands

In mammals, the main function of the salivary glands is to lubricate the ingested food, which helps in mastication and deglutition to protect oral tissues and in some species to initiate enzymatic activity. Salivary glands are present outside the wall of the digestive system and linked with the oral cavity through the duct. The two types of salivary glands include the major salivary glands and the minor salivary glands. The secretions of the salivary glands are serous, mucous, or seromucous

(mixed). Serous cells produce a watery secretion having enzymes, ions, and a small amount of mucin, whereas mucous cells produce a viscous, stringy secretion called mucus [15, 47].

8. Minor salivary glands

Minor salivary glands are present within the wall of the oral cavity and oropharynx, and have short ducts [48]. They are named on the basis of their location:

- Labial glands present in the lips.

- Buccal glands present in the cheeks.

- Palatal glands present in the hard and soft palate.

- Lingual glands situated on the tongue.

The minor salivary glands are present in all three forms, that is, serous, mucous, and seromucous, which are the contributors of serous and mucous secretions through secretary ducts to saliva. Secretary units exist in a variety of forms (i.e., acinar, tubulo-acinar, or tubular). Mucous tubules surrounded by the serous acini frequently develop serous demilunes; however striated ducts (the small ducts) are not its characteristics. The epithelium present in it is the simply squamous to low-cuboidal in shape. Later in the oral cavity, it is changed into stratified squamous form. Glands in the cheeks lie in the middle, dorsal, and ventral rows. The glands of the labial regions are assemblage as superior (nasolabial glands), commissural labial (under the skin along the mouth angle), and inferior labial glands which are connected to the commissural labial glands [15].

The composition of the submandibular gland varies in terms of saliva secretion among different species. The mandibular salivary gland is responsible for the production of a major portion of saliva. These are situated in the ventral and caudal part of the angle of the mandible and are irregularly triangular in shape. The gland has three angles, two surfaces, and three borders. The lateral surface is covered partly by the ventral part of the parotid gland. The medial surface is related to retrophyrangeal lymph node, the pharynx, larynx, and the lingual artery. The mandibular salivary gland is cream-colored or pale yellow, weighing from 5 g to 11 g. It is tubule-alveolar in composition. A thin connective tissue capsule covers the gland and the gland is derived into lobes and lobules by connective tissue septa emerging from the capsule. These connective tissue septa contain ducts, blood vessels, lymphatic, and nerves. The mixed alveoli (seromucous) are more abundantly present in the parenchyma than the other two forms. The duct system of the gland consists of intercalated, striated, and excretory duct forms [49].

Like other ruminants, goats are known to process saliva that acts mainly as a bicarbonate phosphate buffer, which aids in rumination and maintaining electrolyte and water balance, thus the saliva has a role in producing alkaline activity and evenness of the food contents within the sac of rumen and reticulum [50]. After suckling, the milk is overstepped by the reticulo-rumen through the esophageal groove into the true stomach (abomasums) in goat kids. The rumen remains very small in kids due to consuming liquid contents only until and unless the animal receives the fibrous diet. The juvenile animal relies on milk to neutralize the acidic environment in the stomach.

9. Lymphoid tissue of oral cavity of goat

Lymphoid tissue comprises mainly of lymphocytes within the oral cavity and is responsible for maintaining immunity. Such tissues are arranged in diffused and nodular form also called as lymphoid patches. There are two types of lymphoid organs, the primary lymphoid organs comprise of bone marrow and thymus where the development and schooling of the lymphocytes occurs, and secondary lymphoid organs include spleen, lymph nodes, and associated tissues of skin, mucosa, gut, and bronchi,. where the mature naive T and B lymphocytes identify the antigen where they get activated, proliferated and differentiated into effectors and memory types. The tonsils comprise of lymphoid cells (diffuse and nodular), including lingual and palatine, lined by keratinized stratified squamous epithelium [48]. On the other hand, para-epiglottic, pharyngeal, and tubal mucosae are lined by pseudostratified columnar ciliated epithelium on major areas contributing largely to immunity [51].

10. Esophagus

After the pharynx, which is the common cavity for ingested material and the air to pass, a long tube called esophagus is present in the goats. This hollow muscular tube connects the stomach to pharynx. The esophagus in goats passes over the dorsal border of the liver and enters the stomach at the cardia. The cardiac opening in the stomach is opposite to the middle of the eighth intercostal space; it is just to the left of the median plane and about two to three inches below the vertebral column. It opens into stomach at the junction of rumen and reticulum. In kids, the esophagus travels to form an esophageal groove, which serves as a bypass to transfer milk directly into abomasum. In goats, the esophagus consists of majority of the striated muscles. The esophagus has a stratified squamous epithelium lining the hollow organ. It has mucosal folds present for distension. The lamina propria and submucosa have connective tissue (CT) fibers and at the area of the junction with the stomach smooth muscles are arranged in a circular pattern in the inner layer and outer longitudinal within the tunica muscularis [15, 52].

11. Stomach of goat

Like other ruminants, a goat's stomach has four compartments, including rumen, reticulum, omasum, and abomasum (**Figure 4**). Feed undergoes microbial digestion in the fore stomach followed by acidic digestion in the abomasums (true stomach). The larger portion of the fore stomach, the rumen, is regarded as a fermentation vat having the boundless hovering of plant particles related with microbes that are affixed to the mucosal lining cells of the rumen. The inner surface of rumen is coated with minuscule ridge called papillae, which enhances the contact surface area and facilitates improved absorption of digested food ingredients. The inner of the reticulum is honeycomb like in appearance which further adds to the nutrient contact surface area extension [48]. Some of the bacterial digested feed material is absorbed *via* ruminal mucosa and the remaining byproducts are advanced toward omasum containing firm lamellae-like leaves for advanced digestion. Acidic digestions then take place in the abomasums [53]. In addition to mechanical digestion, the rumen presents other valuable properties like the production of Vit-B, synthesis of amino
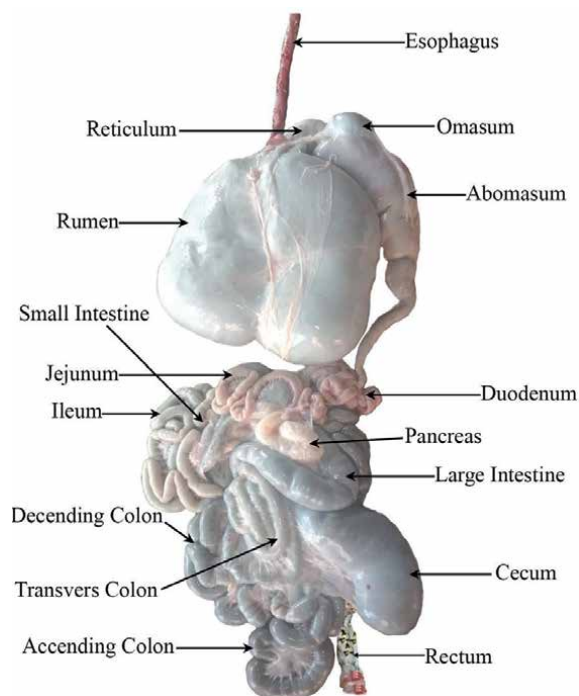
Figure 4.
Digestive system of goat.

acids, and detoxifying anti-nutritional factors like tannins. The fore stomach comprising rumen, reticulum, and omasum is lined by nonglandular keratinized stratified squamous epithelium. The rumen has propria submucosa. And the true stomach has glandular columnar epithelium lining. There are three layers of tunica muscularis–inner oblique, middle circular, and outer longitudinal layer. The lamina muscularis is thicker and has three separate layers. Gastric glands are present in the lamina propria of the mucosal layer in the pyloric region [48, 54–57]. Pylorus is the terminal portion of the stomach, which is characterized by secretions that are largely mucus in nature. This region is separated from the duodenum by a thick circular layer of muscles. At the junction with duodenum, the gastric pits become broader and irregular [58].

The small intestine of most domestic species is quite similar morpho-physiologically. Some of the structural and functional differences in specific regions of the small intestine impart differential functional capabilities to these segments. The small intestine is divided into the following three distinct segments: duodenum, jejunum, and ileum. The major functions of the small intestine are digestion, secretion, and absorption [59, 60]. The small intestinal mucosa has several anatomic adaptations that serve to create an immense surface area to digest and absorb nutrients. These include the plicae circulares (intestinal folds), villi, and microvilli. The villi are the most important area for digestion and absorption of intra-luminal nutrients [61]. It is more elongated in the anterior portion of the gut getting broader toward the ileum. Number of mucous-producing goblets cells increases anterior to posteriorly. The columnar epithelium has a brush border on the top and the mucosa has crypts of Lieberkuhn [62–64]. Columnar cells, Paneth cells, and goblet cells are present in the crypts [24]. Fibrous connective tissue (FCT), blood and lymph vessels are present in

the lamina propria and submucosa. Few of the aggregated lymphoid tissues called Payers patches are present and increase in number toward ileal region. The thickness of the smooth muscles in the muscular mucosa is variable and arranged in thin continuous inner circular and outer longitudinal arrangements. The tunica submucosa is formed by CT, mononuclear cells, having fine blood capillaries along with CT cells, elastic, collagen, and reticular fibers. In duodenum, there are Brunner's glands present in the submucosa which secrete alkaline mucus secretions protecting the intestinal mucosa from the acid released out from the stomach and the viscous mucus lubricates the gut contents [61, 63, 65]. Tunica muscularis thick layer comprising smooth muscle layers similar to the layers present in the mucosa. Mesenteric plexus is present between these layers. Tunica serosa is the last layer containing CT cells, fibers, small capillaries, and flat mesothelial cells. This layer represents the peritoneum and continues with mesentery. The main function of duodenum is to accomplish the initial phase of digestion and mixing of the stomach contents with pancreatic and bile secretions.

Because of the larger surface area of the jejunum, it plays an important role in the absorption of amino acids, fatty acids, sugar, water, minerals, and vitamins. The word ileum means eiliein (Greek word) and is the last part/section of the small intestine in higher vertebrates followed by jejunum. This has fewer diameters than other parts. This portion has smaller circular folds or is even absent in the terminal part and the final absorption of vit. B12, bile salts, and all the remaining important products that are not absorbed in the anterior segments are absorbed in the ileum. These compounds are then absorbed into the bloodstream. The capacity of the small intestine of goats is approximately 2.5 gallons [66].

12. The large intestine

Caecum, colon, and rectum are the three portions of the large intestine. This portion also has all four tunics present in the small intestine that works together to achieve the organs' function. The mucosa is lined by simple columnar epithelium with the handsome number of goblet cells. The lamina propria have rich glandular regions and lymphoid tissues. The muscularis layer is of smooth muscles. There are solitary lymphoid follicles present in the colon over which the dome epithelium is lining on the luminal surface consisting of columnar enterocytes and M cells. Nutrient absorption occurs in the gut *via* the lining epithelium. The submucosa, muscularis, and serosa tunics are the same as that of the small intestine. Muscular contractions mix the intraluminal chyme with microbiota and forward the chyme further caudally. The caecum is a tubular structure located at the beginning of the large intestine also known as the blind gut. The opening of ileo-cecal valve allows the movement of chyme to enter the cecum where the enlarged space permit further mixing of the partially digested material with bacteria. The chyme enters the colon (ascending, transverse, descending, and sigmoid) and rectum through peristaltic muscular contractions [62, 67]. The undigested/partially digested and unabsorbed feed materials take entry in these compartments and further digestion and absorption of salts, water, and important nutrients take place in the large intestine. The more digestion of these materials occurs through microorganisms which is also the function of the large intestine.

Rectum is the final part of the large intestine located dorsally to the urogenital tract and ends on anus. The recto-anal Junction marks the termination of the lamina

muscularis and longitudinal layer of the tunica muscularis, which forms the internal muscular anal sphincter. The anal sphincter is mostly comprised of skeletal muscle. The transition of epithelium columnar to stratified squamous non-keratinized occurs at the junction. The leftover material is getting rid of this portion.

Some differences can be are as follows:

- The lumen of large intestine is much broader.

- There are no villi present in the large intestine.

- Number of goblet cells increased in the intestine proximo-distally.

- Payer's patches are absent in the large intestine.

- There are no plicae circulars in the large intestine.

13. The liver and pancreas

Liver is red-brown in color and is the largest gland of the goat's body, positioned on the right side and just caudal to the diaphragm within the abdominal cavity. This organ has parietal and visceral surfaces. The liver is covered by an FCT Glisson's capsule from which the septa emerge downward and divide the parenchyma into partially completed hexagonal lobules. The central vein is present in the center of the hepatic lobule. The polygonal-shaped hepatocytes are radiated from the central vein area in the form of cords. Sinusoids are present in between the cords where the endothelium and fenestrations are visible. Prominent CT is present in the hepatic triad area at the corner of classical hepatic lobules where hepatic artery, portal vein, and bile ducts are present [68–70].

The liver and pancreas play a pivotal role in digestion. The liver performs metabolic and immunologic functions. It produces bile, which is also stored and then secreted by gallbladder helping the emulsification of fats for digestion. Proteins, fats, and carbohydrates are digested with the help of enzymes secreted by the pancreas in the small intestine. A goat liver also performs different functions like the destruction of hemoglobin, storehouse of glycogen and further converting it into glucose, transformed area into uric acid, detoxification, metabolizing drugs, synthesizing phospholipids and cholesterol, storehouse of vitamins and iron, and the production of almost 10% of the erythropoietin in adult animals [71].

The gall bladder of goat is a pear-shaped sac, yellowish-white in color, which remains filled with green-colored bile juice located at the level of the ninth rib. This structure is lined internally by tall columnar epithelium with occasional goblet cells. Thick muscles at the neck region are thought to be the sphincter of the gall bladder [61].

Pancreas has both the exocrine and endocrine portions and is present in the abdominal cavity. Its head lies in the loop formed by the duodenum and its tail is headed toward the spleen. The major portion is the exocrine comprised of the acini lined internally by the pyramidal acinar cells forming lobules having zymogen granules at their apical portion. The granules are precursors of several digestive enzymes which are secreted into the duodenum *via* duct. The secretion drains from the acini through the intercalated duct, which merges to form an intralobular duct. The later

duct joins to form larger inter-lobular ducts, which enter into the main duct of the pancreas [68, 72].

14. Health and clinical issues that can occur with goat alimentary system

In goats, a range of diseases affecting the gastro-intestinal tract is found, chiefly including bacterial, viral, parasitic, and fungal infections. Oral cavity affections caused by bacterial pathogens are stomatitis caused by a number of bacteria such as Staphylococci, Streptococci, Fusobacterium necrophorum, Sphaerophorus necrophorus, and Actinobacillus lignieresii (Wooden Tongue). The common viral infections include PPR (PPR Virus, mainly Lineage IV), Bluetongue (Orbi virus), ORF (Parapoxvirus), Goat Pox (Goat Pox virus), Foot and Mouth Disease (Aptho virus), etc. Fungal infections are frequently caused by Monilia spp., Candidia spp., Fusarium spp., etc. Pharyngitis and esophagitis are caused by bacteria such as Actinobacilli and Fusobacterium necrophorum besides the pathogens invading down from the oral cavity to pharynx and esophagus. Ovine Herpes virus-2 is the viral agent causing esophagitis in goats [73, 74].

Rumenitis in goats accounts for a significant subclinical disease in survivors of acute episodes, favoring it by serving as a portal for the entry of fungi in this pivotal organ of digestion in goats. Fusobacterium necrophorum may cause secondary infections of abomasum. In Abomasum, a number of parasites belonging to the genera Haemonchus and Mecistocirrus have been recorded. They are large abomasal blood-sucking Trichostrongyles, capable of causing severe anemia and hypoproteinemia. In addition, Ostertagia spp. and related genera, such as Camelostrongylus, Teladorsagia, Marshallagia, and Trichostrongylus axei, are also found in various ruminants, causing chronic abomasitis with mucous metaplasia, achlorhydria, diarrhea, and plasma protein loss [75, 76].

Intestinal diseases affecting goats include Johne's disease generally associated with wasting of body condition, but often not diarrhea mostly targeting the small intestine. The large bowel may be involved in a minority of cases, but the ileum is consistently affected. Acute undifferentiated diarrhea in neonatal goats is frequently associated with enterotoxigenic E. coli, rotavirus, coronaviruses, and Cryptosporidium parvum. Coccidiosis (a protozoan disease) is a multifaceted ailment caused by Eimeria spp. in caprine kids and may occur in animals as young as 3 weeks to 5 months of age. Raised white plaques of coccidia-infected proliferative epithelial cells are found in the terminal ileum; there may be some degree of hemorrhage in severe cases. Some parasites use the peritoneal cavity as their final habitat. Setaria spp. are Onchocercid filarioid nematodes inhabiting the peritoneal cavity of many wild and domestic ungulates, including goats [26, 74, 77].

Gastroenteritis has been recorded in goats >3 weeks of age. The major causes of diarrhea and ill-thrift in goats at pasture are parasitic. The main helminth endoparasite species causing this syndrome are Ostertagia, Nematodirus, and Trichostrongylus. Diarrhea and enterocolitis may also be associated with Clostridium perfringens type D enterotoxemia in goats, although; animals may die quite suddenly without showing any premonitory signs such as diarrhea. C. perfringens type D Enterotoxemia ("pulpy kidney" disease also known as "overeating" disease) is an important disease of goats worldwide resulting in significant mortality. Mycoplasma mycoides may cause acute fibrinous peritonitis in goats, although acute death from septicemia, or arthritis and mastitis are more common. Paratuberculosis caused by

Mycobacterium avium subspecies paratuberculosis frequently produces nodular granulomatous lymphangitis in the mesentery and sometimes caseous or mineralized lymphadenitis [10, 26, 74, 78–80].

15. Conclusion

Both anatomical and physiological study of the GIT and associated organs of domestic goats are essential to be reported. Therefore, the development, histological structures, and functions of the goat gastrointestinal tract, and immune system, nutrition, and clinical issues of the gut are highlighted in this chapter.

Author details

Arbab Sikandar[1]* and Amar Nasir[2]

1 Department of Basic Sciences, sub-campus Jhang, University of Veterinary and Animal Sciences (UVAS), Lahore, Pakistan

2 Department of Clinical Sciences, sub-campus Jhang, University of Veterinary and Animal Sciences (UVAS), Lahore, Pakistan

*Address all correspondence to: arbab.sikandar@uvas.edu.pk

IntechOpen

References

[1] Hashmi HA, Belgacem AO, Behnassi M, Javed K, Baig MB. Impacts of climate change on livestock and related food security implications—Overview of the situation in Pakistan and policy recommendations. Emerging Challenges to Food Production and Security in Asia, Middle East, and Africa. 2021:197-239. DOI: 10.1007/978-3-030-72987-5_8

[2] Saleh AA, Rashad AM, Hassanine NN, Sharaby MA. Sallam SM. History of the Goat and Modern Versus Old Strategies to Enhance the Genetic Performance. 2023. DOI: 10.5772/intechopen.1001106

[3] Rehman A, Jingdong L, Chandio AA, Hussain I. Livestock production and population census in Pakistan: Determining their relationship with agricultural GDP using econometric analysis. Information Processing in Agriculture. 2017;**4**(2):168-177

[4] Naseer Z, Hu H, Yaseen M, Tariq M. Rural women empowerment through social protection programs: A case of Benazir income support programme in Punjab, Pakistan. Journal of the Saudi Society of Agricultural Sciences. 2021;**20**(2):67-74

[5] Khan M, Rashid MA, Yousaf MS, Naveed S, Mohsin I, Rehman HU. Replacing ground Rhodes grass hay with soyhulls in the pelleted diet: Effects on ingestive behavior, nutrient digestibility, blood metabolites, growth performance, and economic viability of intensive fattening Lohi lambs. Tropical Animal Health and Production. 2023a;**55**(3):172

[6] Liang JB, Paengkoum P. Current status, challenges and the way forward for dairy goat production in Asia–conference summary of dairy goats in Asia. Asian-Australasian journal of animal sciences. 2019;**32**(8):1233-1243

[7] Talpur FN, Bhanger MI, Memon NN. Milk fatty acid composition of indigenous goat and ewe breeds from Sindh, Pakistan. Journal of food Composition and Analysis. 2009;**22**(1):59-64

[8] van Leeuwen SS, Te Poele EM, Chatziioannou AC, Benjamins E, Haandrikman A, Dijkhuizen L. Goat milk oligosaccharides: Their diversity, quantity, and functional properties in comparison to human milk oligosaccharides. Journal of agricultural and food chemistry. 2020;**68**(47):13469-13485

[9] Mapiye O, Makombe G, Molotsi A, Dzama K, Mapiye C. Towards a revolutionized agricultural extension system for the sustainability of smallholder livestock production in developing countries: The potential role of icts. Sustainability. 2021;**13**(11):5868

[10] Prank MR, Ahammed MF, Alim MA, Islam MM, Hassan MM, Saifuddin AK, et al. Rearing system, socio-economic status and common diseases frequency of goats in the northern part of Bangladesh. Small Ruminant Research. 2023;**219**:106887

[11] Pawaiya RVS, Singh DD, Gangwar NK, Gururaj K, Kumar V, Paul S, et al. Retrospective study on mortality of goats due to alimentary system diseases in an organized farm. Small Ruminant Research. 2017;**149**:141-146

[12] Zahur AB, Irshad H, Hussain M, Anjum R, Khan MQ. Transboundary animal diseases in Pakistan. Journal of Veterinary Medicine, Series B. 2006;**53**:19-22

[13] Rafiq M, Ameen K. Use of digital media and demand for digitized contents in higher education sector of Pakistan.

The International Information & Library Review. 2012;**44**(3):116-122

[14] Silanikove N. The physiological basis of adaptation in goats to harsh environments. Small Ruminant Research. 2000;**35**(3):181-193

[15] Navarre CB, Baird A, Pugh D. Diseases of the gastrointestinal system. In: Pugh DG, Baird AN, editors. Sheep and Goat Medicine. 2nd ed. Maryland Heights, MO, USA: Elsevier Saunders; 2012. pp. 71-105

[16] Davies G, Oates J, editors. Colobine monkeys: their ecology, behaviour and evolution. Cambridge University Press; 24 Nov 1994

[17] Dubeuf JP, Morand-Fehr P, Rubino R. Situation, changes and future of goat industry around the world. Small Ruminant Research. 2004;**51**(2):165-173

[18] Robbins CT, Spalinger DE, van Hoven W. Adaptation of ruminants to browse and grass diets: Are anatomical-based browser-grazer interpretations valid? Oecologia. 1995;**103**(2):208-213

[19] Ramzan F, Khan MS, Bhatti SA, Gültas M, Schmitt AO. Breeding objectives and selection criteria for four strains of Pakistani Beetal goats identified in a participatory approach. Small Ruminant Research. 2020;**190**:106163

[20] Sikandar A, Adil M, Zaneb H, Arshad M, Ali HM, Khan MA. Concurrent cerebral and extra-cerebral caprine coenurosis: a case report. Pakistan Journal of Life Society and Science. 2018;**16**:55-58

[21] Yaqoob M, Shahzad F, Aslam M, Younas M, Bilal G. Production performance of Dera din Panah goat under desert range conditions in Pakistan. Tropical animal health and production. 2009;**41**(7):1413-1419

[22] Umaraw P, Verma AK, Kumar P. Barbari goats: Current status. In: Sustainable Goat Production in Adverse Environments: Volume II. Cham: Springer; 2017. pp. 29-40

[23] Khan MS, Khan MA, Mahmood SU. Genetic resources and diversity in Pakistani goats. International Journal of Agriculture and Biology. 2008;**10**(2):227-231

[24] Andleeb R, Rajesh R, Massarat K, Baba MA, Masuood J, Dar FA. Histomorphological study of the Paneth cells and Enterochromaffin cells of the small intestine in Gaddi goat. SKUAST Journal of Research. 2016;**18**(1):54-57

[25] Hussain T, Babar ME, Sadia H, Shaheen M, Nadeem A, Ali A, et al. Microsatellite markers based genetic diversity analysis in Damani and Nachi goat breeds of Pakistan. Pakistan Veterinary Journal. 2013;**33**(4):520-522

[26] Sikandar A, Cheema AH, Younus M, Zaneb H. Mycobacterium Avium subspecies Paratuberculosis multibacillary infection (Johne's disease) in a teddy goat. Pakistan Veterinary Journal. 2012;**33**(2):260-262

[27] Kakar AR. Assessing the potential of the indigenous livestock breeds of Baluchistan. In: A Dry net Sci Tech Expertise Technical Report. 2009

[28] Kumar C, Song S, Dewani P, Kumar M, Parkash O, Ma Y, et al. Population structure, genetic diversity and selection signatures within seven indigenous Pakistani goat populations. Animal genetics. 2018;**49**(6):592-604

[29] Saif R, Henkel J, Jagannathan V, Drögemüller C, Flury C, Leeb T. The

LCORL locus is under selection in large-sized Pakistani goat breeds. Genes. 2020;**11**(2):168

[30] Otzule L, Ilgaza A. Goat kids growth and morphological development of stomach in first 60 days of life. Research for Rural Development, Latvia University of Agriculture. 2014;**1**:185-189

[31] Khan S, Jamal MA, Khan IM, Ullah I, Jabbar A, Khan NM, et al. Factors affecting superovulation induction in goats (Capra hericus): An analysis of various approaches. Frontiers in Veterinary Science. 2023b;**10**:10. DOI: 10.3389/fvets.2023.115210

[32] Khurshid MA, Rashid MA, Yousaf MS, Naveed S, Shahid MQ, Rehman HU. Effect of straw particle size in high grain complete pelleted diet on growth performance, rumen pH, feeding behavior, nutrient digestibility, blood and carcass indices of fattening male goats. Small Ruminant Research. 2023;**219**:106907

[33] Ørskov ER. Goat production on a global basis. Small Ruminant Research. 2011;**98**(1-3):9-11

[34] Azim A, Ghazanfar S, Latif A, Nadeem MA. Nutritional evaluation of some top fodder tree leaves and shrubs of district Chakwal, Pakistan in relation to ruminants requirements. Pakistan Journal of Nutrition. 2011;**10**(1):54-59

[35] Devendra C. Use of shrubs and tree fodders by ruminants. In: Shrubs and Tree Fodders for Farm Animals: Proceedings of a Workshop in Denpasar, Indonesia, 24-29 July 1989. Ottawa, ON, CA: IDRC; 1990

[36] Everitt JH, Drawe DL, Lonard RI, Lonard R. Trees, Shrubs & Cacti of South Texas. Texas, USA: Texas Tech University Press; 2002

[37] Horne P, Stür WW. Developing Forage Technologies with Smallholder Farmers: How to Select the Best Varieties to Offer Farmers in Southeast Asia, 1999.

[38] Islam M, Razzaq A, Hassan S, Zubair M, Kalroo MW, Khan A, et al. Influence of rangeland protection and seasonal grazing on aboveground vegetation, forage quality and weight gain of small ruminants—A study in Thar Desert. Pakistan. Journal of Mountain Science. 2023;**20**(2):403-414

[39] Cognie Y, Baril G, Poulin N, Mermillod P. Current status of embryo technologies in sheep and goat. Theriogenology. 2003;**59**(1):171-188

[40] Slack JM. From Egg to Embryo: Regional Specification in Early Development. Cambridge, United Kingdome: The Press Syndicate of The University of Cambridge; 1991

[41] Hyttel P, Sinowatz F, Vejlsted M, Betteridge K. Essentials of Domestic Animal Embryology. Elsevier Health Sciences; 2009

[42] Needham J, Hughes A. A History of Embryology. Cambridge, United Kingdome: Cambridge University Press, University Printing House; 2015

[43] Adhikary GN, Quasem MA, Das SK. Histological observation of thyroid gland at Prepubertal, pubertal and Castracted black Bengal goat. Pakistan Journal of biological Sciences. 2003;**6**(11):998-1004

[44] Arain MA, Khaskheli M, Rajput IR, Faraz S, Rao S, Umer M, et al. Effect of slaughtering age on chemical composition of goat meat. Pakistan Journal of Nutrition. 2010;**9**(4):404-408

[45] Vatta AF, Abbot MA, Villiers JF, Gumede SA, Harrison LJ, Krecek RC, et al. Goat Keepers' Animal Health Care

Manual. South Africa: Agricultural Research Council. Onderstepoort Veterinary Institute with KwaZulu-Natal Department of Agriculture and Environment; 2006. p. 60

[46] Mahdy MA, Abdalla KE, Mohamed SA. Morphological and scanning electron microscopic studies of the lingual papillae of the tongue of the goat (Capra hircus). Microscopy Research and Technique. 2021;**84**(5):891-901

[47] Tadjalli M, Dehghani SN, Ghadiri M. Sialography of the goat parotid, mandibular and sublingual salivary glands. Small Ruminant Research. 2002;**44**(3):179-185

[48] Constantinescu GM. Guide to Regional Ruminant Anatomy Based on the Dissection of the Goat. Amis, USA: Iowa state university press; 2001

[49] Khojasteh SM, Delashoub M. Microscopic anatomy of the parotid and submandibular salivary glands in European hamster (Cricetus cricetus L.). International Research Journal of Basic and Applied Science. 2012;**3**(7):1544-1548

[50] Elewa YH, Ichii O, Otsuka S, Hashimoto Y, Kon Y. Structural changes of goat parotid salivary gland: Pre-and post-weaning periods. Anatomia, histologia, embryologia. 2014;**43**(4):265-272

[51] Casteleyn C, Breugelmans S, Simoens P, Van den Broeck W. The tonsils revisited: Review of the anatomical localization and histological characteristics of the tonsils of domestic and laboratory animals. Clinical and Developmental Immunology. 2011;**2011**:1-14

[52] Islam MS, Awal MA, Quasem MA, Asaduzzaman M, Das SK. Morphology

of esophagus of black Bengal goat. Bangladesh Journal of Veterinary Medicine. 2008;**6**(2):223-225

[53] Wang L, Shah AM, Liu Y, Jin L, Wang Z, Xue B, et al. Relationship between true digestibility of dietary phosphorus and gastrointestinal bacteria of goats. PLoS One. 2020;**15**(5):e0225018

[54] García A, Masot J, Franco A, Gázquez A, Redondo E. Histomorphometric and immunohistochemical study of the goat rumen during prenatal development. The Anatomical Record: Advances in Integrative Anatomy and Evolutionary Biology. 2012;**295**(5):776-785

[55] Giger-Reverdin S, Domange C, Broudiscou LP, Sauvant D, Berthelot V. Rumen function in goats, an example of adaptive capacity. Journal of Dairy Research. 2020;**87**(1):45-51

[56] Gupta V, Farooqui MM, Prakash A, Pathak A, Kumar P. Organogenesis of rumen of goat (Capra hircus) in early prenatal stage (0-50 days) of gestation. Ruminant Science. 2017;**6**:247-254

[57] Membrive CM. Anatomy and physiology of the rumen. In: Rumenology. Cham: Springer; 2016. pp. 1-38

[58] Gupta V, Farooqui MM, Ajay P, Rakesh G. Morphological changes in foetal goat abomasum (Capra hircus). Indian Journal of Veterinary Anatomy. 2016;**28**(2):61-65

[59] Abdelsattar MM, Zhuang Y, Cui K, Bi Y, Haridy M, Zhang N. Longitudinal investigations of anatomical and morphological development of the gastrointestinal tract in goats from colostrum to postweaning. Journal of Dairy Science. 2022;**105**(3):2597-2611

[60] Verma A, Farooqui MM, Prakash A, Pathak A, Singh SP, Gupta V,

et al. Topographical and biometrical anatomy of duodenum in prenatal goats. Indian Journal of Small Ruminants. 2020;**26**(2):214-218

[61] Hassan AA, Nossir HM, Soliman KZ, El-Skeikh EM, Konsowa MM. Computed tomographic, laparoscopic and sectional anatomy of the liver and spleen in goats (Capra hircus). Slovenian Veterinary Research. 2018;**55**:175-186

[62] Kadam SD, Bhosale NS, Aage HM, Kapadnis PJ. Study of histoarchitecture of large intestine in goat. Indian Journal of Animal Research. 2007;**41**(3):196-199

[63] Said AH, Eid AM. Light and scanning electron microscopy of the small intestine of goat (Capra hircus). Journal of Cell and Animal Biology. 2015;**9**(1):1-8

[64] Singh TS, Sathyamoorthy OR, Basha SH, Ushakumary S, Raja K. Histomorphological,Histomorphometrical and histochemical studies on the small intestine of large white Yorkshire pig (sus scrofa domesticus). Journal of Livestock Research. 2021;**11**(2):59-66

[65] Sikandar A, Cheema AH, Adil M, Younus M, Zaneb H, Zaman MA, et al. Ovineparatuberculosis-ahistopathological study from Pakistan. Journal of Animal Plant and Sciences. Pakistan Agricultural Scientists Forum (PAS FORUM); 2013;**23**(3):749-753

[66] Reece WO, Rowe EW. Functional Anatomy and Physiology of Domestic Animals. Hobokin, NJ, USA: John Wiley & Sons; 2017

[67] Braun U, Steininger K, Tschuor A, Hässig M. Ultrasonographic examination of the small intestine, large intestine and greater omentum in 30 Saanen goats. The Veterinary Journal. 2011;**189**(3):330-335

[68] Balasundaram K. Histomorphology of pancreas in goats. Journal of pharmacognosy and Phytochemistry. 2018;7:1711-1713

[69] Khaleel IM, Zghair FS, Naser RA. Immunohistochemical study and identification of alpha and beta endocrine cells of the pancreatic islets in goat (Capra hircus). EurAsian Journal of BioSciences. 2020;**14**(2):6465-6470

[70] Madhan KE, Raju S. Comparative histology of human and cow, goat and sheep liver. Journal of Surgical Academia. 2014;**4**(1):10-13

[71] Singh G, Farooqui MM, Prakash A, Pathak A, Kumar P. Morphogenesis of prenatal liver of goat (Capra hircus). Indian Journal of Veterinary Anatomy. 2012;**24**(1):5-9

[72] Singh D, Prakash A, Farooqui MM, Singh SP, Gautam AK. Development of connective tissue fibres in pancreas of prenatal stages of goat (Capra hircus). International Journal of Current Microbiology and Applied Sciences. 2018;7(7):2878-2883

[73] Baird AN, SHIPLEY CF. Oral-esophageal diseases. Sheep, Goat, and Cervid Medicine-E-Book. 2020;**51**:51-62

[74] Radostits OM, Gay C, Hinchcliff KW, Constable PD, editors. Veterinary Medicine E-Book: A Textbook of the Diseases of Cattle, Horses, Sheep, Pigs and Goats. Elsevier Health Sciences; Amsterdam, Netherlands: Sounders Limited; 2006

[75] Pugh DG, Baird NN. Sheep & Goat Medicine-E-Book. Missouri: Elsevier Saunders; 2012

[76] Rehman T, Iqbal KJ, Anwer A, Abbas RZ, Babar W, Ali A, et al. In vitro anthelmintic efficacy of Citrullus

colocynthis (L.) Schrad on Haemonchus contortus. Veterinarski arhiv. 2021;**91**(3):309-318

[77] Constable PD, Hinchcliff KW, Done SH, Grünberg W. Veterinary Medicine: A Textbook of the Diseases of Cattle, Horses, Sheep, Pigs and Goats. Missouri: Elsevier Saunders; 2016

[78] Abutarbush SM. Veterinary medicine—A textbook of the diseases of cattle, horses, sheep, pigs and goats. The Canadian Veterinary Journal. 2010;**51**(5):541

[79] Mohanta UK, Anisuzzaman A, Farjana T, Das PM, Majumder S, Mondal MM. Prevalence, population dynamics and pathological effects of intestinal helminths in black Bengal goats. Bangladesh. Journal of Veterinary Medicine. 2007;**5**:63-69

[80] Sikandar A. Histopathology: An old yet important technique in modern science. Histopathology. 2018:1. DOI: 10.5772/ intechopen.76908

Pathology of Protein Misfolding Diseases in Animals

Diksha Kandpal, Deepika Lather, Vikas Nehra and Babulal Jangir

Abstract

Protein misfolding diseases are the diseases, which cause transformation of proteins into beta-sheets, forming amyloid fibrils and resulting in aggregate formations and plaques. A wide horizon for occurrence of protein misfolding diseases, includes temperature, pH, surfactant, hydrophobic interaction etc. plays important role. Extensive studies on pathways for protein misfolding converge to mechanism of seed nucleation hypothesis for protein aggregation and misfolding within the cells. Correct folding of proteins is required for normal functioning of the cells and this is accomplished by presence of protein quality control (PQC) system, which make use of endoplasmic reticulum-associated degradation (ERAD), ubiquitin pathway, autophagy, and molecular chaperones. In addition, extrinsic and intrinsic alteration, however, causes misfolding of the protein. Pathological conditions, such as prion diseases, amyloidosis, lung diseases, cancer occurrences, Tay Sach's disease, epidermolysis bullosa, and cataract, are repercussion of protein misfolding. Moreover, the diagnosis of protein aggregates and plaques at an initial stage is challenging. Diagnostic techniques Congo red assay, Thioflavin T binding assay, ANS fluorescence assay, antibody dot blot assay, magnetic resonance imaging, and positron emission tomography are applied but are not routinely used. Although newer techniques are being investigated, lack of suitable biomarkers limits the diagnosis for protein fibril deposition.

Keywords: protein misfolding, protein quality control, protein aggregates, Congo red assay, thioflavin T binding assay, biomarkers

1. Introduction

Proteins are large biomolecules and macromolecules nexus, comprising long chains of different amino acids, thereby conferring proteins specific roles to perform forming essential component of working machinery. Proteins perform vital functions including, catalyzing metabolic reactions, DNA replication, normal structure of the cellular components, response to stimuli, catalyzes, enzymes, performing metabolic activities, and as transport molecules [1]. Although proteins are similar in function yet differ in configuration owing to particular encoding gene of nucleotide sequence and further ensembles protein folding and achieving its characteristic 3D structure or typical native conformation of protein. Protein primarily exist in four forms: primary, secondary, tertiary, and quaternary,

whereas some researchers have reported the fifth form of protein structure called quinary structure [2]. The primary structure comprises of linear chain of amino acids. Secondary structure contains amino acid chains stabilized by hydrogen bonds, forming the polypeptide backbone creating alpha-helix and beta-pleated sheets of the secondary structure. Tertiary structure is determined by the interactions of side chains from the polypeptide backbone [3]. The quaternary structure is formed *via* side-chain interactions between two or more polypeptides [4]. Quinary structure has been identified and refers to the features of protein surfaces that are shaped by evolutionary adaptation [2].

Proteins are dynamic objects, and they arrange themselves in certain conformations to perform correct functions. With respect to structural rearrangements, the structures are referred to as conformation and transitions in between are called conformational changes [5]. Protein folding is ineluctable phenomenon to generate biologically active protein achieving its characteristic structure. Molecular interactions, such as hydrophobic effects, Vander Waals forces, H-bonds, and hydrostatic interactions, exist stably maintaining folded proteins in position and structure. These interactions may either be favorable or unfavorable [6]. The favorable interactions include primarily the enthalpy from Vander Waals packing interactions; secondly, hydrophobic effect or entropy; thirdly, gain of protein-protein Hydrogen bonds; and lastly, electrostatic effects. Unfavorable interaction series include protein conformational entropy and loss of protein-water H-bonding [4, 7]. The correct folding of protein is necessary to perform particular function. Ribosomes and endoplasmic reticulum plays role in synthesizing of proteins and ensures proper folding of the proteins and degrades unfolded protein by various mechanisms (**Figure 1**) [8–10].
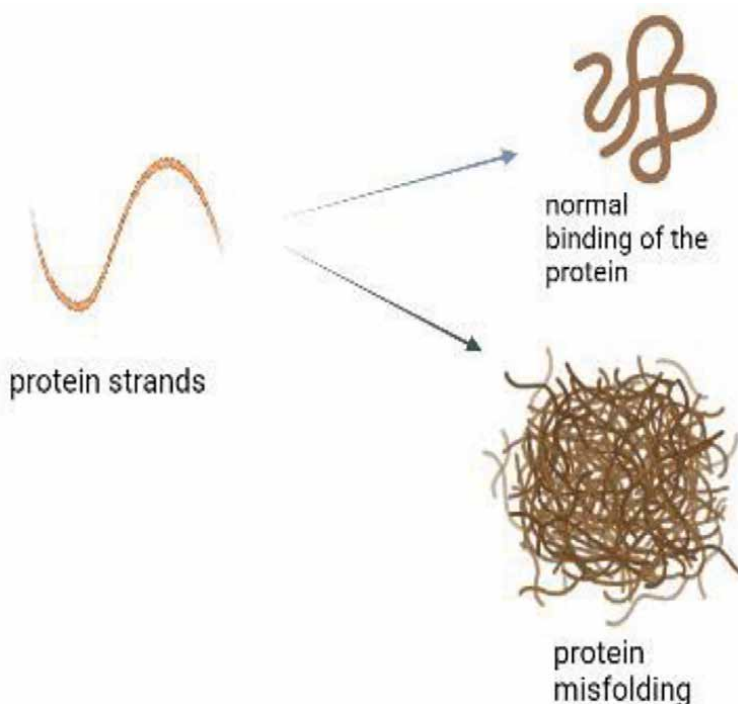

Figure 1.
Depicting the normal binding of the protein when correctly folded and protein structure when misfolding of protein occurs.

2. Mechanism of protein folding and misfolding

Protein folding implies nucleation condensation mechanism, wherein interaction between the residues chiefly leads to the first stage of folding process forming various transition states subsequently resulting in folding of proteins leading to formation of a stable native state [3, 11, 12]. Minimum energy levels are effective for protein folding mechanism, where the lowest energy level helps protein to achieve their stable native state [13, 14]. Initiation of the nucleation process or first phase of the nucleation condensation mechanism prevails from optimum hydrophobic and polar interactions between the formed residues. These interaction results in formation of stable globular structure of protein and serves as quality control system avoiding protein misfolding [10, 15]. Moreover, depending upon the sizes of proteins slightly different mechanisms are adopted for smaller and larger proteins. Smaller proteins undergo two-state mechanisms unlikely to larger protein, where the procedure is more complex with formation of transition states or intermediates or oligomers between the unfolded and fully folded state [16].

Various locations utilized for protein folding, such as in the cells, ribosomes are responsible for protein synthesis in a mechanism called co-translational folding, some folds in cytoplasm after complete protein synthesis, and some folds in endoplasmic reticulum (ER) or mitochondria during translocation [10]. However, some of the polypeptide regions during folding, which are otherwise buried if exposed, lead to formation of unfavorable interactions with other molecules causing protein misfolding. This explains that in protein-folding pathways transient non-native states develop to hide the regions of protein chain, which can cause aggregates on interaction with other molecules commonly the hydrophobic patches [17].

Protein misfolding mechanism and aggregation follow similar trend of seeding nucleation model [3]. This involves two processes or phases, the former phase is
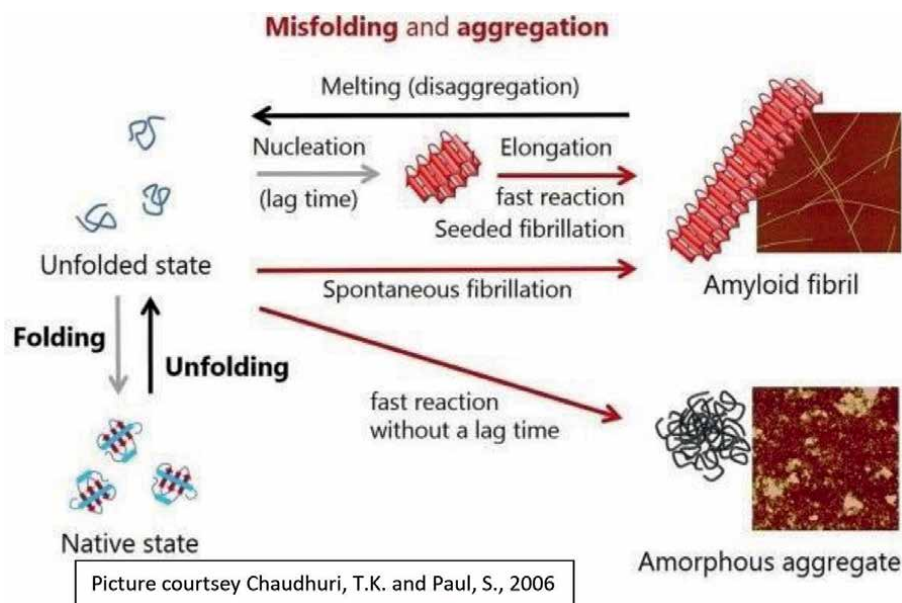

Figure 2.
The picture represents the process that occurs, leading to protein misfolding. Picture courtsey: [21].

called the lag phase, which is responsible for formation of oligomers causing misfolding to occur, and the later phase is called the elongation phase or exponential or polymerization phase [18]. Elaborated studies on the misfolding mechanism reveal that the initial steps are thermodynamically unfavorable and progress slowly until the minimum stable oligomeric unit is formed referred to as seeds [19]. After this step, exponential increase in the rate of formation is observed from oligomers to fibers [20]. The rate of formation can be altered by addition of preformed seeds, which minimizes the lag phase and enhances the polymerization phase. Oligomers are, thereby, considered as best seeds to propagate the misfolding process in an exponential manner (**Figure** 2) [22].

3. Protein quality control system (PQC)

Protein quality control system ensures proper folding of proteins and degradation of the unfolded and partially folded proteins. Usually, the PQC system has the ability to eliminate defective ribosomal products, which have been synthesized as a result of errors in translation or post-translational processes or proteins. Protein quality control system comprises of endoplasmic reticulum-associated degradation, ubiquitin protease pathway, autophagy, and chaperones, which are activated countering misfolded protein and either slow their formation in order to either correct the misfolded protein and refold them or destruct the misfolded protein.

3.1 Endoplasmic reticulum (ER)

Endoplasmic reticulum (ER), besides being a major site for protein production, is one of the major cellular organelles involved in protein homeostasis and quality control. Cellular proteins utilize the ER to attain their folded and posttranslationally modified active state [23]. Although the ER is well furnished for synthesis and folding of significantly high amount of proteins, genetic or environmental alterations are known to stress out the ER promoting misfolding and accumulation of proteins. Unfolded protein response (UPR) mechanism utilized by ER to combat against protein misfolding. UPR is composed of three different transmembrane proteins, including ATF6 (activated transcription factor 6), PERK (double-stranded RNA activated protein kinase, such as ER kinase), and IRE1 (inositol-requiring transmembrane kinase and endonuclease). PERK blocks protein translation by phosphorylating eukaryotic translation initiation (eIF2), and ATF6 (p50ATF6) acts as transcription factor to induce expression of ER-resident chaperones, such as binding protein (BiP). IRE1 alternatively splices XBP1 mRNA. The activation of all three proximal sensors results in the attenuation of protein synthesis through eukaryotic initiation factor-2 (eIF2) kinase and increases protein-folding capacity of the ER. The spliced gene product induces transcription of different genes involved in the ER-associated degradation (ERAD) pathway [24].

The goals of the UPR involve shutting down further protein synthesis to reduce the overload of the ER, secondly, induce ER-resident chaperones to prevent misfolding, and lastly activate ER-associated degradation (ERAD) (IRE1pathway) system to shed off misfolded protein burden using the proteasome. While temporary stress is effectively handled by the UPR, chronic stress leads to continuous accumulation of misfolded protein beyond the capacity of the UPR regulation.

3.2 Ubiquitin (Ub): proteasome pathway (UPP)

Intracellular proteins are degraded by the ubiquitin (Ub)–proteasome pathway (UPP). The UPP consists of enzymes, which attach polypeptide cofactor, Ub onto proteins, and tags them for degradation. This tagging process enables their recognition by the 26S proteasome (large multicatalytic protease complex that degrades ubiquitinated proteins to small peptides). The UPP selectively eliminates misfolded and damaged proteins that arise by missense or nonsense mutations, biosynthetic errors, or damage by oxygen radicals or by denaturation [25]. Three enzymatic components E1, E2, and E3 are required to link chains of Ub onto proteins destined for degradation. E1 or Ub-activating enzyme and E2s or Ub-carrier or conjugating proteins prepare Ub for conjugation and E3 or Ub-protein ligase, recognize specific protein substrate, and catalyze the transfer of activated Ub to it. The initial step in conjugation is activation of Ub at its C-terminus by the enzyme E1. After activation, Ub bound to E1 through thioester linkage is transferred to a sulfhydryl group. The E2s generally are small proteins, containing the cysteine that forms a thioester linkage with the activated Ub. The large number of E2s helps to generate the specificity of the ubiquitination system because specific E2s function in the degradation of various types of substrates, and they can conjugate with various E3s (**Figure 3**) [24, 26, 27].

3.3 Autophagy

Autophagy is a clearance mechanism that degrades damaged organelles and proteins. Normally, it is activated under stress conditions as a protective mechanism to ensure survival and cellular homeostasis by protein turnover. Autophagy is classified in three different categories, chaperone-mediated autophagy (CMA), microautophagy, and macroautophagy, depending on the mechanism used for the capture and degradation of substrates.

In CMA, proteins contain the pentapeptide KFERQ, which is recognized by the chaperone viz., heat shock protein 70 and transported to the lysosome for its hydrolysis. Lysosomes are sites for intracellular protein degradation, which involves uptake of secretory vesicles, portions of the cytoplasm, or whole organelles by lysosomes followed by enzymatic degradation. Microautophagy refers to a process in which some portions of the cytosol are trapped directly by the lysosome without the intervention of chaperones and macroautophagy involves sequestration of damaged organelles or large protein aggregates into cargo vesicles known as autophagosomes that transport the contents to the lysosome for its degradation (**Figure 4**) [28].
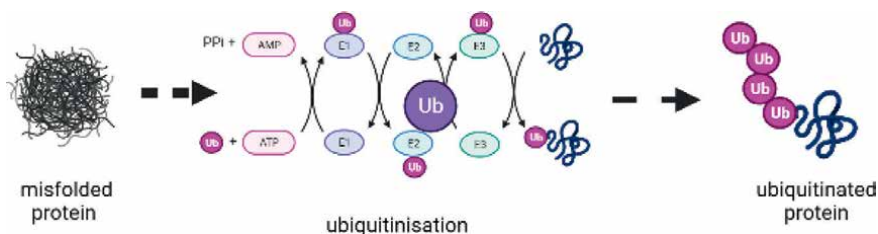

Figure 3.
Picture depicting the process of misfolding protein correction using the ubiquitin (Ub)–proteasome pathway (UPP).
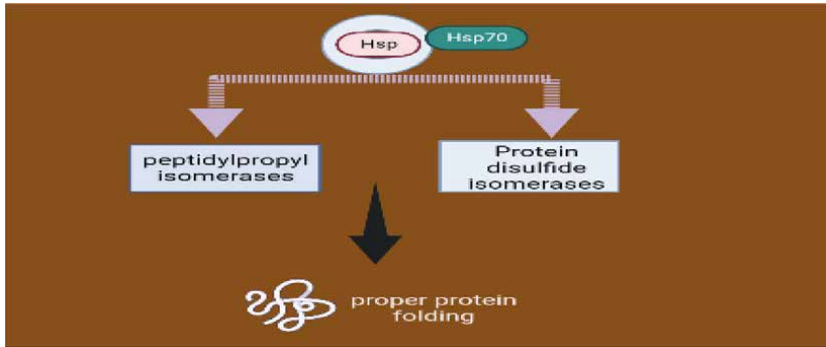
Figure 4.
The picture depicting the role of chaperones or heat shock protein in encountering the misfolding of protein and resolving it through different pathway.

3.4 Chaperones

In general, molecular chaperones are proteins that recognize and bind polypeptides to expose surfaces with specific physicochemical properties, thereby minimizing the potential for aggregation and protecting against attack by proteases [29]. Two different categories of chaperones are identified, folding helper, and holding-type chaperones. Folding helper chaperones comprises of ubiquitous Hsp70/Hsp40/GrpE chaperone system (eukaryotic homologs of the DnaK/DnaJ/GrpE system in *Escherichia coli*) and the large barrel chaperonin complex Hsp60/Hsp10 (eukaryotic homologs) [30–33]. Lectin chaperones calreticulin and calnexin are family of folding helper chaperones without ATPase domain [34]. CLIPs (chaperones involved in protein synthesis) constitute a large family of proteins, and evidence suggests that various CLIPs are associated with different classes of proteins. CLIPs are physically linked to translation mechanisms to control the quality control of newly translated proteins [35, 36]. Chaperones utilize ATP binding and hydrolysis cycles to target

Figure 5.
Summary of factors that are responsible for protein misfolding.

nonnatural polypeptides for folding and unfolding. Several ATP-dependent chaperones, also called protein remodeling factors, mediate target degradation, unfol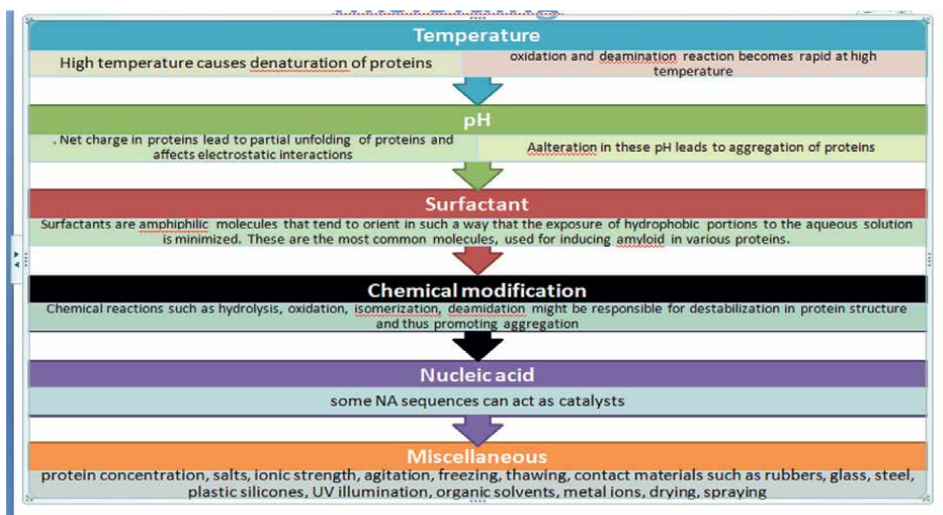ding, or reversal of aggregation [8, 21]. Chaperones target unfolded and partially folded proteins. In particular, it showed a separated hydrophobic region at the center of the folded protein, preventing aggregation by interacting with other molecules [30, 31].

Besides molecular chaperones, other types of folding catalysts that accelerate steps in the folding process, which can otherwise be very slow include protein disulfide isomerases. Protein disulfide isomerases enhance the rate of formation and reorganization of disulfide bonds within proteins and peptidylprolyl isomerases that increase the rate of cis/trans isomerization of peptide bonds involving proline residues [15]. Dysfunction of any of these pathways can, unsurprisingly, lead to protein misfolding diseases (**Figure 5**) [1, 34, 37].

4. Factors affecting protein misfolding

Protein misfolding is a mutation in the gene in question, which results in the misfolding of an amino acid. These mutations in the genetic code are consequently directly related to abnormalities in protein folding, which are either a decrease (loss of function) in the presence of certain proteins that have never been folded into a functional state, or a misfolded protein inside or outside the cell. This situation can always be an igniting point for various diseases as these misfolded proteins are usually insoluble and tend to form aggregates (gains of function). The insoluble nature of protein aggregates results in recessive structures due to their high propensity for intermolecular hydrogen bonding. These are called amyloid fibrils, and as they accumulate, they form amyloid plaques [19, 38].

Incorrect protein folding can occur for a number of reasons, including internal and external factors. The internal factors broadly include, first, somatic mutations in the gene sequence resulting in transformation of proteins that cannot accommodate their native folding. Secondly, errors in the transcription or translation process result in modified proteins that cannot fold correctly. Third criteria include failure of folding and chaperones protective responses. Fourthly, posttranslational modifications of proteins and errors in protein delivery mechanism, and lastly, structural modifications due to environmental changes and induction of protein misfolding by seeding and cross-seeding mechanisms. The most common fate of misfolded proteins is self-aggregation due to exposure of fragments, which are otherwise hidden inside the protein and generate a high level of stickiness [39].

Protein folding is a fine-tuned process that is influenced by several external factors, including electric fields, magnetic fields, temperature, pH, chemicals, space constraints, and molecular density. These factors lead to improper folding of proteins, which leads to proteinopathy. Proteins become unstable at extreme temperatures and become denatured. Likewise, excessive alteration in pH, mechanical forces, and chemical denaturants denature proteins [4]. Denaturation leads to the loss of the tertiary structure of the protein and not the formation of aggregates, but mainly the beta layer of amyloid or amyloid fibrils, which subsequently forms amyloid plaques [7].

High temperature directly affects the conformation of proteins and causes irreversible sometimes reversible denaturation of proteins, which leads to aggregation. High temperature enhances oxidation and deamination reactions and also increases the frequency of hydrophobic interactions, which may lead to protein aggregation. Protein aggregation changes with the pH of the protein, resulting in partial unfolding

of the protein and affecting the electrostatic interactions of protein. Aggregation occurs due to neutralization of charged molecules with enhancement of hydrophobic interactions. The presence of various surfactant molecules, for example, cationic (CTAB, CPC, DTAB), anionic (SDS, SLES, AOT), and nonionic causes protein aggregation. They have a strong effect on protein conformation as they destabilize the protein or stabilize it with subsequent aggregation. Aggregation of proteins occurs due to the interaction of surfactants with opposite charge centers of protein molecules and repulsion of water molecules by hydrophilic tails. Chemical modification is another technique that plays an important role in protein aggregation. Chemical reactions, such as hydrolysis, oxidation, isomerization, and deamidation, can destabilize protein structures and promote aggregation [29]. In addition, the induction of aggregation will be induced by photolytic degradation of proteins, including oxidation of aromatic residues, including histidine, cystine, and methionine.

Posttranslational modifications affect the structure and function of proteins, usually promoting proper folding or leading to improper folding and accumulation. Reducing sugars plays an important role in posttranslational protein modification, forming advanced glycosylation end products (AGEs) in a nonenzymatic process called glycosylation. Protein glycosylation depends on the influence of free amino groups on the polypeptide chain, sugar concentration, and oxidative conditions. It has been noted that amyloid deposits of β-amyloid, tau, prion, transthyretin, and β(2) microglobulin contain glycosylated proteins [40]. The mechanism behind aggregation-promoting glycosylation is that it stabilizes protein aggregates by promoting the formation of covalent cross-links that accumulate over a period of time and are not frequently removed. Proteins also undergo glycosylation at exposed lysine residues, which are also ubiquitination sites, which send proteins to the proteasome for degradation, resulting in clearance damage by the ubiquitin-proteasome system. Thus, the accumulation of proteins in the form of aggregates or in the form of deposits or inclusions in tissues may be beneficial after glycosylation. Various factors that cause protein folding include protein concentration, salinity, and ionic strength.

5. Diseases due to protein misfolding

Diseases, due to protein misfolding, can be broadly categorized into two categories basically the loss of function and the gain of function. Diseases arise because specific protein becomes unfunctional when adopting a misfolded state or undergoes severe impairment of protein trafficking [41]. This is observed in autosomal recessive disorders with loss of function pathology. This type of misfolding comprises of cystic fibrosis, Phenylketonuria, and short chain acyl Co A dehydrogenase. Second type of misfolding occurs by the gain of function, wherein the pathological state originates because of underlying aggregates or concomitant aggregation of proteins [7, 42]. This is further subcategorized into two subtypes. First, dominant inherited diseases [43]. Some researchers illustrate protein misfolding diseases under five different categories namely, improper degradation, mislocalization, dominant-negative mutations, structural alterations with novel toxic functions, and amyloid accumulation [14].

5.1 Prion disease and protein misfolding

Prions cause spongiform encephalopathy known as scrapie in sheep and bovine spongiform encephalopathy or mad cow disease in cattle. Transmissible spongiform

encephalopathy is a protein-folding disease that causes fatal neurodegeneration characterized by vacuoles in the brain. The misfolded protein, named PrPSc, is derived from the endogenous cellular prion protein PrPC. PrPC is a glycoprotein of approximately 231 amino acid residues, which is fixed in plasma. Mature PrPC protein residue is 23–231 amino acid long composed of an independent and flexible N-terminal region (residues 23–120) and a C-terminal globular domain (residues 121–231), *via* the glycolipid anchor phosphatidylinositol that physically interact with each other. Globular domain contains two short leaf-forming antiparallel filaments (aa 128–130 and 160–162 aa for mouse PrPC) and three helices [44, 45]. The hypothesis is that amyloid-like fibrils are formed by two tightly staggered plates in the form of zippers, allowing nucleation to form fibrillar-forming aggregates [36, 46, 47].

Prime event within pathogenesis is the misfolding of the regular shape of the prion protein, PrPC, into the generally protease-resistant-sheet rich isoform, described because the scrapie prion protein (PrPSc), *via* way of means of a conformational rearrangement. The PrPSc constitutes the transmissible agent ("prion"), capable of recruit and convert natively folded PrPC into de novo PrPSc through an autocatalytic process. It is the PrP-TSE protein that can shape amyloid protein aggregates. The purpose for the two absolutely special configurations of the identical protein is not known; however, a vital commentary is if a small quantity of PrP-TSE is brought to a bigger quantity of PrP-C, the "healthy" protein is transformed to the TSE shape [48]. The two variations have wonderful traits glaring of their secondary and tertiary structures. The PrPC is constructed from 40% α-helical and 3% β-helical folds, while PrPSc is folded right into a parallel left-exceeded β-helical shape that has a 30% α-helical and 40% β-helical conformation [45]. There are at the least two proposed fashions for PrPSc autocatalytic propagation. The refolding version assumes that an electricity barrier precludes the preliminary conversion of PrPC to PrPS. The seeding version asserts that PrPC and PrPSc exist in thermodynamic equilibrium, and PrPSc starts to mixture while a particularly ordered monomeric PrPSc (the seed) stabilizes and recruits greater monomeric PrPSc to shape large aggregates [49, 50].

Elucidation of the high-decision shape of prions and aggregated prions has been hard due to problems related to the inherent chemical houses of the proteins. Two mechanisms, the cloud speculation and deformed-template speculation, were proposed for the genesis of prion lines related to classical scrapie. Although the two ideas are noticeably described, they may be now no longer collectively exclusive. The cloud speculation assumes that isolates are constructed from a heterogenous combination of PrPSc conformations (lines), and over time, a permissive conformer arises to turn out to be the fundamental variant [51]. The deformed-template speculation posits that, initially, there may be a fundamental conformer instead of a combination of PrPSc conformations, and adjustments within side the replication surroundings cause trial-and-mistakes seeding activities that generate a brand-new dominant conformer. Both hypotheses postulate the life of more than one conformer inside an isolate that makes a contribution to the discovered variations in sickness phenotype [52].

The key event in pathogenesis is the aberrant folding of the normal form of the prion protein, PrP C, into a commonly protease-resistant leaf-rich isoform, defined as prion protein scrapie (PrPSc) by structural rearrangement. PrPSc is an infectious agent ("prion") that can naturally recruit folded PrPCs and convert them to novel PrPSc through an autocatalytic process. It is the PrP TSE protein that can form an aggregate of amyloid proteins. The reasons for the two completely different configurations of the same protein are unknown, but the normal prion protein PrP C undergoes a conformational change into a self-replicating, misfolded PrPSc conformer.

On the other hand, in the genetic type of disease, a change in the PrPC form may occur due to a genetic mutation of the PRNP gene [44, 53]. The processes that promote development are not fully understood. Indeed, pathogenic mutations, such as G113V and A116V in the N-terminal domain, can induce prion pathogenesis by accelerating misfolding and aggregation and modifying the structure of the palindromic region, which appears to be the intermolecular binding site in oligomers [44].

The defining step in prion infection is the transformation of the PrPC form into the protease-resistant β-sheet. Prion disease is caused by the accumulation of a misfolded form of PrPC called PrPSc. At this time, PrPC expression is necessary and rate-limiting. Transformation of PrPC into the pathological conformer PrPSc is characterized by a significant increase in the secondary structure of the β-sheet [5, 48]. The conversion of PrPC to PrPSc is accompanied by significant structural and biophysical changes in the molecule. When improperly folded, PrPC, rich in α-helices, which normally attaches to cell membranes *via* glycosyl phosphatidylinositol (GPI) anchors, is converted into predominantly single β-sheets [5, 45]. These changes increase resistance to heat and degradation by proteases. Indeed, it has been suggested that prion proteins can experience an environment that can reconstitute disulfide bonds in the endosome, which has been shown to enhance the transition to a fibrillar state [5, 48]. In sheep, the highest concentrations of PRNP mRNA transcripts are found in the thalamus and brain, followed by the cerebellum, spinal cord, spleen, other lymphoid tissues, brainstem, gastrointestinal tract, and reproductive organs.

5.2 Amyloidosis and protein misfolding

Amyloidosis belongs to the group of protein-folding disorders. Various proteins that are soluble under physiological conditions can undergo conformational changes in their β-layer-rich structures, which can then self-assemble into highly insoluble amyloid fibrils. Proteins in a partially folded or misfolded state due to loss of function of the protein's quality control system and various external factors contain open hydrophobic and unstructured regions that contribute to the formation of aggregates [36, 46, 49]. Amyloidosis can be divided into two main classes: localized or focal and systemic. In focal amyloidosis, amyloid fibrils deposit in organs, such as the brain and pancreas, where precursor proteins are synthesized [9, 54]. On the other hand, in systemic amyloidosis, serum precursor proteins, such as immunoglobulin light chain in amyloid amyloidosis (AL), transthyretin in familial amyloid polyneuropathy, and β2-microglobulin in dialysis amyloidosis circulate and polymerize to form amyloid fibrils then settles all over the tissue surface [40, 55]. In addition, the formation of stable aggregate structures can also occur due to hydrophobic decay due to the presence of extraneous debris in solution that changes conditions. On the other hand, electrostatic interaction with hydrophobic forces plays a crucial role in the formation of the complex amyloid fibrils [40].

5.3 Cancer occurence and protein misfolding

The maximum often altered gene in tumors is TP53 encoding the p53 protein. TP53 mutations are related to unfavorable diagnosis in lots of sporadic cancers. The initial stage of TP53 mutations is the loss of wild-kind p53 functions, which represents an essential gain for the duration of most cancers improvement through depriving cells of intrinsic tumor suppressive responses, along with senescence and apoptosis [56]. The tumor suppressor p53, a transcription element that regulates

the cell cycle and apoptosis, is likewise amyloidogenic. In tumor models, each wildkind and mutant p53 protein displays aggregation kinetics and morphology just like the ones of classical amyloidogenic proteins, along with β-amyloid peptide and α- synuclein [14]. Wild type p53 loses its anticancer maneuver, while p53 mutants with enhanced amyloidogenicity show accelerated aggregation. The majority of TP53 mutations are missense, producing single residue substitutions within the protein's DNA-binding domain when compared with most other tumor suppressor genes. However, p53 missense mutant proteins (mutp53) lose the ability to activate canonical p53 target genes, and some mutants exert trans-dominant repression over the wild-type counterpart. The cancer cells are supposed to gain selective advantages by retaining only the mutant form of the p53 protein. This can be explained by the ability of different p53 mutants to reshape the tumor cell's transcriptome and proteome, by virtue of newly established interactions with transcription regulators, enzymes, and other cellular proteins.

Based on this, it has been reported that specific missense mutations in p53 disrupt important cellular pathways, promote proliferation and survival of cancer cells, and promote invasion, migration, metastasis, and chemical resistance. Some of the tumor suppressive activity of wild-type p53 is related to its ability to help cells adapt and survive in moderately stressful conditions, including oxidative and metabolic stress [38]. Mutant p53, similar to wild type, stabilizes and activates in response to tumor-associated stress conditions and may provide cancer cells with the ability to cope with difficult conditions encountered during tumor development, including DNA associated with hyperproliferation. Mutant p53 supports tumor progression by promoting an adaptive response to cancer-associated stress conditions. An oncogenic missense mutant form of p53 (mutp53) can recognize multiple stress effects and act as homeostatic factors triggering adaptive mechanisms. Mutant p53 has been shown to induce a survival response to oxidative stress, promoting protein folding and increasing proteasome activity. The mutant p53 protein is inherently unstable due to proteasome-mediated degradation induced by the E3 ubiquitin ligase MDM2 and CHIP. However, mutp53 protein accumulates in higher amounts in tumor tissues, and this stabilization is necessary to realize pleiotropic oncogenic activity [57].

5.4 Epidermolysis bullosa simplex and protein misfolding

EB simplex results from mutations affecting either keratin 14 (K14) or K5, the type I and type II intermediate filament (IF) proteins. Mutations in the gene encoding collagen, type XVII, alpha 1 (COL17A1), a hemidesmosomal plaque protein required for tight adherence of basal keratinocytes to the basal lamina, account for a special subset of patients with elements typical of both EB simplex and EB junctional dominantly disrupting keratin IF structure [58, 59]. Mutations in the K14 rod domain elicit the formation of aggregates of amorphous proteins in the cytoplasm. Such aggregates are diagnostic of the most severe form of EB simplex. In an experiment with mice, homozygous null for K14, K5, or plectin displayed the key features of EB simplex revealing that cell fragility is largely a loss of function phenotype, containing a K14 mutation causing simple EB compared to *in vitro* reconstituted filaments in wild-type K5 and K14 proteins contains an Arg125 → Cysor K5 mutation, 1649delG exhibiting significantly lower elasticity in low (linear) strain mode is easily broken. If the response of misfolded proteins cannot resolve these aggregates, the cell's protein homeostasis machinery is overloaded. This induces cellular stress and can affect the phenotype of cells and tissues *in vivo* [60].

5.5 Lung diseases and protein misfolding

UPR activation is induced by several pathogens associated with respiratory diseases, including cystic fibrosis, asthma, and COPD. Toll-like receptor (TLR) activation and bacterial infection can trigger UPR. TLR2 and TLR4, specifically activate IRE1 to promote the release of inflammatory mediators. Respiratory pathogens can also interfere with UPR. Intracellular pathogens, such as bacteria, replicate in ER-associated compartments and selectively block IRE1 pathway activation [61]. Secreted bacterial toxins can modulate the UPR. For example, pyocyanin from *Pseudomonas aeruginosa* induces a similar response in the alveoli evidenced by XBP1 splicing and BiP induction. *Aspergillus fumigatus* is a fungal pathogen that interacts with airway protection in a variety of ways to cause broncho-pulmonary aspergillosis. We found that the expression of BiP was increased in lung tissue. Administration of *A. fumigatus* to rats induced pulmonary UPR and airway hyper-responsiveness. Although the mechanisms are not fully elucidated, they include the generation of mitochondrial reactive oxygen species (ROS) and impaired PDI function leading to ER stress. Many viruses cause ER stress, including RSV, influenza A virus (IAV), Coxsackie virus A16, SARSCoV1, and SARSCoV2 (COVID-19). The mechanism of virus-induced ER stress may involve abundant translation of viral proteins that inhibit their ability to fold. It has been reported that IAV induces inflammation and apoptosis in primary human bronchial epithelial cells by activating IRE1 with little or no activation of PERK or ATF6. Picornaviruses, such as rhinoviruses, can benefit from IRE1 activation because they can promote autophagy, and picornaviruses use autophagosomes as RNA replication sites. In contrast, RSV was reported to induce noncanonical UPR activation with IRE1 and ATF6 activation but not PERK, whereas IRE1 inhibits RSV replication, suggesting that inhibition of this UPR arm may be detrimental to RSV infection [62].

5.6 Taysach's disease and protein misfolding

Lysosomal storage diseases (LSDs) are comprised magnificence group of rare diseases of numerous pathologies. Their distinctive characteristics include dysfunction of the endosome–lysosome system, which in lots of instances ends in the accumulation of toxic metabolites and death at molecular level. A subset of LSD includes GM2 gangliosidoses. GM2 gangliosidoses are a series of associated disorders resulting from insufficiency of active β-hexosaminidase A (HexA). HexA enzyme processes GM2 ganglioside to GM3 ganglioside in the lysosome. Inactivation or loss of HexA causes toxic metabolite buildup of GM2, leading to disease formation and cell death. Tay–Sachs disease (TSD) is clinically described with the aid of using mutations with HEXA gene. The HexA enzyme is made from the HEXA and HEXB genes, which encode α and β subunits, respectively with 60% similarity on the amino acid. They are synthesized on the endoplasmic reticulum (ER), wherein they are glycosylated and form intramolecular disulfide linkages and dimerize. The structural similarities among the chains form more than one isozyme through differential affiliation such as HexA (αβ), HexS (αα), and HexB (ββ). HexB is the most stable of the complexes and HexA is the only species capable of processing GM2 ganglioside. This led to hypothesis development stating low β production promotes heterodimerization over β homodimerization. In the Golgi apparatus, specific glycans are modified with mannose 6-phosphate (M6P), allowing for the trafficking of Hex enzymes to lysosomes. In the lysosome, presentation of the GM2 ganglioside substrate from the bilayer to the active site of HexA additionally requires the adaptor protein GM2-activator. Loss of function in either subunit of HexA or its adaptor protein can lead to GM2 gangliosidosis [63].

5.7 Miscellaneous conditions due to protein misfolding

5.7.1 Hypoxia

Hypoxia induces UPR at several targets, including airway epithelial cells and the mechanisms by which this occurs are not fully understood. Therefore, there are several ways, in which hypoxia can cause ER and UPR stress. First of all, reactive oxygen species formed under hypoxia can modulate UPR activation by directly or indirectly affecting BiP and interfering with the formation of disulfide bonds [64]. Redox-sensitive PDI chaperones are restored during protein folding. It is reduced by electron transfer to ER oxido-reduction (ERO1), which then requires molecular oxygen for reoxidation and restoration of function. In addition, since ERO1 is a target of hypoxia-inducing factor (HIF), hypoxia may modulate disulfide bond formation in several ways.

5.7.2 Idiopathic pulmonary fibrosis

Idiopathic pulmonary fibrosis (IPF) is a scarring disease histologically characterized by the presence of fibroblastic lesions. Despite antifibrotic therapy, the prognosis is grave. Fewer researchers have shown that ER stress plays an important role; however, the biological mechanisms that cause the condition are still unclear. Alveolar type II (AT2) cells secrete surfactant protein C (SFTPC) and mutations in surfactant protein C (SFTPC) are associated with familial IPF and profound UPR activation. Many of these mutations disrupt the BRICHOS SFTPC domain, which acts as a distinct chaperone to promote SFTPC folding. Infringement of SFTPC folding can lead to protein aggregation and activation of all UPR cancers. In a mouse model, these mutations interfere with lung morphogenesis, either directly leading to fibrosis or increasing the lung's sensitivity to secondary infections that lead to pulmonary fibrosis [62].

5.7.3 Cataract

Cataract is defined as a clouding of the transparent lens inside the eye, reducing the amount of light and subsequently reducing vision. The natural lens is a crystalline substance and the precise structure of water and protein creates a clear pathway for light to pass through. Crystallin, the major protein of the mammalian eye lens, exists in the α-polydisperse B-crystallin form, and each with a molecular weight of approximately 20 kDa. Members of the alpha (α) and β γ crystallin family are the major soluble lens proteins. A- crystalline is an ATP-independent chaperone that effectively binds to damaged or partially unfolded proteins and dissociates them to prevent large-scale protein aggregation. A- crystalline comprises of αA and αB subunits and belongs to family of heat shock proteins [34, 65, 66]. Alpha-crystallin depends on external conditions, such as pH and temperature, quaternary structure, ionic strength, and concentration [67]. In addition to the lens, it is widely found in many other tissues, including the brain, lung, spleen, heart, and skeletal muscle, where it acts as a chaperone and interacts with several partially folded target proteins. Alpha-crystallins prohibit the formation and precipitation of αB- and α-crystallin, as well as ordered protein aggregates (amyloid fibrils).

Proteomic analysis of lens proteins revealed deamidation, oxidation, glycosylation, and shortening as various factors associated with damage. Deamidation is one of the most common damages to crystallins, introducing a negative charge to proteins by converting residues of glutamine to glutamate. Asparagine is also susceptible to

deamidation, and both residues are transformed into cataract aggregates. Several oxidation sites targeting tryptophan, cysteine, and methionine residues have been identified in crystallin. Deamination decreases the stability of βA3 and βB1 crystallins and increases the tendency to aggregation. Destabilization, due to lifetime accumulation of covalent modifications/alteration, can lead to partial unfolding of proteins, which can lead to the formation of intermediate conformations exposing previously hidden hydrophobic residues. Hence, proving that destabilization of the native state of the lens protein due to covalent bond damage leads to aggregation [66].

6. Diagnosis

Identification of protein aggregates can be divided into three classes: (i) visualization of protein aggregates in biopsies, (ii) monitoring of marker peptides in body fluids, and (iii) visualization of protein aggregates *in vivo* using imaging techniques [68].

6.1 Thioflavin T binding assay

The use of Thioflavin T (ThT) and its derivatives is perhaps the simplest and most widely used method for monitoring the aggregation of amyloidogenic proteins. ThT is a low molecular weight dye exhibiting fluorescence emission when fibrillar protein aggregates bind to the β-layer groove structure. Traditionally, ThT has been used to detect amyloid fibrils because of the characteristic sigmoidal increase in fluorescence that occurs between the monomeric state and the ends of the fibrils [69, 70] beside ThT also binds to fibrillar aggregates containing β-sheet groove binding sites (fibrillar oligomers and fibrils). Prefibrillar aggregates of β-sheet structure contain few binding sites than fibril thereby showing low frequency of fluorescence [71]. Thus, ThT could indicate the presence of toxic circular fibrin and fibrin oligomers, but not the presence of pre-fibrin oligomers that do not have a clear β-sheet structure [72].

6.2 Congo red binding assay

Congo red (CR) is a small molecule probe traditionally used to identify amyloid fibrils, especially in the form of brain tissue or *in vitro* deposits. CR binds to β-rich structures present in amyloid fibrils and exhibits a characteristic green birefringence with cross-polarization. Newer studies have revealed the use of CR to study fibrillar aggregates [5, 55, 71, 72].

6.3 ANS fluorescence analysis

1-anilinonaphthalene-8-sulfonate (ANS) is one of the most commonly used fluorescent probes for characterization. ANS provides an assessment of surface hydrophobicity, depicting increase in fluorescence intensity and a blue shift (decrease in wavelength) when exposed to hydrophobic regions of the protein surface [73]. The interaction and subsequent destruction of the bilayer of the hydrophobic lipid membrane is considered as one of the main mechanisms conferring toxicity to cells in diseases involving prefibrillar aggregation. Therefore, assessment of the surface hydrophobicity of protein aggregates could potentially be very useful for the study of fibrillar protein aggregates [74]. Indeed, a recent study of prefibrillar oligomers of Aβ42 peptide showed an increase in fluorescence and a

change in blue color upon exposure to the ANS compared to fibrils and monomers, as well as a correlation between increased ANS fluorescence and toxicity. In certain areas of monitoring prefibrillar protein aggregates, ANS is used less frequently than CR and ThT [72, 75].

6.4 Antibody dot blot assay

Due to the difficulty to obtain high-resolution crystal structures of protein aggregates (especially fibrillar aggregates), structure-specific antibodies that help identify and control the state of amyloidogenic protein aggregates have been developed in the past decade. In a study by Glabe [76] have developed three conformation-specific antibodies important for the detection of physiologically relevant fibrillar aggregates: A11 (recognizing fibrillar oligomers but not fibrillar conformers) and OC (fibrillar oligomers, fibrillar conformers) [77]. These conformation-specific antibodies have the inhibitory ability of Aβ aggregation modulators, inhibition of toxic A11-reactive Aβ aggregation formation by diamond blue G (BBG), and low molecular weight inhibitor [78]. Although the application of fibrillar protein aggregates has provided an important understanding of the properties of fibrillar protein aggregates and the effectiveness of potential therapeutics, recent studies suggest caution should be exercised in the use and interpretation of results. First, due to the transient nature of the pre-fibrillar aggregates compared to the final-state conformers, it is very difficult to prepare homogeneous samples of pre-fibrillar aggregates that react exclusively with A11, OC, or αAPF (no cross-reactivity) *in vitro* [79]. It has proven difficult. Preparation of homogeneous prefibrillar aggregates. Second, when testing the inhibitory/modulatory activity of foreign compounds on protein aggregates in several study groups, false-positive antibody reactivity was observed in some cases. Because of these two factors, care must be taken when designing experiments and interpreting the results of these antibodies [72].

Direct observation of amyloid plaques *in vivo* is also used as a diagnostic tool for protein aggregation. Although this direct observation is attractive for clinical use, it is not routinely practiced. Technologies such as ELISA, magnetic resonance imaging (MRI), positron emission tomography (PET), and diffusion tensor imaging are being developed for the direct diagnosis of amyloid plaques based on visual inspection of enhanced images [80, 81]. However, all these methods are based solely on a qualitative approach and rely on the detection of visible changes in the central nervous system. Although some work has been done to quantify amyloid load in PET image analysis, the results are very limited. More recent advances in MRI are primarily based on the use of nanoparticles to localize plaques [82, 83]. For example, the use of magnetic nanoparticles bound to curcumin or hollow manganese oxide nanoparticles bound to specific antibodies. These two nanoparticle methods increase the specificity and sensitivity of the method to protein aggregates. However, these approaches are not routinely used and may not meet the need for diagnosis before irreversible tissue damage occurs [68].

7. Conclusion

Protein misfolding is the cause of many diseases, and new discoveries about protein misfolding have led to the study of another aspect of protein misfolding described as self-aggregation or self-activation. Various diagnostic approaches have been used to

detect protein aggregates *in vitro* and in living cells. Traditional methods, dye-binding assays, TEM, CD, and FTIR analysis, have been widely used to monitor amyloid fibril formation *in vitro*. Recently, AFM and dot blot assays using conformation-specific antibodies have been used to characterize physiologically important pro fibrillar protein aggregates. A limitation of diagnostic techniques for dye-binding assays is the inadequate detection of prefibrous oligomers by current dyes. Lack of biomarkers and antibodies in protein aggregate detection prohibits prompt diagnosis of conditions relative to protein misfolding. Therefore, as discussed the main theme in therapeutic approach for misfolding of proteins relies on most effective procedure for early diagnosis and understanding the fundamental mechanisms of protein aggregation. Chaperone-related therapeutic measures are being explored for treatment of protein misfolding diseases. Also, the ubiquitin protease system and unfolded protein responses are being explored molecularly to achieve new insight into misfolding of proteins.

Authors' contributions

Dr. Deepika Lather, Dr. Vikas Nehra has contributed toward the design, proper arrangement, and sectioning of the review topic. Dr. Babulal Jangir contributed in recent approaches and diagnostics in protein misfolding diseases. Diksha Kandpal has reviewed the articles and data available and written and compiled the manuscript.

Funding

No funding received.

Competing interests

Authors declare that there are no competing interests.

Ethical approval

No ethical approval needed as it is a review-based article.

Availability of data and materials

No data available.

Author details

Diksha Kandpal*, Deepika Lather, Vikas Nehra and Babulal Jangir
College of Veterinary Sciences, Lala Lajpat Rai University of Veterinary and Animal
Sciences, Hisar, Haryana, India

*Address all correspondence to: diksha.kandpal@gmail.com

IntechOpen

References

[1] Cuanalo-Contreras K, Mukherjee A, Soto C. Role of protein misfolding and proteostasis deficiency in protein misfolding diseases and aging. International Journal of Cell Biology. 2013;**2013**:638083

[2] Sanvictores T, Farci F. Biochemistry, Primary Protein Structure. Treasure Island, FL: StatPearls Publishing; 2020

[3] Gianni S, Guydosh NR, Khan F, Caldas TD, Mayor U, White GW, et al. Unifying features in protein-folding mechanisms. Proceedings of the National Academy of Sciences. 2003;**100**(23):13286-13291

[4] Roshni KG. Protein folding, misfolding, and coping mechanism of cells—A short discussion. Open Journal of Cell Protein and Science. 2021;**4**(1):001-004. DOI: 10.17352/ojcps, 4

[5] Lin JC, Liu HL. Protein conformational diseases: From mechanisms to drug designs. Current Drug Discovery Technologies. 2006;**3**(2):145-153

[6] Goloubinoff P. Recent and future grand challenges in protein folding, misfolding, and degradation. Frontiers in Molecular Biosciences. 2014;**1**:1

[7] Denny RA, Gavrin LK, Saiah E. Recent developments in targeting protein misfolding diseases. Bioorganic & Medicinal Chemistry Letters. 2013;**23**(7):1935-1944

[8] Bross P, Corydon TJ, Andresen BS, Jørgensen MM, Bolund L, Gregersen N. Protein misfolding and degradation in genetic diseases. Human Mutation. 1999;**14**(3):186-198

[9] Zaman M, Khan AN, Zakariya SM, Khan RH. Protein misfolding, aggregation and mechanism of amyloid cytotoxicity: An overview and therapeutic strategies to inhibit aggregation. International Journal of Biological Macromolecules. 2019;**134**:1022-1037

[10] Englander SW, Mayne L. The nature of protein folding pathways. Proceedings of the National Academy of Sciences. 2014;**111**(45):15873-15880

[11] Fersht AR. Optimization of rates of protein folding: The nucleation-condensation mechanism and its implications. Proceedings of the National Academy of Sciences. 1995;**92**(24):10869-10873

[12] Kukic P, Pustovalova Y, Camilloni C, Gianni S, Korzhnev DM, Vendruscolo M. Structural characterization of the early events in the nucleation–condensation mechanism in a protein folding process. Journal of the American Chemical Society. 2017;**139**(20):6899-6910

[13] Nölting B, Agard DA. How general is the nucleation–condensation mechanism? Proteins: Structure, Function, and Bioinformatics. 2008;**73**(3):754-764

[14] Valastyan JS, Lindquist S. Mechanisms of protein-folding diseases at a glance. Disease Models & Mechanisms. 2014;**7**(1):9-14

[15] Baldwin RL. The nature of protein folding pathways: The classical versus the new view. Journal of Biomolecular NMR. 1995;**5**(2):103-109

[16] Matthews CR. Pathways of protein folding. Annual Review of Biochemistry. 1993;**62**(1):653-683

[17] Hartl FU, Hayer-Hartl M. Molecular chaperones in the cytosol: From nascent

chain to folded protein. Science. 2002;**295**(5561):1852-1858

[18] Chaturvedi SK, Siddiqi MK, Alam P, Khan RH. Protein misfolding and aggregation: Mechanism, factors and detection. Process Biochemistry. 2016;**51**(9):1183-1192

[19] Kundu D, Prerna K, Chaurasia R, Bharty MK, Dubey VK. Advances in protein misfolding, amyloidosis and its correlation with human diseases. 3 Biotech. 2020;**10**(5):1-22

[20] Morales R, Moreno-Gonzalez I, Soto C. Cross-seeding of misfolded proteins: Implications for etiology and pathogenesis of protein misfolding diseases. PLoS Pathogens. 2013;**9**(9):e1003537

[21] Chaudhuri TK, Paul S. Protein-misfolding diseases and chaperone-based therapeutic approaches. The FEBS Journal. 2006;**273**(7):1331-1349

[22] Soto C, Estrada L, Castilla J. Amyloids, prions and the inherent infectious nature of misfolded protein aggregates. Trends in Biochemical Science. 2006;**31**(3):150-155

[23] Dobson CM. Protein misfolding, evolution and disease. Trends in Biochemical Sciences. 1999;**24**(9):329-332

[24] Huang Q, Figueiredo-Pereira ME. Ubiquitin/proteasome pathway impairment in neurodegeneration: Therapeutic implications. Apoptosis. 2010;**15**(11):1292-1311

[25] Lecker SH, Goldberg AL, Mitch WE. Protein degradation by the ubiquitin–proteasome pathway in normal and disease states. Journal of the American Society of Nephrology. 2006;**17**(7):1807-1819

[26] Ciechanover A, Schwartz AL. The ubiquitin-proteasome pathway: The complexity and myriad functions of proteins death. Proceedings of the National Academy of Sciences. 1998;**95**(6):2727-2730

[27] Ciechanover A. The ubiquitin–proteasome pathway: On protein death and cell life. The EMBO Journal. 1998;**17**(24):7151-7160

[28] Menzies FM, Moreau K, Rubinsztein DC. Protein misfolding disorders and macroautophagy. Current Opinion in Cell Biology. 2011;**23**(2):190-197

[29] Gandhi J, Antonelli AC, Afridi A, Vatsia S, Joshi G, Romanov V, et al. Protein misfolding and aggregation in neurodegenerative diseases: A review of pathogeneses, novel detection strategies, and potential therapeutics. Reviews in the Neurosciences. 2019;**30**(4):339-358

[30] Ciechanover A, Kwon YT. Protein quality control by molecular chaperones in neurodegeneration. Frontiers in Neuroscience. 2017;**11**:185

[31] Hartl FU, Bracher A, Hayer-Hartl M. Molecular chaperones in protein folding and proteostasis. Nature. 2011;**475**(7356):324-332

[32] Saibil H. Chaperone machines for protein folding, unfolding and disaggregation. Nature Reviews Molecular Cell Biology. 2013;**14**(10):630-642

[33] Grantcharova V, Alm EJ, Baker D, Horwich AL. Mechanisms of protein folding. Current Opinion in Structural Biology. 2001;**11**(1):70-82

[34] Barral JM, Broadley SA, Schaffar G, Hartl FU. Roles of molecular chaperones in protein misfolding diseases. In: Seminars in Cell & Developmental Biology. Vol. 15, No. 1. UK: Academic Press; 2004. pp. 17-29

[35] Amm I, Sommer T, Wolf DH. Protein quality control and elimination of protein waste: The role of the ubiquitin–proteasome system. Biochimica et Biophysica Acta (BBA)-Molecular Cell Research. 2014;**1843**(1):182-196

[36] Sweeney P, Park H, Baumann M, Dunlop J, Frydman J, Kopito R, et al. Protein misfolding in neurodegenerative diseases: Implications and strategies. Translational Neurodegeneration. 2017;**6**(1):1-13

[37] Nakamura T, Lipton SA. Cell death: Protein misfolding and neurodegenerative diseases. Apoptosis. 2009;**14**(4):455-468

[38] Bellotti V, Stoppini M. Protein misfolding diseases. The Open Biology Journal. 2009;**2**(1):228-234

[39] Moreno-Gonzalez I, Soto C. Misfolded protein aggregates: Mechanisms, structures and potential for disease transmission. In: Seminars in Cell & Developmental Biology. Vol. 22, No. 5. UK: Academic Press; 2011. pp. 482-487

[40] Chiti F, Dobson CM. Protein misfolding, amyloid formation, and human disease: A summary of progress over the last decade. Annual Review of Biochemistry. 2017;**86**:27-68

[41] Bucciantini M, Giannoni E, Chiti F, Baroni F, Formigli L, Zurdo J, et al. Inherent toxicity of aggregates implies a common mechanism for protein misfolding diseases. Nature. 2002;**416**(6880):507-511

[42] Winklhofer KF, Tatzelt J, Haass C. The two faces of protein misfolding: Gain-and loss-of-function in neurodegenerative diseases. The EMBO Journal. 2008;**27**(2):336-349

[43] Hartl FU. Protein misfolding diseases. Annual Review of Biochemistry. 2017;**86**:21-26

[44] Bernardi L, Bruni AC. Mutations in prion protein gene: Pathogenic mechanisms in C-terminal vs. N-terminal domain, a review. International Journal of Molecular Sciences. 2019;**20**(14):3606

[45] Poggiolini I, Saverioni D, Parchi P. Prion protein misfolding, strains, and neurotoxicity: An update from studies on mammalian prions. International Journal of Cell Biology. 2013;**2013**:910314

[46] Knowles TP, Vendruscolo M, Dobson CM. The amyloid state and its association with protein misfolding diseases. Nature Reviews Molecular Cell Biology. 2014;**15**(6):384-396

[47] Soto C, Pritzkow S. Protein misfolding, aggregation, and conformational strains in neurodegenerative diseases. Nature Neuroscience. 2018;**21**(10):1332-1340

[48] Kupfer L, Hinrichs W, Groschup MH. Prion protein misfolding. Current Molecular Medicine. 2009;**9**(7):826-835

[49] Morales R, Estrada LD, Diaz-Espinoza R, Morales-Scheihing D, Jara MC, Castilla J, et al. Molecular cross talk between misfolded proteins in animal models of Alzheimer's and prion diseases. Journal of Neuroscience. 2010;**30**(13):4528-4535

[50] Norrby E. Prions and protein-folding diseases. Journal of Internal Medicine. 2011;**270**(1):1-14

[51] Cassmann ED, Greenlee JJ. Pathogenesis, detection, and control of scrapie in sheep. American Journal of Veterinary Research. 2020;**81**(7):600-614

[52] Murakami T, Ishiguro N, Higuchi K. Transmission of systemic AA amyloidosis in animals. Veterinary Pathology. 2014;**51**(2):363-371

[53] Imran M, Mahmood S. An overview of animal prion diseases. Virology Journal. 2011;**8**(1):1-8

[54] Woldemeskel M. A concise review of amyloidosis in animals. Veterinary Medicine International. 2012:1-12

[55] Picken MM. The pathology of amyloidosis in classification: A review. Acta Haematologica. 2020;**143**(4):322-334

[56] Butler JS, Loh SN. Folding and misfolding mechanisms of the p53 DNA binding domain at physiological temperature. Protein Science. 2006;**15**(11):2457-2465

[57] Mantovani F, Collavin L, Del Sal G. Mutant p53 as a guardian of the cancer cell. Cell Death & Differentiation. 2019;**26**(2):199-212

[58] Coulombe PA, Lee CH. Defining keratin protein function in skin epithelia: Epidermolysis bullosa simplex and its aftermath. Journal of Investigative Dermatology. 2012;**132**(3):763-775

[59] Shinkuma S, McMillan JR, Shimizu H. Ultrastructure and molecular pathogenesis of epidermolysis bullosa. Clinics in Dermatology. 2011;**29**(4):412-419

[60] Coulombe PA, Kerns ML, Fuchs E. Epidermolysis bullosa simplex: A paradigm for disorders of tissue fragility. The Journal of Clinical Investigation. 2009;**119**(7):1784-1793

[61] Greene CM, McElvaney NG. Protein misfolding and obstructive lung disease. Proceedings of the American Thoracic Society. 2010;**7**(6):346-355

[62] Bradley KL, Stokes CA, Marciniak SJ, Parker LC, Condliffe AM. Role of unfolded proteins in lung disease. Thorax. 2021;**76**(1):92-99

[63] Dersh D, Iwamoto Y, Argon Y. Tay–Sachs disease mutations in HEXA target the α chain of hexosaminidase A

to endoplasmic reticulum–associated degradation. Molecular Biology of the Cell. 2016;**27**(24):3813-3827

[64] Díaz-Villanueva JF, Díaz-Molina R, García-González V. Protein folding and mechanisms of proteostasis. International Journal of Molecular Sciences. 2015;**16**(8):17193-17230

[65] Banerjee PR, Pande A, Shekhtman A, Pande J. Molecular mechanism of the chaperone function of mini-α-crystallin, a 19-residue peptide of human α-crystallin. Biochemistry. 2015;**54**(2):505-515

[66] Moreau KL, King JA. Protein misfolding and aggregation in cataract disease and prospects for prevention. Trends in Molecular Medicine. 2012;**18**(5):273-282

[67] Markossian KA, Yudin IK, Kurganov BI. Mechanism of suppression of protein aggregation by α-crystallin. International Journal of Molecular Sciences. 2009;**10**(3):1314-1345

[68] Strømland Ø, Jakubec M, Furse S, Halskau Ø. Detection of misfolded protein aggregates from a clinical perspective. Journal of Clinical and Translational Research. 2016;**2**(1):11

[69] Ramirez-Alvarado M, Kelly JW, Dobson CM, editors. Protein Misfolding Diseases: Current and Emerging Principles and Therapies. Vol. 14. New Jersey, USA: John Wiley & Sons; 2010

[70] Reinke A, Gestwicki JE. Structure-activity relationships of amyloid beta-aggregation inhibitors based on curcumin: Influence of linker length and flexibility. Chemical Biology & Drug Design. 2007;**70**:206. [PubMed: 17718715]

[71] Hudson S, Ecroyd H, Kee TW, Carver J. The thioflavin T fluorescence

assay for amyloid fibril detection can be biased by the presence of exogenous compounds. The FEBS Journal. 2009;**276**:5960. [PubMed: 19754881]

[72] Gregoire S, Irwin J, Kwon I. Techniques for monitoring protein misfolding and aggregation in vitro and in living cells. Korean Journal of Chemical Engineering. 2012;**29**(6):693-702

[73] Hawe A, Sutter M, Jiskoot W. Extrinsic fluorescent dyes as tools for protein characterization. Pharmaceutical Research. 2008;**25**:1487. [PubMed: 18172579]

[74] Ladiwala ARA, Dordick JS, Tessier PM. Aromatic small molecules remodel toxic soluble oligomers of amyloid beta through three independent pathways. The Journal of Biological Chemistry. 2011;**286**:3209. [PubMed: 21098486]

[75] Hadley KC, Borrelli MJ, Lepock JR, McLaurin J, Croul SE, Guha A, et al. Multiphoton ANS fluorescence microscopy as an *in vivo* sensor for protein misfolding stress. Cell Stress and Chaperones. 2011;**16**(5):549-561

[76] Glabe CG. Structural classification of toxic amyloid oligomers. The Journal of Biological Chemistry. 2008;**283**:29639. [PubMed: 18723507]

[77] Kayed R, Head E, Thompson JL, McIntire TM, Milton SC, Cotman CW, et al. Common structure of soluble amyloid oligomers implies common mechanism of pathogenesis. Science (New York, N.Y.). 2003;**300**:486

[78] Kayed R, Head E, Sarsoza F, Saing T, Cotman CW, Necula M, et al. Fibril specific, conformation dependent antibodies recognize a generic epitope common to amyloid fibrils and fibrillar oligomers that is absent in prefibrillar oligomers. Molecular Neurodegeneration. 2007;**2**:18. [PubMed: 17897471]

[79] Wong HE, Qi W, Choi HM, Fernandez EJ, Kwon I. ACS Chemical Neuroscience. 2011;**2**:645. [PubMed: 22860159]

[80] Chen S, Svedendahl M, Antosiewicz TJ, Kall M. Plasmon-enhanced enzyme-linked immunosorbent assay on large arrays of individual particles made by electron beam lithography. ACS Nano. 2013;**7**(10):8824-8832

[81] Schmidt ME, Chiao P, Klein G, Matthews D, Thurfjell L, Cole PE, et al. The influence of biological and technical factors on quantitative analysis of amyloid PET: Points to consider and recommendations for controlling variability in longitudinal data. Alzheimer's & Dementia. 2015;**11**(9):1050-1068

[82] Cheng KK, Chan PS, Fan S, Kwan SM, Yeung KL, Wang YXJ, et al. Curcumin-conjugated magnetic nanoparticles for detecting amyloid plaques in Alzheimer's disease mice using magnetic resonance imaging (MRI). Biomaterials. 2015;**44**:155-172

[83] Kim JH, Ha TL, Im GH, Yang J, Seo SW, Lee IS, et al. Magnetic resonance imaging of amyloid plaques using hollow manganese oxide nanoparticles conjugated with antibody aβ1-40 in a transgenic mouse model. Neuroreport. 2013;**24**(1):16-21

Chapter 4

New Studies on the Gaits Displayed by Miocene, Pliocene, and Pleistocene Fossil Horse Trackways

Elise Renders and Alan Vincelette

Abstract

The authors here apply a refined methodology to determine the gaits of fossil equids. Miocene trackways of *Cremohipparion* near Jumilla, Spain, contain three sets of tracks of equids trotting at around 2.9–3.4 m/s, crossed by another three sets of tracks of perhaps younger equids at play galloping at around 5.2–5.6 m/s. Other Miocene trackways include three sets of *Hippotherium* near Osoppo, Italy, galloping at around 6.2–6.5 m/s, and one of *Scaphohippus* from Barstow, California, in the United States, likely engaged in a rack (or less likely a trot) at 2.1 m/s. Pliocene trackways include one *Hipparion* near Elche, Spain, trotting at around 3.5 m/s, and three trackways of *Eurygnathohippus* from Laetoli, Tanzania, of equids racking (with one perhaps engaged in a running walk) at around 2.1–3.1 m/s, including tracks of what is likely a foal being supervised by its mare. Finally, a Pleistocene trackway of *Equus* near Cardston, Alberta, Canada, shows a horse in a gallop at around 6.6 m/s. Hence, Miocene to Pleistocene fossil trackways reveal that equids in the past possessed standard gaits (trot, gallop) as well as alternative lateral gaits (rack), and had similar herding behaviors found in modern horses today.

Keywords: horse gaits, fossil horses, equids, horse trackways, mammal behavior, mammal locomotion

1. Introduction

Quadrupedal gaits have been variously classified in terms of symmetry (i.e. symmetrical gaits wherein the motion of the limbs on one side of the animal is mirrored by the motion on the other side, versus asymmetrical gaits where it is not); temporal foot sequence (i.e. lateral sequence wherein the sequence of limbs lifting off the ground is left hind-left front-right hind-right front versus diagonal sequence wherein the sequence of limbs is left hind-right front-right hind-left front); temporal couplet pairings (i.e. lateral-couplet wherein the ipsilateral pairs of limbs land closer together in time versus diagonal couplet wherein the diagonal pairs of limbs land closer together in time); coordination of limbs (i.e. laterally coordinated gaits wherein ipsilateral limb pairs move forward together in unison or near unison,

versus diagonally coordinated gaits wherein diagonal limb pairs do so, versus square gaits wherein each limb moves more or less independently); and beats (i.e. two-beat gaits with ipsilateral or diagonal limb pairs contacting the ground close together, versus three-beat gaits involving a hind limb pair contacting the ground followed by independent front limbs contacts, and four-beat gaits wherein all four limbs contact the ground independently). For more on the classification of quadrupedal gaits see [1–7].

The slower gaits are four-beat walking gaits. They are symmetrical, involve a pendulum-like action of swinging legs wherein all four limbs operate relatively independently of each other (i.e. square), lack suspended phases (i.e. have a duty factor above 0.50 as hind limbs are on the ground for more than 50% of the stride cycle), and possess alternating three- and two-limb support structures. Such walks may be lateral-sequence diagonal-couplet (as in salamanders and hedgehogs), diagonal-sequence diagonal-couplet (as in crocodilians and primates), or lateral-sequence (ipsi)lateral-couplet (as in carnivores and ungulates). Most medium-speed gaits have periods of suspension wherein all four limbs are off the ground at the same time (and so possess a duty factor of less than 0.50), and are two-beat gaits that involve coordination of ipsilateral or diagonal limbs with bouncing or spring-like mechanics. The diagonally coordinated trot, with a two-limb diagonal support structure and diagonal couplets, is the medium-speed gait of most quadrupeds. A few quadrupeds, such as camels, employ the ipsilaterally coordinated pace, with a two-limb ipsilateral support structure and ipsilateral couplets. The fastest gaits are asymmetrical and involve the coordination of contralateral legs operating in a leaping and strut-like manner, with extensive periods of four-limb suspension. If all four limbs are employed together we have the pronk or stott common to antelopes; if the contralateral hind limbs are employed in unison we have the bound (half or full) of rabbits; and finally if the contralateral hind limbs are employed sequentially then we have the gallop, either transverse as in ungulates with hind and fore legs mirroring each other, or rotary as in carnivores without such mirroring [2–4, 8–13].

Among mammals, horses possess one of the most diverse gait-sets so-far known [5, 6, 14, 15]. Various breeds have been observed employing 14 out of around 17 major quadrupedal gaits [2, 3, 13, 14]. Not only do horses utilize the standard square four-beat lateral-sequence lateral-couplet walk, along with the diagonally coordinated two-beat diagonal-sequence diagonal-couplet trot, and the asymmetrical three-beat canter and transverse four-beat gallop (with a footfall sequence of left hind-right hind-left front-right front), but select breeds can also employ more unusual gaits. For example, the diagonally coordinated lateral-sequence diagonal-couplet walk (fox walk) and two-beat lateral-sequence diagonal-couplet trot (fox trot) are found in the Missouri Fox Trotter and Walkaloosa [16]. Also occurring are intermediate speed laterally coordinated gaits including the paso corto and paso largo of the Paso Fino Horse [17], the running walk (four-beat) and stepping pace (two-beat) of the Tennessee Walking Horse, the four-beat rack of the American Saddlebred and related tölt of the Icelandic Horse, and the two-beat pace of the Icelandic and Standardbred [18, 19]. Horses also on occasion utilize the asymmetrical rotary gallop (for quick initial bursts) with a footfall sequence of right hind-left hind-left front-right front, the asymmetrical half bound leap (for jumping over obstacles or in the ring) off the back pair of legs, as well as the even more unusual stott (in the ring or when startled) wherein a horse leaps into the air with all 4 ft employed simultaneously as in the Lipizzaner [2, 3, 13, 14].

Traditionally the square lateral-sequence lateral-couplet walk, the diagonally coordinated trot, the asymmetrical gallop, and sometimes the asymmetrical canter,

were considered to be the natural gaits of the horse whereas the laterally coordinated pace, rack, fox trot, and running walk were considered to be "artificial" gaits as they did not occur in all horse breeds and were not always spontaneously expressed in those breeds in which they did occur. It was thus hypothesized that such gaits were introduced by humans, either through breeding or training. For example, Hildebrand, one of the pioneers in the study of animal gaits, wrote that the horse, on account of the training provided by humans, "has learned to be versatile in the selection of gaits and also to use gaits (termed artificial) that are unnatural to the species and unique to itself" ([14], p. 701). Such a view was perhaps influenced by the words of Muybridge [20] who claimed of the rack that "It is an unnecessary and unnatural gait of the horse, and it is scarcely probable that the ancients trained the animal to its use." And more recently the abstract of a study on Tennessee Walking Horse gait genetics implied the running walk's recent development, stating "Following domestication, man selected the horse primarily for the purpose of transportation rather than consumption; this selective strategy created divergent traits for locomotion" ([21], p. 1377).

Be that as it may, there is now solid evidence from fossil horse trackways that ipsilaterally coordinated four-beat running gaits including the rack and perhaps running walk occurred in extinct horse lineages [22–25]. There is also literary and artistic evidence of the presence of lateral gaits in ancient horses. For example, Pliny the Elder, in his *Naturalis historia* 8.57 of 77 CE, talks of theldones [Asturcón] horses from the Asturias of Northern Spain that had an easy gait involving ipsilateral pairs of legs moving in unison [mollis alterno crurum explicatu glomeratio]. In addition, the famous Flying Horse of Gansu statue (ca. 220 CE) and various reliefs from the Chinese Han dynasty show horses in lateral gaits, and a Turkestan painting from ca. 700 CE shows a horse and camel pacing side by side ([18, 26], pp. 291–306; [27]). Hence the nature and occurrence of lateral "artificial" or what we now prefer to call altenative lateral gaits in horses in the present and past is well worth exploring.

We have previously examined contemporary horse gaits and the tracks they leave behind and have employed them to determine the gaits displayed by fossil horses [22–25]. We here refine our methodology and apply it to the study of fossil horse trackways found to be gaitable, i.e. trackways of single individuals with a series of four or more prints.

2. Materials and methods

Previously published photos, diagrams, and data regarding the footprints left by fossil horses were examined in order to isolate or estimate these key linear kinematic values and footprint patterns for fossil horse trackways [22–25, 28–32]. In particular, data from the following 15 trackways were examined: GQ-1 from the Rainbow Basin, Barstow, California of 14.5 Ma ([25], p. 162, Table 5, and p. 163, Figure 5; as well as new material presented below); HSA-9, HSA-10, HSA-11, HSA-12, HSA-13, and HSA-14 from the Hoya de la Sima site in the Jumilla-Ontur Basin near Jumilla, Murcia, Spain formed around 8.7–7.8 Ma ([33], p. 260, Figure 3, p. 263, Table 1, and pp. 264–265); OS-3, OS-4, and OS-5 from Colle di Osoppo, Osoppo, Italy of ca. 6.0–5.3 Ma ([28], p. 225, Figure 4, and pp. 229–230, Tables 1–3 and 6–8); SC-1 from the Sierra del Colmenar section of the Bajo Segura Basin, outside of Elche, Spain formed 4.9–4.2 Ma ([29], p. 12, Figure 2); LAET-A, LAET-B, and LAET-C from Site G in the Upper Laetoli beds of Tanzania from 3.7 Ma ([22], pp. 472–473, Tables 12.5–12.8,

pp. 476–477, Figures 12.16 and 12.17); and WB-1 from the Wally's Beach deposit at St. Mary's Reservoir, Cardston, Canada formed more recently around 13,000–11,000 years ago ([30], p. 218, Figure 16).

Key linear parameters and ratios were recorded from the data, sketches, and descriptions of the fossil horse trackways, as were the footprint patterns found therein. Based upon our previous work on modern horse gaits [7, 23–25, 34], and further refined here, the key linear kinematic parameters, ratios, and footprint patterns useful for the determination of horse gaits are as follows (definitions modified from [35]; see **Figure 1**).

Footprint width (FW): Greatest distance in centimeters across the middle portion of the hoof impression taken perpendicular to direction of travel (akin to greatest measurement across quarters, or central portion, of hoof).

Footprint length (FL): Distance in centimeters between anterior and posterior edges of hoof impression taken parallel to direction of travel (akin to measurement between toe and heel of hoof).

Stride length or cycle length (SL): Distance in meters between the anterior portion (i.e. toe of hoof) of successive footprints of the same foot parallel to the orientation of the trackway (ideally between left hind impressions if possible). The stride length tends to increase as a gait gets faster.

Stride length/horse height ratio (SL/H): Dimensionless speed ratio found by dividing stride length by horse height at the withers. As gaits get faster this number
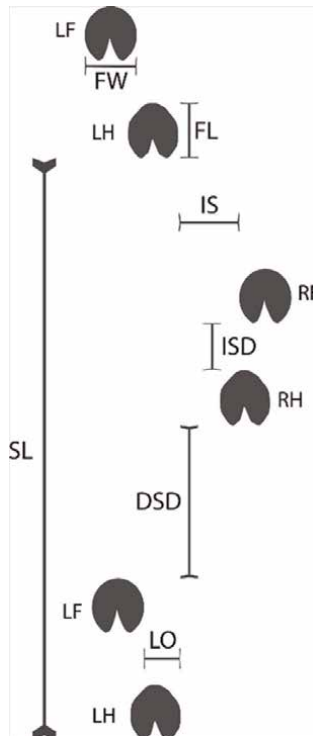

Figure 1.
Measurements taken of horse trackway (LH = left hind; LF = left front; RH = right hind; RF = right front). FW = footprint width; F = footprint length; ISD = ipsilateral step distance; DSD = diagonal step distance; LO = lateral offset. IS = interior straddle; and SL = stride length.

increases. In walking gaits this value is usually less than 1.0, between 1.0 and 2.0 in intermediate speed gaits, while in very fast gaits it can be above 2.0.

Distance between diagonal steps (DSD): Measurement in centimeters between anterior (i.e. toe) and posterior (i.e. heel) edges of contralateral front and hind hoof prints parallel to the orientation of the trackway.

Distance between ipsilateral steps (ISD): Measurement in centimeters between anterior (i.e. toe) and posterior (i.e. heel) edges of ipsilateral front and hind hoof prints parallel to the orientation of the trackway.

Ipsilateral step distance [overstep; overstrike]/Stride length ratio (ISD/SL): Distance between ipsilateral steps divided by the stride length. The ipsilateral overstep [overstrike] can reach as high as 15–30% in fast ipsilaterally coordinated gaits.

Diagonal/Ipsilateral step distance ratio (DSD/ISD): Distance between diagonal steps divided by distance between ipsilateral steps. This value is above 0.5 in square gaits, but increasingly lower than 0.5 in laterally coordinated gaits, and exceeds 1.0 in diagonally coordinated gaits.

Symmetry between diagonal and ipsilateral steps ([DSD1/DSD2 + ISD1/ISD2]/2): ½ × (diagonal step distance 1/diagonal step distance 2) + (ipsilateral step distance 1/ipsilateral step distance 2).

Average interior straddle (IS) [gauge]: Average distance in centimeters between quarters of contralateral front and hind hoof prints measured perpendicular to the orientation of the trackway. In the walk and running walk this value is typically positive but in gaits with high-lateral coordination the hind limbs are free to come in or cross the centerline without interference and so this value is often negative.

Interior straddle/hind hoof width (IS/HW): Ratio of average interior straddle divided by average hind hoof width. This value is negative in fast laterally-coordinated gaits such as the rack and pace, around zero in slow walks and trots, and positive in fast walks and trots.

Average foot pair lateral offset (LO): Average distance in centimeters between quarters of closest hoof print pairs whether formed by ipsilateral, diagonal, or contralateral front or contralateral hind measured perpendicular to the orientation of the trackway. This value is low when ipsilateral pairs of feet are close together but high when diagonal pairs are close together.

Foot pair LO/FW: Ratio of average foot pair lateral offset divided by average width of hoof print at quarters. This value is high for gaits with diagonal pairs landing close together in space but low for gaits with lateral pairs landing close together in space.

Angle of hoof impression (HA): Though we did not incorporate this data here as more study is needed, we also recommend measuring the angle each hoof impression makes (line drawn between anterior (toe) center and anterior (heel) posterior margins of hoof impression) in relation to a line drawn parallel to the orientation of the trackway. If 3D image generating software is available and made use of (which would be ideal) it would also be advisable to record any angle of deviation from the horizontal the hoof makes. This may yield important data allowing discrimination of gaits in the future or showing aspects of conformation, slippage, or change of direction.

The first key step in determining the gaits displayed by fossil horses is to determine the footfall sequence found in these trackways, and for this purpose it is necessary to distinguish fore feet (manus) from hind feet (pes). This is possible for modern and fossil horses as from the Miocene onward the front hooves of horses tend to be wider, more isometric (with a length/width ratio closer to 1.00) and circular in shape, and rounder at the tip, whereas the hind hooves tend to be narrower, less isometric and more oval in shape, and possess a more pointed tip (see **Figure 2** below; see [7]).
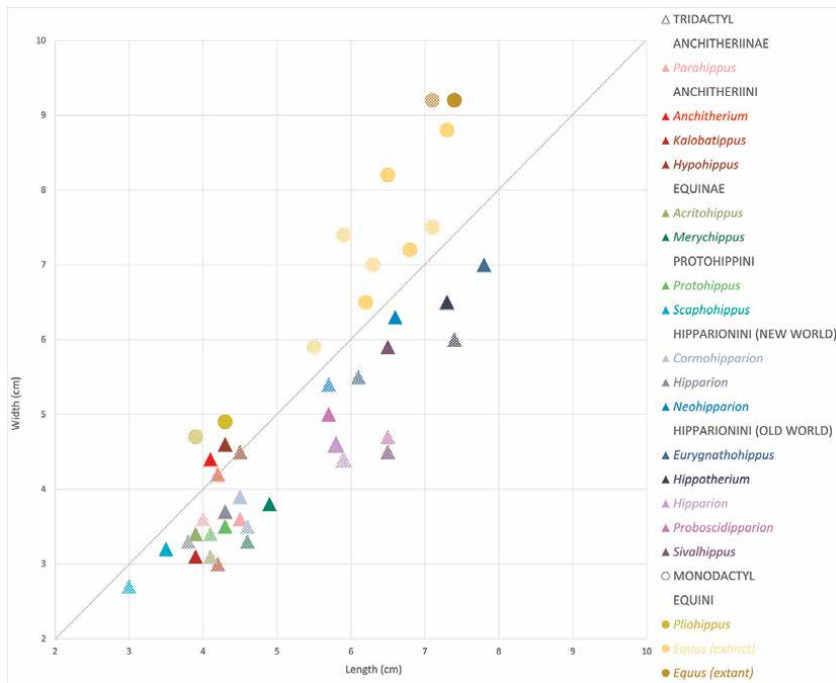
Figure 2.
Bivariate plot of length vs. width for central ungual phalanx (3PhIII) of fossil equids with isometric line. Hooves above line are wider than long (common in monodactyl species) and hooves below line are longer than wide (common in tridactyl species). Front hooves (manus) are solid in color while hind hooves (pes) are cross hatched.

The second key step for the determination of horse gait from tracks is estimation of the height (at withers) of the horse that made the tracks. This is difficult as one does not always know the species, age, gender, genetics, or development of the trackmaker. This is why trackway data is important, especially the size of the front hoof print. Still correlation of hoof size with horse height is lower (0.41) than that of a correlation of other skeletal elements such as the skull (0.83–91), metacarpal (0.90–0.95), metatarsal (0.87–0.91), and phalanges (0.81–0.91) (see [34, 36–40]). Moreover, the allometric ratios of the different limb bones can vary from one species to another [41–43] and this can affect height estimations. For these reasons, we believe that height of the trackmaker is best estimated by combining data from horse trackways and associated horse species osteology, giving 50% of the weight to the tracks themselves as they are the primary known factor about the print maker, a print maker whose species is a matter of some inference and whose population height can be variable, then giving 25% weight to the skull (if available) which correlates well with the size of fossil horses, and finally giving 25% weight to the other postcranial elements that closely correlate with overall height such as the metacarpal, metatarsal, proximal phalanx, and distal phalanx. This method allows different lines of evidence to estimate print-maker height in cases when the exact size and body ratios in relation to height are unknown for the printmaker.

After determining the measurements of the front hoof track, as well as associated skeletal elements such as the skull, metacarpal, metatarsal, and phalanges, it is necessary to multiply these values height estimation multipliers appropriate to the fossil

horse tribe or grouping. We have calculated such multipliers elsewhere based upon heights of fossil horse species with complete skeletons, thereby arriving at multipliers for the different fossil horse subfamilies and tries including: Eocene subfamilies Propalaeotheriinae and Hyracotheriinae; the Oligocene subfamily Anchitheriinae; the late Miocene tribe Hipparionini; the Pliocene and Pleistocene tribe Equini; as well as the paraphyletic early Miocene merychippine group consisting of the genera *Acritohippus*, *Merychippus*, and *Scaphohippus* [7]. We also developed scaled hoof height estimation multipliers based upon known values in the modern horse where height at withers is 13.16 times size of front hoof [40] and 21.62 the size of the front distal phalanx or coffin bone. For these multiplier values see Appendix A **Table A1** (as well as [7]). Assuming then the species of the trackmaker can be determined, the following formula is ideal (if not one is forced to rely on trackway data alone):

$$0.25(\text{CL} \times \text{CLMs}) \times$$

$$0.25[(\text{MT} \times \text{MTMs}) + (\text{MC} \times \text{MCMs}) + (\text{1P3} \times \text{1P3Ms}) + (\text{3P3} \times \text{3P3Ms})]/4) \times$$

$$0.50(\text{FFL} \times \text{FFLMs}) \tag{1}$$

where CL = maximal skull length measured from the tip of the incisive bone to the nuchal crest; MT = greatest metatarsal III length, MC = greatest metacarpal III length, 1P3 = greatest proximal phalanx III length, 3P3 = greatest distal phalanx III length; FFL = front footprint length, and CLM, MTM, MCM, 1P3M, 3P3M, and FFLM are the multipliers for the matching fossil horse groupings (s).

With the footfall pattern determined and height of trackmaker estimated one can then reconstruct the gait of the trackmaker using five key linear track ratios (see **Table 1**): Step symmetry calculation (SS), stride length/horse height (SL/HT), interior straddle/hind hoof width (IS/HW), ipsilateral step distance/stride length (ISD/SL), and diagonal/ipsilateral step distance (DSD/ISD). The first three taken together distinguish asymmetrical from symmetrical gaits, and the latter three distinguish symmetrical gates. This can be seen by through Principal Component Analysis (see **Figure 3**). Based upon dimensionless speed, gaits are separated into slow walks (SL/HT = 0.78–1.09) and fast walks (SL/HT = 1.10–1.18); slow trots (SL/HT = 1.32 = 1.51) and fast trots (SL/HT = 1.55–1.80); slow running walks (SL/HT = 1.13–1.36) and fast running walks (SL/HT = 1.59–1.60); slow racks (SL/HT = 1.18–1.24) and fast racks (SL/HT = 1.39–1.70).

Gait	Average stride length (cm)	Average dimensionless speed (stride length/ height at withers)	Average ipsilateral step distance/ stride length	Average diagonal/ ipsilateral step distance	Average step symmetry (for ipsilateral and diagonal Steps)	Average interior straddle/ hind hoof width	Average lateral offset/ hind hoof width
Slow walk	145.4	1.02	−0.06	−7.96	0.92 (0.86, 0.97)	0.17	0.15
Fast walk	159.7	1.13	−0.01	11.75	0.86 (0.79, 0.94)	0.04	0.23
Slow trot	179.0	1.30	−0.11	−5.02	0.94 (0.92, 0.96)	0.15	0.29
Fast trot	240.9	1.71	−0.01	11.70	0.88 (0.80, 0.96)	0.16	0.39
Running walk	213.8	1.40	0.16	1.21	0.90 (0.93, 0.87)	0.00	—

Gait	Average stride length (cm)	Average dimensionless speed (stride length/ height at withers)	Average ipsilateral step distance/ stride length	Average diagonal/ ipsilateral step distance	Average step symmetry (for ipsilateral and diagonal Steps)	Average interior straddle/ hind hoof width	Average lateral offset/ hind hoof width
Slow rack	173.00	1.21	0.10	2.54	0.83 (0.78, 0.88)	−0.12	0.21
Fast rack	215.7	1.51	0.28	0.37	0.83 (0.95, 0.71)	−0.37	0.58
Stepping pace	240.0	1.59	0.31	0.26	0.89 (0.88, 0.90)	−0.15	0.59
Canter/ gallop	241.7/ 303.6	1.59/ 1.89	0.28/ 0.25	0.40/ 0.61	0.42 (0.68, 0.16)/ 0.53 (0.69, 0.36)	0.15/ 0.48	—/ —

Table 1.
Key linear measurements and ratios of modern horse trackways in different gaits (data from [25, 34]; and original data, 2022).
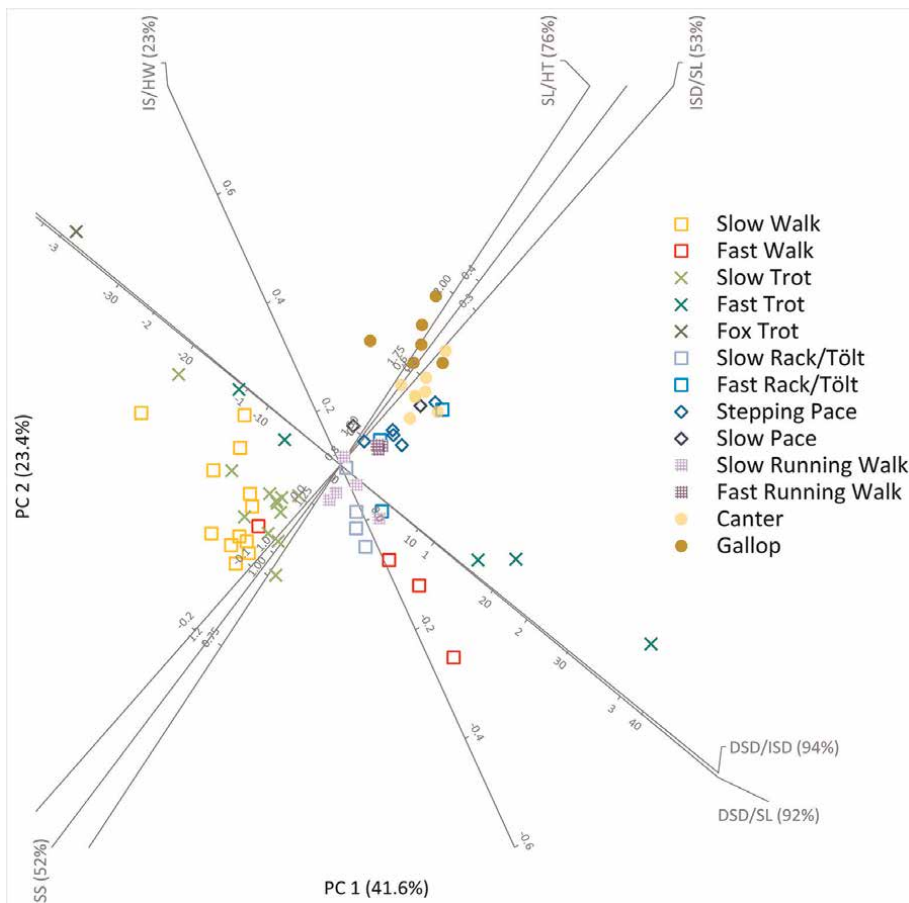

Figure 3.
Principal component analysis of horse gaits for six key factors: step symmetry (SS); interior straddle/hoof width (IS/HW); stride length/height (SL/HT); ipsilateral step distance/stride length (ISD/SL); diagonal step distance/ stride length (DSD/SL); and diagonal/ipsilateral step distance (DSD/ISD).
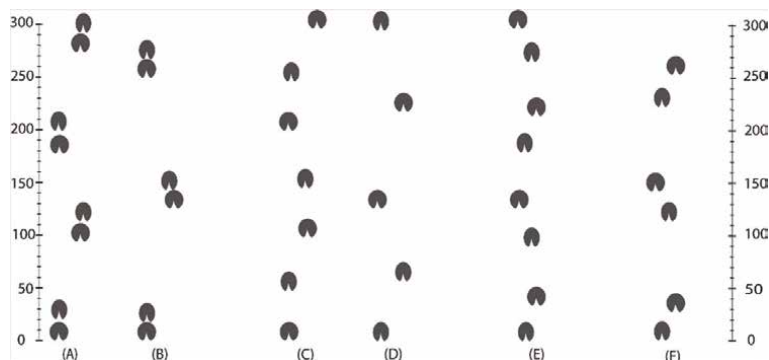
Figure 4.
Footprint patterns of various gaits in modern horses. In the fast walk (A) there is a small stride length with a small overstep of ipsilateral hind feet resulting in distinct lateral pairs of prints in roughly parallel lines and a diagonal step distance much larger than the ipsilateral one. The fox trot, true fast trot, and slow rack (B) forms a trackway similar to that of the walk with lateral pairs of prints lining up more or less in parallel but possesses a greater stride length. In the running walk (C) there is a large overstep yielding no obvious pairs of prints as the ipsilateral step distances and diagonal step distances are roughly equivalent with themselves. This should be contrasted with the gallop (D) which also lacks obvious print pairings but which has a much greater stride length and in which there is greater variance within the ipsilateral and diagonal step distances and a sequence of contralateral feet. In the fast rack or tölt (E) the ipsilateral step length is much greater than the diagonal one resulting in diagonal pairs of prints that form a bowed pattern with a large stride length and hind impressions that often cross over the centerline. In the stepping pace and true pace (F) there is an even greater stride length and the diagonal pairs of prints occur very close together as the ipsilateral step distance is much larger than the diagonal one. The scale in centimeters.

The asymmetry of the galloping gait is reflected in the step symmetry (SS) calculation (i.e. $\frac{1}{2} \times$ [DSD1/DSD2 + ISD1/ISD2]). Symmetrical gaits of the horse (walk, rack, trot, running walk) tend to have a step symmetry between 0.80 and 1.00 while asymmetrical gaits of horses (canter and gallop) tend to have a step symmetry between 0.25 and 0.70. In symmetrical horse gaits, the three ratios of ipsilateral step distance/stride length (ISD/SL), diagonal/ipsilateral step distance (DSD/ISD), and interior straddle/hoof width (IS/HW), can go a long way in distinguishing one gait form another. Ipsilateral step distance/stride length (ISD/SL) is around −0.15 to 0.50 in walking and trotting gaits, but around 0.10–0.40 in the rack or pace. The diagonal/ipsilateral step distance (DSD/ISD) tends to have high negative or positive values in the walk and trot (−20 to −3 in slower versions, 3–20 in faster versions) whereas it is usually quite low in ipsilaterally coordinated gaits such as the rack, pace, and running walk (0.20–3.00). Finally, the interior straddle/hind hoof width ratio (IS/HW) tends to be positive in the walk and trot, but negative in the ipsilaterally coordinated gaits of running walk, rack, and pace (see **Figure A1** [7, 25]).

Finally, to determine gait of a fossil horse trackmaker it is useful to compare the trackway with the standard footfall patterns and sequences left by modern horses in various gaits (see **Figure 4**). The galloping trackway is asymmetrical, and so will have a footfall sequence with two contralateral hind limbs landing in succession, whereas the other gaits being symmetrical will contain ipsilateral and diagonal pairs of limbs landing in succession. Walking, trotting, and slow racking gaits leave trackways with ipsilateral pairs of feet landing close together with a slight understep, overstep, or capping. Fast racking and pacing gaits have diagonal pairs of feet landing close together, with hind feet often crossing over the centerline. Galloping gaits have contralateral pairs of feet landing close together, but along with the running walk, often leave trackways of isolated prints without any obvious pairings, or with the canter leave a 1-2-1 pattern with the pair consisting of an overstep of ipsilateral feet.
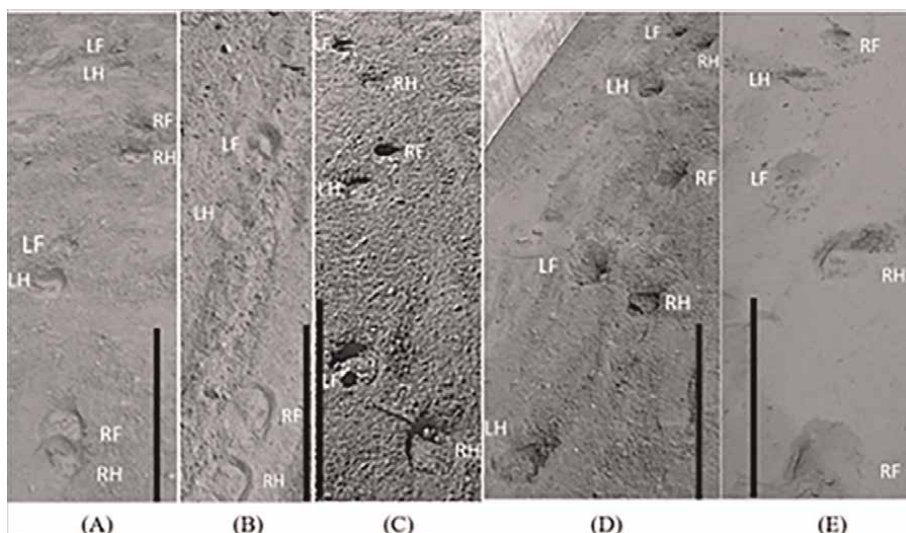
Figure 5.
Photographs of modern horses in various gaits. A. Slow walk of a Shetland Pony (horse 22), stride length = 129 cm; B. Slow Trot of a Sicilian Donkey (horse 25), stride length = 142 cm. C. Pace of a Tennessee Walking Horse (horse 1), stride length = 210 cm; D. Left-lead canter of a Shetland Pony (horse 24), stride length = 188 cm; and E. Running walk of a Tennessee Walking Horse (horse 1), stride length = 180 cm. Black bars are 50 cm long.

Lastly, the stride length is least with walking gaits, increases with medium speed trotting and racking gaits, and is greatest with galloping gaits (**Figure 5**). Stride length/height, which tends to be 1.10 or lower in a walk, 1.10–2.00 in a medium-speed trotting or pacing gait, and 1.50–2.50 in a gallop (see **Table 1** above).

The last step is to estimate the speed of the trackmaker. For this purpose the authors have come up with a modified Alexander formula based upon study of modern horses in various gaits and speeds [7, 44], which is as follows:

$$v = 0.72 g^{0.50} S^{0.81} H^{0.21} \tag{2}$$

where v is the velocity in meters/second, g is the gravitational constant of 9.81 m/s^2, S is the stride length in meters, H is the height of the horse at the withers in meters, and 0.23 is the speed multiplier.

3. Results

3.1 Trackways suggestive of diagonally coordinated trotting gaits in horses

Four fossil equid trackways suggesting a slow trotting gait are found at two different sites (see **Tables 1** and **2** below). Three of these occur near each other at the Hoya de la Sima site in the Jumilla-Ontur Basin near Jumilla, Murcia, Spain from ca 8.7–7.8 Ma ([31, 33]; see **Figures 6A** and **7A** above and below). Here overlapping tridactyl prints containing a large central hoof along with two smaller lateral hooves were preserved in gypsum layers and set down on a lake shore in the upper Tortonian (European Mammal Neogene Zone 11, hereafter MN 11). The size of the central hoof impression at the Hoya de la Sima site was around 9.3 cm in length and 7.5 cm in width (HSM-2). Three of the trackways (HSA-9, HSA-10, and HSA-11) contain impressions

Species	Track-way	Age (Ma)	Height of horse (cm)	Front central foof print length/width (cm)	Hind central hoof print length/width (cm)	Stride length (cm)	Lateral step length (cm)	Diagonal step length (cm)	Lateral offset of hoof pairs (cm)
Scaphohippus sumani	GQ-1	14.5	77.5	5.0/3.5	5.2/3.5	ca. 97.2	33.3	5.3	1.3
Cremohipparion mattewi	HSA-9	8.7–7.8	100.7	9.3/ca. 7.5 (HSM-2)	–/–	137.0	ca. –9.6	56.0	0.0
Cremohipparion mattewi	HSA-10	8.7–7.8	100.7	9.3/ca. 7.5 (HSM-2)	–/–	ca. 167.0	ca. –9.6	ca. 62.9	0.0
Cremohipparion mattewi	HSA-11	8.7–7.8	100.7	9.3/ca. 7.5 (HSM-2)	–/–	152.0	ca. –7.3	63.6	0.0
Cremohipparion mattewi	HSA-12	8.7–7.8	100.7	9.3/ca. 7.5 (HSM-2)	–/–	277.4	58.1, 51.6	51.6, 58.1	—
Cremohipparion mattewi	HSA-13	8.7–7.8	100.7	9.3/ca. 7.5 (HSM-2)	–/–	277.4	58.1, 58.1	51.6, 51.6	—
Cremohipparion mattewi	HSA-14	8.7–7.8	100.7	9.3/ca. 7.5 (HSM-2)	–/–	309.7	64.5, 64.5	64.5, 51.6	—
Hippotherium malpassii	OS-3	6.0–5.3	110.1	8.4/7.5	–/–	344.0	77.5, 76.5	75.0, 80.0	—
Hippotherium malpassii	OS-4	6.0–5.3	109.6	8.3/8.4	–/–	361.5	84.0, 81.0	80.5, 84.0	—
Hippotherium malpassii	OS-5	6.0–5.3	102.5	7.0/7.5	–/–	343.0	81.0, 89.0	68.0, 77.0	—
Hipparion fissurae	SC-1	4.9–4.2	99.8	ca. 6.5/4.4	ca. 7.7/4.4	173.8	ca. –13.5	65.7	ca. 0.0
Eurygnathohippus hasumense	LAET-A (adult)	3.7	122.1	8.8/8.0	7.5/6.5	137.0	34.5	18.0	ca. 6.5
Eurygnathohippus hasumense	LAET-B (mare)	3.7	123.9	9.1/8.0	7.6/6.7	138.9	ca. 27.7	25.1	—
Eurygnathohippus hasumense	LAET-C (foal)	3.7	87.9	6.4/4.0	6.1/4.1	94.4	23.9	10.8	ca. 4.0
Equus lambei	WB-1	ca. 0.01	120.5	10.5/10.5	–/–	356.6	87.3, 70.9	56.4, 100.0	—

Table 2.
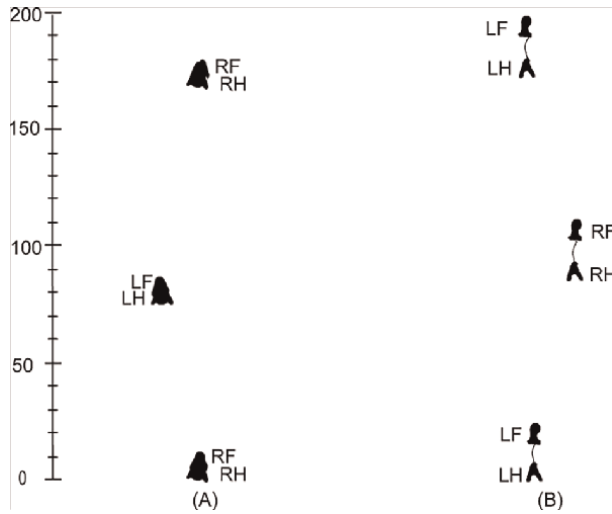*Linear kinematic parameters of fossil horse trackways.*

Figure 6.
Trackways of fossil horses in a slow trot (scale in cm). A. Trackway HAS-11 of Cremohipparion matthewi *from the Hoya de la Sima site near Jumilla, Spain (after [33]) set down on a lake shore around 8.7–7.8 Ma. B. Trackway SC-1 of* Hipparion fissurae *from the Bajo Segura Basin near Elche, Spain (after [29]) made in coastal sands around 4.9–4.2 Ma.*
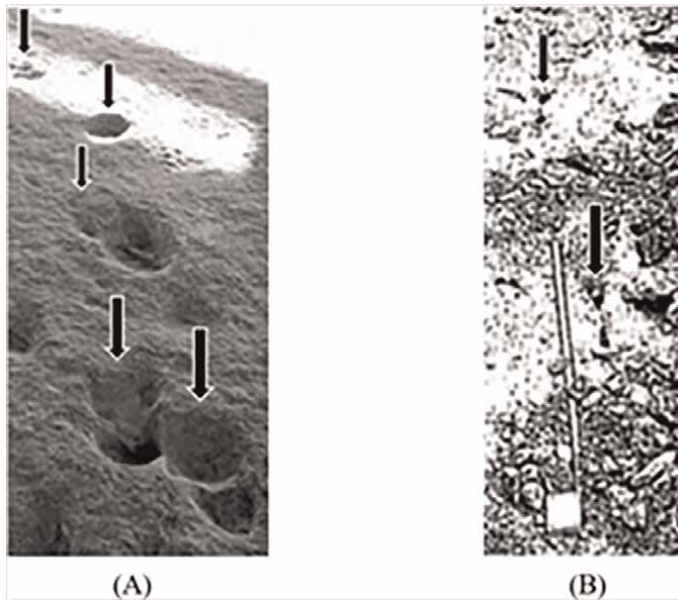
Figure 7.
Photographs of trackways of trotting fossil horses. A. Pliocene trackways HAS-11 and HSA-9 of Cremohipparion matthewi *from the Hoya de la Sima site near Jumilla, Spain (close-up of Figure 14C from [45], used with permission); and B. Pliocene trackway SC-1 of* Hipparion fissurae *near Elche, Spain (close-up of Figure 4C from [29], used with permission). Arrows show prints and direction of travel.*

in which ipsilateral hind feet understep and partially overlap the front feet as suggested by a hoof impression with a rounded tip and shorter length located anteriorly. Trackway HSA-9 is 9.5 m long and contains 15 impressions of overlapping

hooves, each impression around 14.5 cm long and 11 cm wide consisting of a large central hoof around 8.2–10.1 cm long typically followed by lateral toe impressions. The diagonal step distance is around 56.0 cm and the stride length is 137.0 cm. Trackway HSA-10 is 5.5 m long and contains eight impressions of overlapping hooves, each impression around 12.9 cm long and 10.8 cm wide. The diagonal step distance is ca. 62.9 cm and the stride length (steps 1–5) is around 167.0 cm. Trackway HSA-11 is 4.1 m long and contains six impressions consisting of overlapping hooves measuring around 15.1 cm long and 12.3 cm wide. The diagonal step distance is around 63.6 cm and the stride length is 152.0 cm. The interior straddle is around 20 cm.

There is also a trackway consisting of 10 hoof impressions in ipsilateral pairs located in the Sierra del Colmenar section of the Bajo Segura Basin, near the town of Elche, in the Alicante Province of Spain, likely of a trotting horse from around 4.9–4.2 Ma ([29]; see **Figures 6B** and **7B** above). The trackway (SC-1) was laid down in early Pliocene (MN 14) evaporitic coastal muddy sands. The central footprint impressions are around 6.5 cm long and 4.4 cm wide, and the interior straddle between ipsilateral pair prints averages around 13.4 cm (12.7–14.1 cm) indicating a wide gauge trackway. The ipsilateral pairs of the trackway seem to contain an understepping separation of the front foot from the hind foot of 7 cm (−13.5 cm total) linked by an odd groove that Lancis and Estevéz [29] postulate is due to hoof sliding, or in our view a toe (side?) scraping across the ground prior to full foot impact. The understep is indicated by the fact that the

Figure 8.
Photograph of modern horse (horse 19) in medium trot with some overstep, stride length = 265 cm. Bar is 50 cm in length.

anterior print is rounder in front while the posterior one is more oval in front, though the hind print is wider than the front print (perhaps due to partial collapse of sediment around the front foot). Hence we postulate a trotting gait (as seen in **Figure 8** above) here though further study is warranted. As such the diagonal step distance (intercouplet distance) separating the ipsilateral pairs averages around 65.7 cm (65.0 cm, ca. 66.4 cm) and the stride length is about 173.8 cm.

3.2 Trackways suggestive of laterally coordinated gaits in fossil horses

As we have previously argued there are also trackways suggestive of laterally coordinated intermediate-speed gaits in fossil horses (see **Tables 1** and **2** below).

The best preserved of these trackways are those of three hipparionin horses laid down in volcanic ash at Locality 8, Site G, in the Upper Laetoli beds in Tanzania some 3.66 Ma ([22–25]; see **Figures 9B,C** and **10E** below). The trackways, 151 to 251 cm in length, contain eight to 13 prints [23, 24]. Trackway LAET-A of an adult horse had ipsilateral step distances (footprints 2–6) that averaged 34.5 cm and diagonal step distances that averaged 18.0 cm, a stride length of 137.0 cm, with the prints forming a bowed or wave-like pattern made by diagonal pairs with lateral offsets around 6.5 cm ([22], 473). Trackway LAET-B of an adult horse (and likely a mare as it parallels and overlaps the trackway of a juvenile), had ipsilateral step distances (footprints 1–5) that averaged 25.1 cm and diagonal step distances that averaged around 27.7 cm, a stride length of 138.9 cm, and consisted of four isolated foot impressions with no obvious pairings. Finally, trackway LAET-C of a juvenile horse, had ipsilateral step distances (footprints 6–10) averaging 23.9 cm and diagonal step distances that averaged 10.8 cm, a lateral offset around 4.0 cm, with a stride length of 94.4 cm, and a trackway that is bowed with distinct diagonal pairs of hoof impressions. The central hoof prints from the Laetoli horse trackways themselves yield the following approximate measurements: LAET-A (adult), front hooves (manus) 8.8 cm long by 8.0 cm
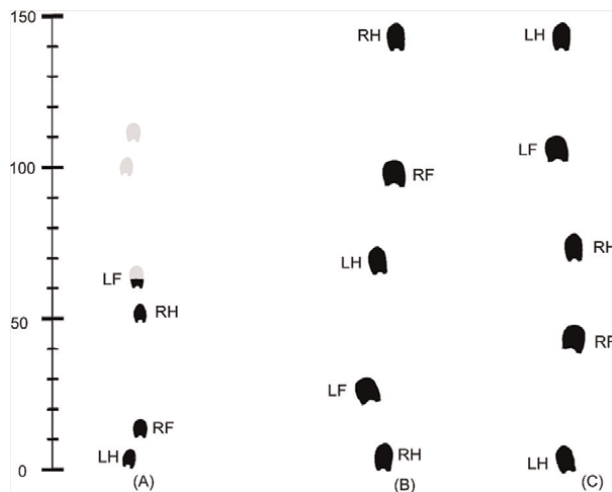
Figure 9.
Laterally-coordinated gaits in fossil horses (scale in cm). A. Trackway GQ-1 showing rack or tölt of Scaphohippus sumani *(after [25]). The impressions (grayed-out where missing) were laid down on a lake shore in the Mud Hills near Barstow, California around 14.5 Ma. B, Trackway LAET-A showing the species* Eurygnathohippus hasumense *in a rack or tölt (after [22–24]). The prints were formed in volcanic ash some 3.7 Ma at Laetoli, Site G, in Tanzania. C. Trackway LAET-B of prior species in a running walk (or rack).*

Figure 10.
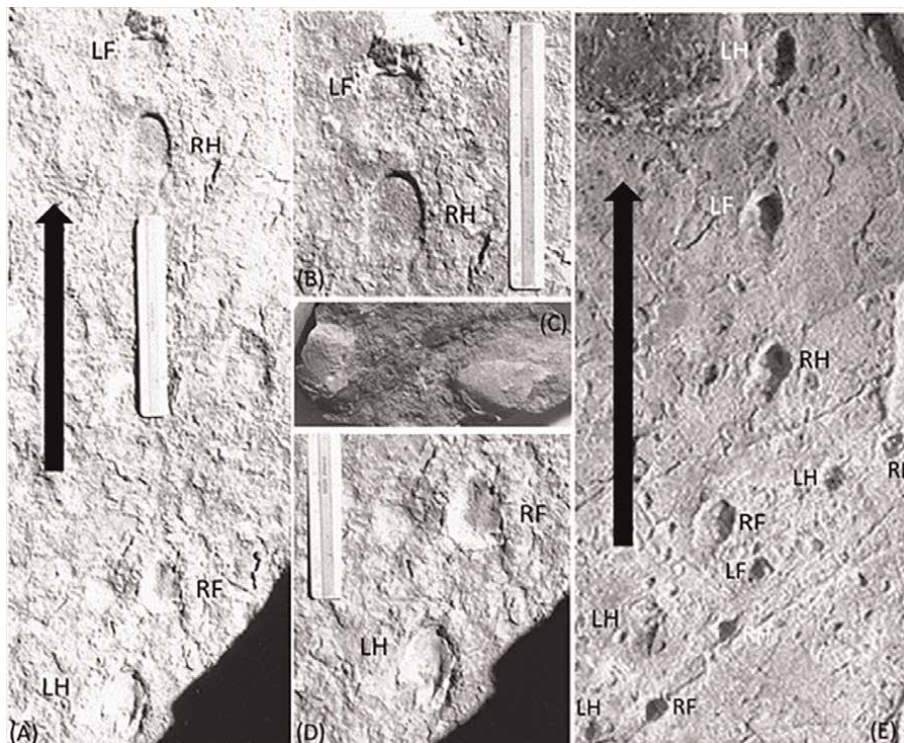*Photographs of intermediate speed laterally-coordinated gaits in fossil horses. A. Mold of Miocene trackway GR-1 of* Scaphohippus sumani *made on site at the Mud Hills near Barstow, California; B. Close up of upper pair of GR-1 hoof prints (ruler repositioned from original); C. Cast of upper pair of GR-1 hoof prints (ruler repositioned from original); D. Close up of lower pair of GR-1 hoof prints; E. Pliocene trackways LAET-B and LAET-C of mare in running walk to left and juvenile in rack or tölt beside her to the right made by* Eurygnathohippus hasumense *from Laetoli Site G in Tanzania. The mare prints have posterior distal mud adhesion that adds to impression length.*

wide and hind hooves (pes) 7.5 cm long and 6.5 cm wide; LAET-B (adult), front hooves (manus) 9.1 cm long by 8.0 cm wide and hind hooves (pes) 7.6 cm long by 6.7 cm wide; LAET-C (juvenile), front hooves (manus) 6.4 cm long by 4.0 cm wide and hind hooves (pes) 6.1 cm long by 4.1 cm wide. The adult Laetoli trackways ([22], pp. 476–477, Figures 12.16 and 12.17) possessed negative interior straddle (narrow gauge) measurements of ca. −0.5 cm (LAET-A), −2.0 cm (LAET-B), and 0.0 cm (LAET-C).

Another fossil horse trackway (GQ-1; ichnospecies *Hippipeda araiochelata*), one 61 cm long, also seems to be indicative of a lateral racking gait, this time of a middle Miocene merychippine horse ([25]; see **Figures 9A** and **10A–D** below). The trackway consists of four footprints set down at the edge of a lake some 14.5 Ma which were excavated from Greer Quarry in the Barstow Formation of the Mud Hills outside of Barstow, California [25, 32, 46]. The footprints were found on a rock slab exposed in convex epirelief from which a rubber mold was made (SBCM L1816-3436). One of the hoof impressions is incomplete but one can distinguish fore feet (manus) from hind feet (pes) based upon the other three impressions due to the fact that the hind foot impressions are more pointed at the tip and longer while the front foot impressions are more rounded at the tip and have a ratio of length to width
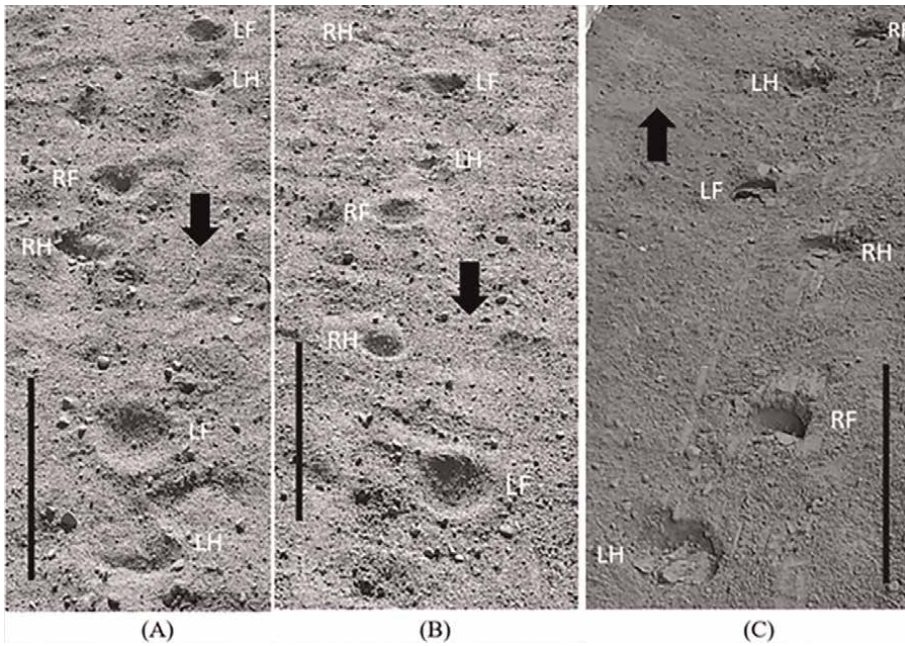
Figure 11.
Laterally coordinated gaits of modern horses. A. Slow rack (show gait) with overstepping lateral pairs in a Rocky Mountain Horse (horse 10), stride length = 180 cm; B. Fast rack (pleasure gait) with understepping diagonal pairs of a Rocky Mountain horse (horse 11), stride length = 201 cm; C. Slow pace with diagonal pairs of a Tennesse Walker (horse 1), stride length = 208 cm. Bars are 50 cm in length. Arrows show direction of travel.

closer to 1.0. Trackway GQ-1, when reconstructed according to an assumption of constant speed, has a stride length of around 97.2 cm, ipsilateral step distances of 33.3 cm, diagonal step distances averaging 5.3 cm, and lateral offsets of diagonal pairs averaging 1.3 cm in which the hind feet understep the front feet. The interior straddle is −0.1 cm [25]. The tracks themselves possess a front central hoof (manus) impression measuring 5.0 cm long by 3.5 cm wide, and a hind central hoof (pes) impressions measuring around 5.2 cm long by 3.5 cm wide [25, 32, 46]. One can see the resemblance of these trackways to those of modern horses in alternative lateral gaits (see **Figure 11A–D**).

3.3 Trackways suggestive of asymmetrical galloping gaits in fossil horses

Seven fossil horse trackways, from three different sites, are indicative of a galloping gait (see **Tables 1** and **2** below). Three trackways (HSA-12; HSA-13; HSA-14) occur at the same Hoya de la Sima site in the Jumilla-Ontur Basin near Jumilla, Murcia, Spain where the trotting trackways are found ([31]; see **Figures 12A** and **13A** above). They too were originally made on lake shore sediments of the upper Tortonian (MN 11) around 8.7–7.8 Ma. Trackway HSA-12 is 9.6 m long and consists of 21 individual impressions. The manus (front foot) print is around 9.3 cm long and 7.5 cm wide. The step lengths of HSA-12 (steps 1–5) are ca. 58.1, 51.6, 51.6, and 58.1 cm and the stride length is around 277.4 cm. Trackway HSA-13 is 3.3 m long and contains five to seven partly overlapping hoof impressions 14.9 cm long by 13.7 cm wide. The step distances (steps 1–5) are ca. 51.6, 58.1, 51.6, and 58.1 cm and the stride length is around
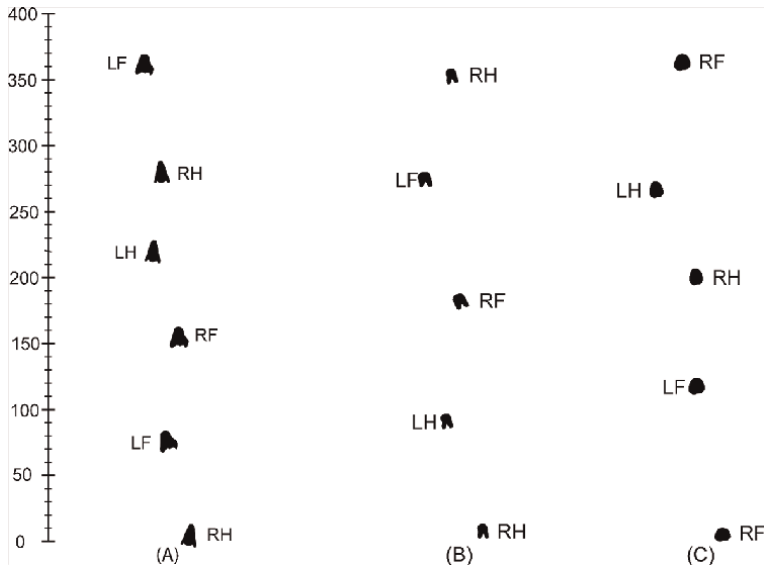
Figure 12.
Trackways (cm scale) of fossil horses in a gallop. A. Trackway HSA-14 of Cremohipparion matthewi *from the Hoya de la Sima site near Jumilla, Spain (after [33]) made on a lake shore ca. 8.7–7.8 Ma; B. Trackway OS-3 of* Hipparion fissurae *laid down in a flood plain near Osoppo, Italy some 6.0–5.53 Ma (after [28]). C. Trackway WB-1 of* Equus lambei *made 13–11 kyr in Wally's Beach fluvial sands near Cardston, Canada (agter [30]).*
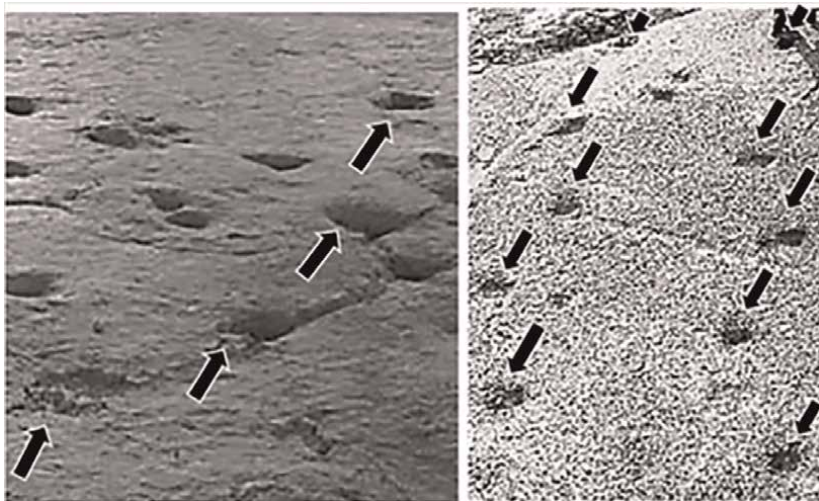
Figure 13.
Photographs of fossil horse galloping trackways. A. Pliocene trackway HSA-14 of Cremohipparion matthewi *near Jumilla, Spain (close-up of Figure 10 from IGME, PT085, used with permission); B. Pliocene trackways OS-4 and OS-3 of* Hipparion fissurae *near Osoppo, Italy (close-up of Figure 15 from Venturini and Discenza, 2009, used with permission). Arrows show prints and direction of travel.*

277.4 cm. Finally trackway HSA-14 is 2.5 m long and contains four to six impressions 14.4 cm long by 12.6 cm wide. The steps distances (steps 1–5) are ca. 64.5, 64.5, 64.5, and 51.6 cm and the stride length is around 309.7 cm.

Three more likely galloping trackways occur near each other on the Colle di Osoppo, near Osoppo, Friuli Venezia Giulia, Italy [28]. The prints were set down in a flood plain near a river in the late Messinian between 6.0 and 5.3 Ma. The three trackways (OS-3, OS-4, and OS-5) are between 8.4 and 9.2 m long and consist of 11 individual footprints which have large central hooves measuring 7.0–10.0 cm long by 6.0–10.0 cm wide, along with two small lateral hoof impressions located posteriorly. The central hoof foot impressions are around 8.4 (OS-3), 8.3 (OS-4), and 7.0 cm (OS-5) in length (see **Figures 12B** and **13B** below). Trackway OS-3 contained step lengths (steps 4–8) of 75.0, 77.5, 80.0, and 76.5 cm, and a stride length of 344.0 cm. Trackway OS-4 contained step lengths (steps 7–11) of ca. 80.5, 84.0, 84.0, and 81.0 cm, and a stride length of 361.5 cm. Trackway OS-5 contained step lengths (steps 3–7) of 68.0, 81.0, 77.0, and 89.0 cm, and a stride length of 343.0 cm. Trackway OS-5, however, warrants further study as orientation of impressions at odd angles and poor preservation suggests the trackway may not belong to a single individual, nor that prints numbering 6 to 11 cross back and forth over trackway OS-4 several times.

Vincelette [25] also provided footprint parameters, based upon scale drawings [30], for a late Pleistocene set of footprints likely made by *Equus lambei* in fluvial sands and silts at the Wally's Beach deposit (DhPG-8) from the drained bottom of St. Mary's Reservoir near Cardston in Alberta, Canada (see **Figure 12C** below). The trackway (WB-1; ichnospecies *Hippipeda cardstoni*) is 401 cm long and consists of five prints 10.5 cm in both length and width made some 13,000–11,000 years ago. The stride length was around 356.6 cm long, with the distance between isolated footprints being 100.0, 70.9, 56.4, and 87.3 cm. One can see the resemblance of these tracks to a modern horse's gallop (see **Figure 14** below).

Figure 14.
Photograph of Tennesse Walking Horse (horse 19) in a left-lead gallop, stride length = 465 cm. Bar is 50 cm.

4. Discussion

Modern horses (unless possessing a rare mutation) possess only one toe per leg, which consists of the previous central metapodials (metacarpals and metatarsals III) and phalanges (first, second, and third phalanges III). They evolved from early Eocene horses which were tetradactyl in the front limbs and tridactyl in the hind limbs, and from late Miocene tridactyl horses. The earliest horses studied here, from the Miocene and Pliocene, were all tridactyl, though the second and fourth digits were reduced in size. Quite often the lateral toes do not make impressions in the substrate, suggesting the horses are "functionally monodactyl" [46], and that the lateral toes have specialized functions, though this has been much debated [47]. The Pleistocene horses studied here were monodactyl.

Comparison of the data obtained from the fossil horse trackways with key kinematic parameters (**Table 3**) and footprint patterns (**Figures 4** and **5** above) of modern horses leads to the recognition of four different gaits in fossil horse trackways, the trot, the running walk, the rack, and the gallop.

4.1 Diagonal trotting gaits in fossil horses

As noted earlier, four fossil equid trackways best match a slow trotting gait (see **Tables 2–4**, and **Figures 6–8** above). This is based upon the fact that they are set down in a pattern of capping or slightly overstepping ipsilateral prints (ipsilateral step distance/stride length ranging from −0.05 to −0.08), at a moderate speed (stride length 130–180 cm; stride length/height ratios of 1.36–1.66), with a large negative

Species	Trackway	Stride length/ height	Diagonal/ ipsilateral step distance	Ipsilateral step distance/ stride length	Interior straddle/ hind hoof width	Lateral offset/hind hoof width
Scaphohippus sumani	GQ-1	1.25	0.16	0.34	−0.29	0.37
Cremohipparion matthewi	HSA-9	1.36	−5.83	ca. −0.07	0.27	0.00
Cremohipparion matthewi	HSA-10	1.66	−6.55	ca. −0.06	0.27	0.00
Cremohipparion matthewi	HSA-11	1.51	−8.71	ca. −0.05	0.27	0.00
Cremohipparion matthewi	HSA-12	2.75	1.00	0.20	0.57	—
Cremohipparion matthewi	HSA-13	2.75	0.89	0.21	1.10	—
Cremohipparion matthewi	HSA-14	3.08	0.90	0.21	0.30	—
Hippotherium malpassii	OS-3	3.12	1.01	0.22	1.17	—
Hippotherium malpassii	OS-4	3.30	1.00	0.23	0.71	—
Hippotherium malpassii	OS-5	3.35	0.85	0.25	0.13	—
Hipparion fissurae	SC-1	1.74	−4.87	−0.08	ca. 3.05	0.00
Eurygnathohippus hasumense	LAET-A	1.12	0.52	0.25	−0.31	ca. 1.00
Eurygnathohippus hasumense	LAET-B	1.12	0.91	0.18	−0.07	—
Eurygnathohippus hasumense	LAET-C	1.07	0.45	0.25	0.25	ca. 0.98
Equus lambei	WB-1	2.96	0.99	0.22	0.67	—

Table 3.
Key ratios for fossil horse lateral gait trackways.

Species	Trackway	Pattern	Foot pairs	Relation of foot pairs	Gait	Estimated velocity (m/s)
Scaphohippus sumani	GQ-1	Bowed	Diagonal	Understep	Rack	2.09
Cremohipparion matthewi	HSA-9	Parallel	Lateral	Understep	Trot	2.91
Cremohipparion matthewi	HSA-10	Parallel	Lateral	Understep	Trot	3.42
Cremohipparion matthewi	HSA-11	Parallel	Lateral	Understep	Trot	3.17
Cremohipparion matthewi	HSA-12	Isolated	None (contralateral)	—	Gallop	5.16
Cremohipparion matthewi	HSA-13	Isolated	None (contralateral)	—	Gallop	5.16
Cremohipparion matthewi	HSA-14	Isolated	None (contralateral)	—	Gallop	5.64
Hippotherium malpassii	OS-3	Isolated	None (contralateral)	—	Gallop	6.26
Hippotherium malpassii	OS-4	Isolated	None (contralateral)	—	Gallop	6.51
Hippotherium malpassii	OS-5	Isolated	None (contralateral)	—	Gallop	6.15
Hipparion fissurae	SC-1	Parallel	Lateral	Understep	Trot	3.53
Eurygnathohippus hasumense	LAET-A	Bowed	Diagonal	Understep	Rack	3.03
Eurygnathohippus hasumense	LAET-B	Isolated	None (ipsilateral)	—	Running Walk or Rack	3.08
Eurygnathohippus hasumense	LAET-C	Bowed	Diagonal	Understep	Rack	2.09
Equus lambei	WB-1	Isolated	None (contralateral)	—	Gallop	6.57

Table 4.
Major gait characteristics and velocity for fossil horse trackways.

diagonal/ipsilateral step length ratio of −5.0 to −10.0. Though a slow rack can also set down prints in ipsilateral pairs this usually occurs at shorter stride lengths (stride length/height around 1.20) and is accompanied by an interior straddle that is close to zero or negative as hind feet can cross the center line as there is less foot interference [25, 34]. Here though the interior straddle of the tracks varies from around 0.6–1.1 cm.

Three of these trackways (HSA-9, HSA-10, and HSA-11) are from the Hoya de la Sima site near Jumilla, Spain [31, 33] consisting of overlapping tridactyl prints of ipsilateral feet formed around 8.7–7.8 Ma (see **Figures 6A** and **7A** below).

Three species of tridactyl hipparionins are found in MN 11 strata in nearby Spain, a smaller form *Cremohipparion matthewi*, a larger form *Hipparion laromae*, and even larger forms *Cremohipparion mediterraneum* and *Hipparion longpipes* [48–50]. In Pleistocene and extant horses the length of the hoof is around 1.8–2.0 times the length of the distal phalanx bone, in Miocene horses the hoof length is around 1.0–1.3 times the length of the distal phalanx III bone [7, 32]. In Pliocene horses the hoof size would presumably land between these two values (see [46], 27, **Table 1**, who notes changes

in hoof wall thickness over time). Hence we can estimate the hoof size to be around 1.4–1.7 times the length of the distal phalanx III. As *H. laromae* from Rome had a distal phalanx III (i.e. 3PhIII) 6.5 cm long by 6.2 cm wide, albeit from slightly later MN 10 strata [50], this suggests it would make a central hoof impression around 9.1–11.1 cm long whereas the impressions made by the central hoof in the substrate at the Hoya de la Sima site were around 8.0–9.3 cm long. This would seem to rule out *H. laromae* as the trackmaker, as well as the slightly larger forms of *C. mediterraneum* and *H. longpipes*. The smaller hipparionin species then, *Cremohipparion matthewi* [periafricanum], which had a size around 79% that of *H. laromae* and an estimated hoof size of 7.2–8.8 cm long would seem to be the best candidate for the trackmaker and is tentatively assigned here.

Cremohipparion matthewi from MN 11 strata at the Puente Minero site, Teruel Province, Spain, has a row of upper cheek teeth (PM-1350; P^2–M^3) 11.3 cm long, a metatarsal III (PM-960) 19.2 cm long, and a hind first phalanx III (PM-771) 4.7 cm long [50]. The type specimen from Samos had a skull (LGPUT OK-557) around 31.9 cm long with a row of upper cheek teeth around 11.2 cm long, associated metacarpals that averaged around 20.5 cm long, along with a metatarsal 21.4 cm long [51], and footprints around 9.3 cm long by 7.5 cm wide.

Using the hipparionin multipliers (**Table A1**) we arrive at the following estimated heights: 82.1 cm (from the skull), 97.5 cm (from the metatarsal), 94.5 cm (from the hind first phalanx), and 112.3 cm (from the footprints). Assigning 25% weight to both the skull and postcrania and 50% to the footprints gives a height estimation of 100.7 cm for the trackmaking *Cremohipparion matthewi*. This in turn would yield the following stride length/height ratios: 1.36 (HSA-9), 1.66 (HSA-10), and 1.51 (HSA-11), indicative, along with the overlapping or understepping ipsilateral foot pairs, of a slow trot at around 2.9–3.4 m/s using our modified Alexander formula.

The other trackway (SC-1) suggesting a trotting gait was located in the Sierra del Colmenar section of the Bajo Segura Basin, near Elche, Spain and formed around 4.9–4.2 Ma ([29]; see **Figures 6B** and **7B** above). The trackway was likely made by the tridactyl horse species *Hipparion fissurae* found in similar strata [52–55]. Postcranial remains of *H. fissurae* from the MN 14 zone in Spain [52] include third metacarpals (GL 1+68, GL 370, GL 92+127, VAR 1-43) averaging 24.3 cm in length, third metatarsals (GL 142, GL 304, GL 391+390, FSL-SN, LA 90, LCA 81-42; VAR 132, VAR 144) averaging 26.8 cm in length, and first phalanges III averaging 6.4 cm in length in the front legs (GL 133, GL 374, GL 409, LA 127, LCA 8168, NM 18078) and 6.1 cm in the hind legs (GL 22, LA 91, LA 93, LA 137, LA 138, NM 18079, NM 18087, ORR 32, ORR 48, VAR 1-112, VA 31). The front central hoof impressions were around 6.5 cm long. A skull of the species found near Pavlodar, Kazakhstan, from ca. 5.5–5.3 Ma, measured about 38.4 cm long [55].

If we use the hipparionin multipliers (**Table A1**), we arrive at the following height estimations for the trackmaker: 97.9 (from the skull), 139.7 cm (from the third metacarpal), 136.1 cm (from the third metatarsal), 131.4 cm (from the anterior first phalanx III), 127.3 cm (from the posterior first phalanx III), and 78.5 cm (from the footprints). The footprint height estimation is here much lower than the skeletal estimations suggesting the presence of a young individual here, different bone length proportions than the norm, or perhaps incorrect species assignment. In any case, by assigning 50% weight to the footprints, 25% to the postcrania, and 25% to the skull, we arrive at a height estimate of 99.8 cm for the *Hipparion fissurae* trackmaker. This in turn yields an ipsilateral step/stride length ratio of −0.08, a diagonal/ipsilateral step distance ratio of −4.87, and a stride length/height ratio of 1.74, which along with the

understepping ipsilateral pairs strongly suggest a slower trotting gait, one which occurred at around 3.5 m/s using our modified Alexander formula. This trackway did have an unusually large interior-straddle for a trot, however.

4.2 Lateral gaits in fossil horses

As we have previously noted, there are also trackways suggestive of laterally coordinated intermediate-speed gaits in fossil horses (see **Tables 2–4**, and **Figures 9–11** above). This gait identification is suggested by footprint patterns wherein diagonal feet land near each other (low diagonal/ipsilateral step distance ratio of 0.15–0.95) at an intermediate speed (stride length of 90–150 cm; 1.20–1.50 stride length/height), with much overstepping (a large ipsilateral step distance/stride length ratio of 0.25–0.59). The other key identifying feature is the possession of a negative interior straddle (narrow gauge trackway), as laterally coordinated gaits have less potential limb interference and allow the hind limbs to cross the center line of the gait (possibly for balance and/or increased speed).

The tridactyl trackways (LAET-A; LAET-B; LAET-C) of the Upper Laetoli beds in Tanzania that formed some 3.66 Ma ([22–24]; see **Figures 9B, C** and **10E** above) were likely made by the species *Eurygnathohippus hasumense* found in nearby strata of a similar geological age [25, 56–61]. Two metacarpals (WM 1635/92 and WM 1669/92) from the Kiloleli Member (ca. 4-3 Ma) of the Manonga Valley, Tanzania, assigned to *E. hasumense* averaged 24.1 cm in length [57]. There is also a skull (AL 340-8) assigned to *E. hasumense* from the younger Denan Dora II beds (ca. 3.2 Ma) of Hadar, Kenya that measures ca. 51.5 cm, along with metacarpals (AL 155-156) averaging 26.2 cm [41, 62]. An incomplete skull (WM 1528/92) from the Manonga Valley, Tanzania seems slightly larger in size (1:1.04 ratio) than the one from Hadar, Kenya based upon muzzle-length comparisons [57], which would make it 53.6 cm long if fully propor-tional. There is also a front proximal phalanx III from Laetoli (LAET 2357, Loc. 10) 6.8 cm long that is likely from this same species ([22], 475, Table 12.9). Central hoof impressions were 8.8 and 9.1 cm long for the adult trackways A and B, and 6.4 cm long for the juvenile trackway C. Finally radii of the species from Manonga (WM 368/94) and Hadar measure around 31.2 and 32.5–34.5 cm, respectively. Intraspecific height variation is also observed here and likely elsewhere as can be seen in the variation in size of horse astragali from the Upper Laetoli Bed localities 2, 6–8, 14, 16, and 22 (plotted in [22], p. 475, Figure 12.15). The postcranial material from the Upper Ndolanya Beds noted in our previous publications [22, 25] has now been more defin-itively assigned to the more gracile hipparionin species *Eurygnathohippus cornelianus* and not included herein.

If we take the above values and multiply them by the hipparionin height estima-tion multipliers (**Table A1**), we end up with the following height estimates in centi-meters: 136.7 (from the skull), 138.6 (from the third metacarpal), 139.6 (from the front proximal phalanx III), and 106.2 (A), 109.8 (B), and 77.2 (C) from the hoof impressions. If, following the method noted above, we assign the 50% weight to the footprint, 25% to the skull, and 25% to the postcranial measurements, we arrive at the following size estimations for the adult *Eurygnathohippus hasumense* track makers: adult horse A, 122.1 cm; adult horse B, 123.9 cm. The juvenile horse C had a size of around 87.9 cm if its skeleton was proportionate in size to the adult horses.

This yields the following key ratios for the three trackways. For trackway LAET-A: diagonal/ipsilateral step distance, 0.52; ipsilateral step distance/stride length, 0.25; stride length/horse height, 1.12; lateral offset/hind hoof width, 1.00; and for trackway

LAET-B: diagonal/ipsilateral step distance, 0.90; ipsilateral step distance/stride length, 0.18; stride length/horse height, 1.12; and lateral offset/hind hoof width, 0.81. And for trackway LAET-C: diagonal/ipsilateral step distance, 0.45; ipsilateral step distance/ stride length, 0.25; stride length/horse height, 1.07; lateral offset/hind hoof width 0.98.

The gait displayed by the three individuals (two adults and one juvenile) in these trackways have been variously described as a running walk [23–25], a singlefoot [22], or a tölt (Islandpferde Reitbuch, 286). Part of the inspiration for this study was to be able to reexamine these trackways and see if we could distinguish exactly which lateral gait(s) were displayed in the Laetoli hipparionin horses. We now believe we can. The values and characteristics noted above suggest that *Eurygnathohipus hasumense* adult horse A and juvenile horse C were engaged in a rack or tölt. This is indicated by the gaits having the diagonal/ipsilateral step distance ratios around 0.50 or less, as well as the bowed or wave-like pattern of prints formed by diagonal pairs, and a very narrow gauge trackway with negative interior straddles for adult horse A (−2.0 cm) and foal C (0.0 cm). Adult horse B, likely a mare traveling near her offspring (horse C), instead seems to have employed a running walk gait (though a rack at an intermediate speed is also a possibility). This is suggested by the footprints lacking readily identifiable pairs, a diagonal/ipsilateral step ratio of 0.90, and a slightly negative interior straddle (−0.5 cm). It may be that the mare utilized a running walk instead of a rack in order to more easily travel at a velocity matching her foal. There is a possibility that the mare employed an intermediate-speed rack which can lay down isolated prints resembling a running walk, but one would tend to expect an even more negative interior straddle (see [7, 34]). Based upon our modified Alexander formula these gaits would have taken place at around 3.0–3.1 m/s for the adults (LAET-A and LAET-B) and 2.1 m/s for the foal (LAET-C).

Another fossil horse trackway (GQ-1; ichnospecies *Hippipeda araiochelata*), one 61 cm long, of a middle Miocene merychippine horse from Greer Quarry outside of Barstow, California, also arguably displays a laterally coordinated gait ([25]; see **Figures 9A** and **10A–D**). Previously the four hoof impressions (GQ-1), laid down on the edge of a lake some 14.5 Ma which, and found at Greer Quarry outside of Barstow, California, had been assigned to *Scaphohippus intermontanus*. This was based upon its distal phalanx III matching the hoof impression closely, albeit a bit snuggly suggesting a very narrow hoof wall [25, 32], as opposed to the slightly smaller species *Scaphohippus sumani*, or the much larger *Hypohippus affinis* and *Megahippus mckennai*, found nearby in strata of a similar geological age. However, a recent study with which we agree argues that the *S. intermontanus* material should be reassigned to *S. sumani* due to intraspecific variability in tooth complexity between the two populations [63]. In fact, Merriam [64] only distinguished the postcrania of the two merychippine species by size, wherein larger material was assigned to *S. intermontanus* and smaller material to *S. sumani* [64]

The size of the *Scaphohippus sumani* printmaker can be estimated from cranial and postcranial material, as well as the prints, according to the method described above. A skull of the species from the Barstow Formation (Ba2), California (UMCP 21386) measures 33.6 cm, another skull (UCMP 21385) from the same locality is of proportionate length, and a third skull AMNH 87301) from the slightly older Olcott Formation (Ba1), Nebraska, measures around 31.5 cm [64, 65]. Barstow formation postcranial material includes a metacarpal (UCMP 22372) measuring 16.5 cm, metatarsals (UCMP 19817 and 23,130) measuring 18.1 and 18.3 cm in length, a front proximal phalanx III (UCMP 22372) around 3.9 cm long, a hind proximal phalanx III around 3.8 cm long (UCMP 19817), a front distal phalanx III (UCMP 22372) that

measured around 3.5 cm long by 3.2 cm wide, a hind distal phalanx III (UCMP 19817) measuring around 3.0 cm long by 2.7 cm wide [32, 64], and a front hoof impression 5.0 cm long by 3.5 cm wide.

If we take these measurements and multiply them by the protohippin multipliers (**Table A1**), we arrive at the following height estimations in centimeters: 91.4 (from the skull), 90.3 (from the metacarpal), 89.5 (from the metatarsals), 93.9 (from the front proximal phalanx III), 89.1 (from the rear proximal phalanx III), 76.1 (from the front distal phalanx III), 78.6 (from the hind distal phalanx III), and 66.2 (from the front hoof). The height estimation from the front hoof is here somewhat lower than that derived from the other dimensions suggesting perhaps a young individual, bone proportionality differences from those found in *Protohippus*, or perhaps misidentification of species. By again giving 50% weight to the footprints, 25% to the skull, and 25% to postcranial measurements we arrive at a height estimation for the *Scaphohippus sumani* printmaker of 77.5 cm.

This yields the following ratios for the GQ-1 trackway: stride length/height, 1.25; diagonal/ipsilateral step distance, 0.16; ipsilateral step distance/stride length, 0.34; lateral offset/hind hoof width, 0.37. The trackway also seems to display a somewhat bowed pattern of prints with diagonal pairs of feet landing close together. Due to the large lateral offsets that occur in different directions within the print pairs and form a somewhat bowed pattern, we interpret the gait in trackway GQ-1 to again be a laterally coordinated rack or tölt. However, given that there are only four impressions (one incomplete) and that the lateral offset is not large, it is possible, though less likely, for the trackway to be formed by a slow trot (in a horse with poor conformation or changing directions). A rack is more likely though, due to the bowed pattern, the fact the hind hooves both cross the centerline, and there is a lateral offset/hind hoof width ratio above 0.25 (see **Table 3**). The large understep, 1.06 times the hoof length, also better matches that of a rack or stepping pace, wherein the understep is 0.60–1.50 the hoof length, versus a slow trot, wherein the understep is usually 0.35–0.55 the length of the hoof, even if it can reach 0.80–0.85 the length of the hoof at times [7, 25, 34]. On the whole then, the trackway is similar to ones made by living horses in a fast rack (or tölt) or stepping pace (see **Figure 11** above). The value of stride length/height of 1.25, however, somewhat puzzlingly more resembles that of a slow rack than a fast one as is also the case with the *Eurygnathohippus* values, even as the footprint patterns match those of a fast rack. It could be that the horse heights are slightly overestimated here (due to the tracks being by a young individual or species with different limb proportions than *Protohippus*), or that horses are capable of a greater overstep at slower speeds than seen in our study. Further study of the *Scaphohippus* prints has also revealed that the first hind impression points slightly to the right rather than paralleling the center line and that the expected stride length/height is a bit lower than expected for a fast tolt. This is a bit puzzling but can occur in the rack or trot due to change of direction or poor limb conformation [22–25, 32]. The evidence here, therefore, best fits the gait of a rack or tölt, one at a speed of around 2.1 m/s using the modified Alexander formula, made by a member of the *Scaphohippus sumani* species. However, the evidence is not as conclusive as with the Laetoli prints noted above and it is possible that this trackway is from the gait of a tro.

4.3 Galloping gaits in fossil horses

Trackways evidencing a galloping gait are somewhat common in fossil horses, perhaps as such forceful hoof impressions are more likely to be preserved (see **Tables 2–4**,

and **Figures 12–14** above). As noted above, evidence for a galloping gait occurs in seven fossil horse trackways from three different sites. All of these trackways had long stride lengths (270.0–370.0 cm) and stride length/height ratios above 2.75, suggesting high speed and presented four independent hoof impressions (i.e. no obvious foot pairings). The trackways did sometimes display more symmetry than is typical for the gallop in modern horses where it averaged 0.63 (extrapolated from [25]). Here the symmetry [(DSD1/DSD2 + ISD1/ISD2)/2] varied between 0.88 to 0.90 at the Hoya de la Sima site (HSA-12 and HSA-14) to 1.00 (HSA-13), between 0.90 (OS-5) to 0.96 (OS-3 and OS-4) at the Colle di Osoppo site, and was 0.69 (WB-1) at the Wally's Beach site. Still, assuming proper individuation of footprints in the trackway, the long stride length and lack of obvious foot pairs strongly suggests a galloping gait.

Three galloping trackways (HSA-12; HSA-13; HSA-14) occur at the same Hoya de la Sima site near Jumilla, Spain where the trotting trackways are found ([31]; see **Figures 12A** and **13A**) and were likely made by the same tridactyl species of the horse *Cremohipparion matthewi* described above, which had an estimated height of 100.7 cm. This would yield stride length/height ratios of 2.75 (HSA-12), 2.75 (HSA-13), and 3.08 (HSA-14), indicative of left-, right-, and left-lead gallops, respectively, at speeds of around 5.2–5.6 m/s using the Original Alexander formula for such a fast gait.

The three galloping trackways located near each other on the Colle di Osoppo, near Osoppo, Friuli Venezia Giulia, Italy ([28]; see **Figures 12B** and **13B** above) were probably formed by *Hippotherium malpassii*, known from late Messinian deposits in Italy [66, 67]. *Hippotherium malpassii* had an incomplete skull (IGF 5286 V) of a juvenile specimen measuring ca. 22.5 cm, metacarpals (IGF 8192 V and 9397 V) that were 21.4 and 21.6 cm long, a metatarsal (IGF 8193 V) measuring 24.0 cm long, proximal phalanges III (IGF 9390 V and 9391 V; NHMB JH129, JH 158, Nonnumb1) that averaged 6.3 cm long (58.4–67.0), and left central hoof impressions 8.4 (OS-3), 8.3 (OS-4), and 7.0 (OS-5) cm long. Utilizing the *Hippotherium* multipliers (**Table A1**) yields heights of the trackmaker of 131.2 cm (from the metacarpals), 128.4 cm (from the metatarsals), and 128.0 cm (from the proximal phalanges III). The *Hippotherium* hoof multiplier (**Table A1**) results in estimated heights of 91.0 cm (OS-3), 89.9 (OS-4), and 75.8 (OS-5). Lacking a good skull-length measurement, applying the formula of 50% weight given to the hoof values and 50% weight to the postcrania, we arrive at height estimations of 110.1 cm (OS-3), 109.6 cm (OS-4), and 102.5 cm (OS-5) for the trackmaking *Hippotherium malpasii* individuals.

This gives very high values of stride length/height of 3.12, 3.30, and 3.35, respectively. The high ratio of stride length/height as well as the trackway consisting of four independent prints, plus, the fact that the distance between the prints varies, consisting of short, long, and intermediate steps, strongly suggest a galloping gait here, not the trot as suggested by Dalla Vecchia and Rustioni [28] who perhaps misinterpreted the capped trotting trackway shown in Renders [23, 24] as being isolated impressions. Two of the gallops possessed a left-lead (OS-3 and OS-4) and the other a right-lead (OS-5) as reconstructed by Dalla Vecchia and Rustioni [28] and occurred at speeds of 6.2–6.5 m/s using the Modified Alexander Formula.

The trackway WB-1 formed by the late Pleistocene monodactyl horse in fluvial sands and silts at the Wally's Beach deposit (DhPG-8) of St. Mary's Reservoir near Cardston in Alberta, Canada, has previously been referred to horse skeletal remains found at Wally's Beach assigned to the species *Equus conversidens* ([25, 30, 68]; see **Figure 12C** above). Further study, however, has caused us to question that specific identification. The skeletal morphology of the Wally's Beach *Equus* contains features now excluded from the definition of *E. conversidens* [69], namely, infundibulae on at

least one of the lower incisors (typically I^3), and lower molars with a moderately-long ectoflexid that approaches the isthmus but does not penetrate it. The Wally's Beach horses, however, do have more of a deep U-shaped linguaflexid rather than a V-shaped or shallow U-shaped one, cheek teeth with a moderate anterior heel and moderately long protocones, and thick, short legs rather than long stilt-like ones. Such characteristics match closely with the specimens of *Equus lambei* found in Gold Run Creek in the Yukon Territory and in the Bluefish Caves near Edmonton, Ontario, Canada [70–75], as well as with populations formerly classified as *E. conversidens* from a site in the city of Canyon, Randall County, Texas, and a few other Texas locations [70, 76]. McNeil [68], after a careful comparison, placed the Wally's Beach individuals in *E. conversidans* rather than *E. lambei*, but this was based mainly on size ratio differences rather than discrete characteristics, apart from the smaller and less common canines in the Wally's Beach populations, more complex plications on upper cheek teeth of the Wally's Beach specimens, and more prominent and angular masseter ridges on the skulls of the Wally's Beach horses as compared to *E. lambei* specimens from the Bluefish Caves in the Yukon Territory. We, however, do not consider these differences profound enough to differentiate the two populations of horses on a specific level and indeed *E. lambei* found at Canyon, Randall County, Texas have somewhat complex plications in the upper cheek teeth [70, 76]. The Yukon *E. lambei* skull (USNM 8426) has a fairly prominent masseter ridge as well [75], and McNeil [68] admits that other Yukon specimens of *E. lambei* have well-defined masseter ridges approaching those from Wally's Beach. Hence we consider the Wally's Beach fossil horses to be members of the species *E. lambei* rather than *E. conversidens* (see also [77]). A third option would be to group the Wally's Beach horses with modern horses in *Equus ferus* [70], but we believe the shorter size of the Wally's Beach horses overall, along with their possession of short but moderately-stout metapodials, a broad skull with a quite convex ventral border of the mandible, and the greater presence of canines in certain populations (such as in the Bluefish Caves though not at Wally's Beach) preclude that assessment. Hence we assign the prints to *Equus lambei*, preferring to keep this taxon distinct from that of *Equus alaskae* which some authors combine it with [78].

In any case, skeletal remains are found in the same Wally's Beach strata as the footprints, and the phalanges match the prints closely. Such horses from Wally's Beach possessed a skull that averaged 41.3 cm in length, a metacarpal averaging 21.6 cm, a metatarsal averaging 26.1 cm, a hind proximal phalanx III (1PhIII) that averaged 8.1 cm, and a hind distal phalanx III (3PhIII) that averaged 5.7 cm in length, along with a humerus that averaged 28.4 cm in length and the radius 31.5 cm [68], and the central hoof impressions were 10.5 cm long. Using the horse height estimation multipliers for extinct *Equus* species (**Tables A1** and **A2**), and the skeletal material from Wally's Beach itself, would yield the following height estimations: 90.9 (from the skull), 117.1 (from the third metacarpal), 127.9 (from the third metatarsal), 129.7 (from the proximal phalanges), 133.5 from the distal phalanges, and 138.2 cm from the front hoof impression. Using our height estimation formula of assigning 50% weight to the prints, 25% to the skull, and 25% to the postcrania would yield an estimated height of 120.5 cm for the trackmaker of the species *Equus lambei*. This would give a large ratio of stride length/height of 2.96 and be indicative of a gallop, along with the occurrence of short, intermediate, and long step distances rather than more uniform ones. Such a gallop would have been a left-lead one that occurred at a speed of 6.6 m/s using the Modified Alexander Formula.

4.4 Walking gaits in fossil horses

So far very few walking equid gaits have been identified from fossil trackways, perhaps because the horse is less likely to leave a trail in the softer impact of the walk. Recently what does seem to be such a walking trackway [DR-1] was uncovered in regard the recently extinct Giant Cape Zebra (*Equus capensis*) from Driefontein, South Africa, 14 km east of Still Bay. The trackway was made in coastal sands around 109–161 ka. The trackway consists of 12 tracks and is 320 cm long in toto. One cycle of understepping prints has a stride length of ca. 144 cm, an ipsilateral step distance [ISD] of −27.5 cm, a diagonal step distance [DSD] of ca. 33.3 cm, an average lateral offset of ca. 5.1 cm, and an interior straddle of ca. −2.0 cm. The average SDL though was 147 cm, the average ISD was −25.7 cm, and the average DSD was 23 cm. The front hoofprint measured ca. 13.74 cm in length and 12.44 cm in width and the hind footprint (noticeably more oval in shape) measured ca. 15.44 cm in length and 11.15 cm in width ([79], pp. 6–7 and Figure 5).

The height of Equus capensis can be estimated on the basis of comparisons with modern zebra skeletal dimensions (see **Tables A3** and **A4**). The hippotigrine multipliers are 2.64 for the cranium, 6.15 for the third metacarpal, 5.44 for the third metatarsal, 16.36/17.29 for anterior and posterior first phalanx, 22.95 for anterior third phalanx, and 17.32/17.11 for manus and pes hoof measurement, and 13.74 and 12.72 for manus and pes print measurement. Equus capensis has the following skeletal maximal lengths: cranium = 56.0 cm, metacarpal = 21.6 cm, metatarsal = 25.4 cm, phalanx I (manus/pes) = 8.4/8.1 cm, phalanx III manus = 7.7 cm, and the print of the fossil specimen was ca. 13.74 cm long for the manus and 15.44 cm long for the pes. These values yield the following height estimations in cm of *Equus capensis*: 147.8 (from cranium), 132.8 (from third metacarpal), 138.2 (from third metatarsal), 137.4/140.0 (from first phalanx), 176.7 (from third phalanx), 188.8/196.4 (from footprints), or yielding a final height estimate of 169.5 cm (from our formula). This is a bit larger than the estimation of 135.0–159.0 cm in Eisenmann [42], due to the very large nature of the footprints.

With this height estimation we have the following key trackway parameters of SL/HT = 0.85; ISD/SL = −0.18; DSD/SL = 0.23; DSD/ISD = −1.30; LO/HHW = 0.46; IS/HHW = −0.18. These parameters most closely agree with the gait of a walk (taking place at around 0.77 m/s via the original Alexander formula for slow gaits), though the negative interior straddle (and wavy print pattern) have some resemblance to a slow ambling gait such as a running walk (see **Figures 4** and **5E**). Might it be that when traveling over slippery terrain horses tend to shift their limbs interiorly and closer to or straddling the centerline for balance? If so some gaits that appear to be very slow racking ones would actually be trotting ones. More study of this issue is warranted. Alternatively, ancient equines might be capable of very slow alternative lateral gaits, perhaps on slippery substrates. Still trackway DR-1 seems to most closely match that of a walking gait.

5. Conclusion

We find that horses displayed a great variety of gaits in the past, perhaps matching their current repertoire. The footprints studied above show they were capable of both intermediate-speed laterally coordinated gaits such as the running walk and rack or tölt, the diagonally coordinated trot which is the common current medium-speed gait

in horses and zebras, and the transverse gallop. All these gaits are found in tridactyl Miocene horses (15–3.5 Ma) and provided a variety of options for locomotion. Laterally coordinated gaits allow surer footing in intermediate speed gaits when traveling over uneven or muddy terrain; for they provide a diagonal base of support (pace) or continual ground contact throughout the stride (rack or running walk). Following Sondaar [84], such lateral gaits would have been easier than diagonal gaits on the more flexible fetlock joints of tridactyl horses and so helped to prevent injury [22]. Intermediate speed diagonal gaits, such as the trot, are more efficient than lateral ones for longer periods of travel, and so would have been favored for migratory needs.

If these laterally coordinated gaits were common in fossil horses, exactly when horses lost the ability to perform laterally coordinated gaits and retained only the trot, as in zebras, is hard to determine. Janis and Bernor [47] argue that the evolution of monodactyl limbs in *Dinohippus*, *Pliohippus*, and *Equus* in the Miocene built upon a pre-existing suspensory apparatus system in the horse limbs (first seen in tridactyl members of the subfamily Equinae) that allowed elastic return of bouncing energy during the stride cycle, and that this in turn would favor development of the trot for more efficient locomotion over long distances. They speculate that as horses began to adapt to the more open plains they required longer dietary migrations, which in turn favored the development of monodactyly and a trotting gait. Tridactyl horses, even functionally monodactyl ones with reduced lateral legs, would have had mechanical reasons, according to Janis and Bernor [47], to utilize lateral gaits as these allowed for fast locomotion over shorter distances with less hyperextension and compression of the limb joints and for great stability on uneven terrain with a diagonal base of support. This may well be one reason horses and zebras began to lose the ability to engage in lateral gaits. We do find, however, trotting gaits present in tridactyl horses as well as lateral ones in this study. In any case the function of the reduced lateral digits in the Miocene and Pliocene is still in dispute as lateral hoof impressions occurred in some of the trackways studied above (HSA-9 to 14; OS-3 to 5; LAET-B) but not in others (LAET A; GQ-1), and in the LAET-B impression (n. 7) the side toe impressions occur in a more anterior location and more deeply, suggesting lots of flexing of the fetlock joint and use of the side toes for extra support, whereas the side toe impressions in trackways HSA-9 to 14 and OS-3 to 5 tend to occur at the rear of the central hoof impression and less deeply, suggesting light contact during extreme flexion or deep impressions. The lateral digits likely had more than one function such as aiding in limb stabilization, balance, and proprioception, preventing over-compression of the joints, and giving increased traction on uneven or slippery surfaces and during rapid turns [23, 24, 47, 85].

Moreover, the evolution of the passive stay apparatus is also complex as it occurs in the monodactyl *Dinohippus* (ca. 10.3 Ma) horse to the greatest degree but is also found in the earlier tridactyl horses *Acritohippus stylodontus* (ca. 15.3–14.9 Ma) and *Hypohippus equinus* (ca. 20.4–16.0 Ma), perhaps having arisen independently in the latter [86–89]. Hence we are still in the early stages of untangling the biomechanics and functional anatomy of fossil horse feet.

Genetic studies have concluded that laterally coordinated gaits in modern horses trace back to a gene mutation that occurred around the time of horse domestication prior to 10,000 years ago [21], or, for some breeds, to a genetic mutation arising in ninth century England [90]. Genetical studies suggest then that the modern ability to perform lateral gaits in select horse breeds is a parallel evolutionary innovation rather than a reversion to an ancestral condition. This would make sense, as after

domestication riders would have preferred smoother more comfortable gaits over less comfortable ones; hence laterally coordinated gaits would have been prized. Indeed fossil horse trackways show lateral gait parameters indicative of higher-speed racks even though they seem to have been performed at slower speeds. So the particular mechanisms and limb coordinations used in fossil horses may have been different than in modern horses, but this is not clear.

Also of interest is the social behavior evident in the Pliocene trackways. Four zones display multiple horses engaging in the same or similar gaits nearby each other, probably at around the same time. We see three series of prints (HSA-9, HSA-10, HSA-11) of the species *Cremohipparion matthewi* located next to each other and orientated in the same general direction displaying a trot at the Hoya de la Sima site near Jumilla, Murcia, Spain around 8.7–7.8 Ma [31, 33]. Three other print series (HSA-12, HSA-13, HSA-14) located near each other and orientated in the same general direction at the same Hoya de la Sima all show horses in a gallop, as do two or three similar trackways (OS-3, OS-4, and OS-5) of *Hippotherium malpassii* found at the Colle di Osoppo site, near Osoppo, Italy from ca. 6.0–5.3 Ma [28]. Finally, three horse trackways of the species *Eurygnathohippus hasumense* orientated in the same direction and in similar medium-speed gaits [two in a rack or tölt (LAET-A and LAET-C) and another in a running walk (LAET-B)] located near each other occur at Laetoli site 8-G in Tanzania were laid down around 3.7 Ma. This shows a common occurrence found in wild horses and zebras today of herding behavior displayed during locomotion. Hence it appears that horses have long been a social species and move together in a herd. We also see evidence of differing gaits within the herd (assuming the trackways were made close in time to each other). At the Hoya de la Sima site in Jumilla, Spain, there are not just three sets of galloping prints side by side proceeding in the same direction but there are also three trackways of horses engaged in a trot (HSA-9, HSA-10, HSA-11) located side by side and going in the same direction but crossing over the galloping tracks at a perpendicular angle (HSA-12, HSA-13, HSA-14). This could be due to some of the younger horses playing while the older horses were traveling to a certain location, as happens in modern herds (Renders, pers. observations). Two of the trotting track-ways (HSA-9-10) had slightly smaller hind footprints averaging 13.7 cm in length and 10.9 cm in width, consistent with juvenile trackways, as compared to the galloping trackways (HSA 12-14) which averaged 14.6 cm in length and 13.4 cm in width [31, 33]. The hind footprint of trotting trackway HSA-11, however, was fairly large at 15.1 cm long by 12.3 cm wide so might have been that of an adult. In the Laetoli *Eurygnathohippus* site we see two horses, an adult (LAET-A) and a juvenile (LAET-C), with trackways displaying a rack or tölt, while the trackway of what is likely a mare (LAET-B), in that it slows down and crosses over the juvenile trackway, displays a running walk or intermediate-speed rack. Here as noted earlier the mare may have used a slightly different laterally coordinated gait to match the speed of her foal or avoid a collision.

There are a few other fossil horse sites that constitute trample grounds with multiple individuals leaving footprints. It is possible that further fieldwork may be able to isolate individual trackways for which gait can be determined [91–95]. Additional study would also be beneficial in regard to unshod horse hoofs of modern horses and the impressions they make in various substrates such as sand, mud, ash, and snow. Regarding fossil horses, more work correlating front and hind central coffin bone measurements with horse height would be helpful, especially for Eocene and Oligocene horses.

5.1 Sample availability

The *Scaphohippus sumani* footprints came from a quarry and had to be preserved in molds before they were destroyed. The molds and portions of the original trackway are housed at the San Bernardino County Museum, Redlands, California: location SBCM 1-130-394, holotype SBCM L1816-3436 (though at last report they are listed as missing; see photos in **Figure 10A–D** above, however, of the molds displaying the trackway). A few of the *Equus lambei* footprints are housed at the Royal Alberta Museum, Edmonton, Alberta: specimens DhPg-8 3840-3843, while several trackways have been resubmerged at St. Mary's Reservoir, Alberta, Canada. The *Eurygnathohippus hasumense* footprints are still located underground at Site G in Laetoli, Tanzania (a cast made of a portion of the trackway can be found in the Olduvai Gorge Museum, Tanzania). A few of the footprints of *Cremohipparion matthewi* found at the Hoya de la Sima site are housed at the Museo Municipal of Jumilla, Spain, but the bulk of the trackways are now protected by a structure at the trackway site. The trackways located at the Sierra del Colmenar site near Elche, Spain and the Colle di Osoppo site near Osoppo, Italy are still located in the field.
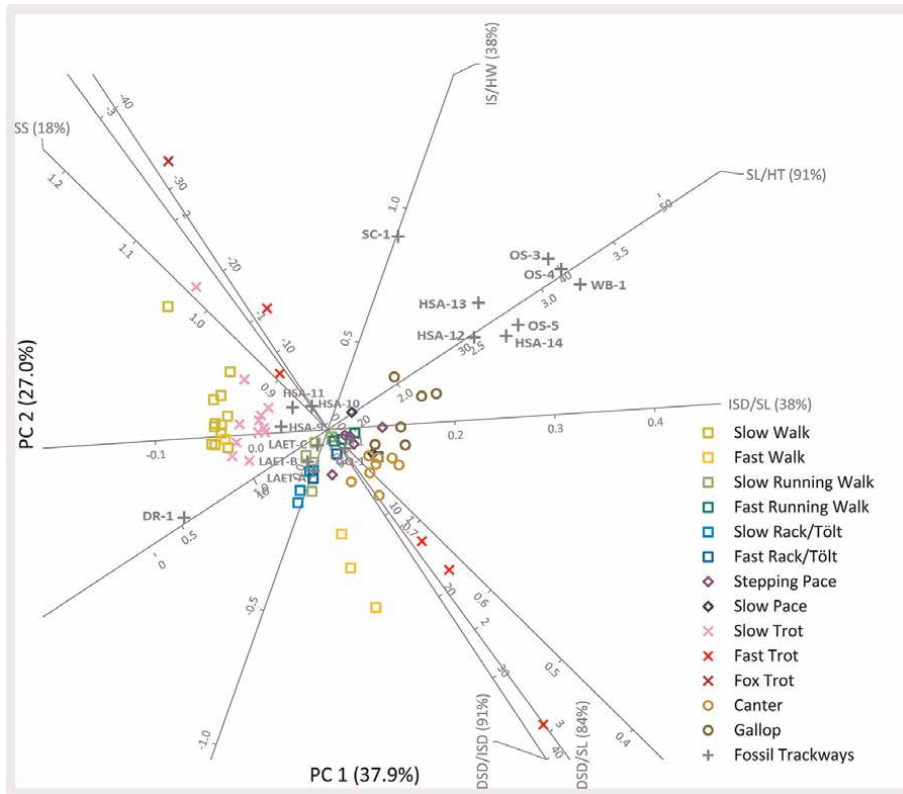
Acknowledgements

Appendix A

Figure A1.
Six-factor principal component analysis of fossil horse trackways plotted against modern horse trackways: step symmetry (SS); interior straddle/hoof width (IS/HW); stride length/height (SL/HT); ipsilateral step distance/ stride length (ISD/SL); diagonal step distance/stride length (DSD/SL); and diagonal/ipsilateral step distance (DSD/ISD). Trackways SC-1, OS-3, OS-4, OS-5, HSA-12, HSA-13, HSA-14, and WB-1 parameters indicative of galloping gaits; HSA-9, HSA-10, and HSA-11 parameters indicate of trotting gaits; trackways LAET-A, LAET-B, and LAET-C parameters indicative of racking gait (or running walk); and trackway DR-1 suggestive of walk.

Equine group	Height/ cranium	Height/ metacarpal III	Height/ metatarsal III	Height/ proximal (1st) phalanx III (front) (hind)		Height/ distal (3rd) phalanx III (front) (hind)		Height/front hoof length (print)
Propalaeotheriinae	**1.97**	**6.25**	**5.56**	**30.00**	**27.27**	**37.5**	**30.00**	**22.83**
Eurohippus	1.97	6.25	5.56	30.00	27.27	37.5	30.00	22.83
Hyracotheriinae	2.55	7.44	5.44	29.50	23.80	32.37	25.25	19.70
Sifrhippus	2.62	8.11	5.95	32.45	23.80	35.70	25.50	21.73
Protrorohippus	2.52	6.76	5.15	26.54	—	34.50	—	21.00
Orohippus	2.50	7.45	5.22	—	—	26.92	25.00	16.39

Equine group	Height/ cranium	Height/ metacarpal III	Height/ metatarsal III	Height/ proximal (1st) phalanx III (front) (hind)		Height/ distal (3rd) phalanx III (front) (hind)		Height/front hoof length (print)
Propalaeotheriinae	**1.97**	**6.25**	**5.56**	**30.00**	**27.27**	**37.5**	**30.00**	**22.83**
Anchitheriinae, basal	2.92	5.15	4.19	35.58	30.84	27.29	22.51	16.61
Mesohippus	2.63	5.23	4.00	35.38	30.67	24.21	23.00	14.74
Miohippus	3.20	5.06	4.38	35.78	31.01	30.37	22.02	18.49
Merychippines	2.77	5.40	4.68	24.30	23.42	23.91	24.42	14.55
Acritohippus	2.77	5.40	4.68	24.30	23.42	23.91	24.42	14.55
Protohippini	2.72	5.47	4.92	24.08	23.45	21.73	26.21	13.23
Protohippus	2.72	5.47	4.92	24.08	23.45	21.73	26.21	13.23
Anchitheriini	3.20	5.25	4.72	29.61	27.82	22.08	22.69	13.44
Kalobatippus	3.44	5.07	4.38	33.03	29.44	22.08	20.38	13.44
Hypohippus	2.96	5.42	5.05	26.19	26.19	—	25.00	13.16
Hipparioni	2.55	5.75	5.08	20.53	20.87	19.83	20.11	12.07
Hipparioni, New World	2.64	4.73	4.17	19.65	20.98	21.27	22.65	12.95
Neohipparion	2.64	4.73	4.17	19.65	20.98	21.27	22.65	12.95
Hipparioni, Old World	2.50	6.26	5.54	20.98	21.67	19.11	17.57	11.63
Hippotherium	2.73	6.10	5.35	20.31	20.31	17.80	17.57	10.83
Plesiohipparion	2.27	6.42	5.73	21.64	23.02	20.42	—	12.43
Equini, basal	2.99	6.48	5.89	21.88	24.02	28.49	31.41	17.34
Pliohippus	2.99	6.48	5.89	21.88	24.02	28.49	31.41	17.34
Equini, caballoid, extinct	2.20	5.42	4.90	14.90	16.01	20.88	21.33	12.71
Equus	2.20	5.42	4.90	14.90	16.01	20.88	21.33	12.71
Equini, extant (*Equus ferus caballus*)	2.51	6.08	5.33	15.84	15.84	21.62	22.54	13.16
Other Perisssodactyla								
Tapiroidea, *Helatelidae*	2.83	5.97	4.51	18.41	23.26	22.10	27.63	7.73
Rhinocerotoidea, *Hyrachus*	2.58	7.81	6.48	28.32	34.88	—	30.07	—
Palaeotheriidae, *Palaeotherium*	2.53	9.79	11.71	47.24	—	—	—	—

Table A1.
Height/skeletal element ratios (multipliers) for fossil horses (after [7]).

Gait	Diagonal/ ipsilateral step distance	Ipsilateral step distance/ stride length	Interior straddle/ hind hoof width	Lateral offset/ hoof width	Average stride length/ height	Diagonal/ ipsilateral step distance multiplier for SL/H
Slow walk (n = 14)	−7.96	−0.06	0.17	0.15	1.02	−0.13
Fast walk (n = 4)	11.75	−0.01	0.04	0.23	1.13	0.10
Slow trot (n = 11)	−5.02	−0.11	0.15	0.29	1.30	−0.25
Fast trot (n = 6)	11.70	−0.01	0.16	0.39	1.71	0.15
Running walk (n = 8)	1.21	0.16	0.00	—	1.40	1.16
Slow rack/Tölt (n = 4)	2.54	0.10	−0.12	0.21	1.21	0.48
Fast rack/Tölt (n = 3)	0.37	0.28	−0.37	0.58	1.51	4.08
Stepping pace (n = 5)	0.26	0.31	−0.15	0.59	1.59	6.12
Slow pace (n = 2)	0.26	0.30	0.10	1.12	1.49	5.73
Canter (n = 8)	0.40	0.28	0.15	—	1.59	3.98
Gallop (n = 6)	0.61	0.25	0.48	—	1.89	3.10

Table A2.
Average linear stride ratios for various gaits (data from [25, 34]; original data, 2022).

Species	Geologic age (Ma)	Height at withers (cm)	Cranial basilar length (cm)	Metacarpal III length (cm)	Metatarsal III length (cm)	Proximal (1st) phalanx III length front/hind (cm)	Distal (3rd) phalanx III length front/hind (cm)	Hoof print length front/hind (cm)	Specimen and source
Equus capensis	1	—	56.0	21.6	25.4	8.4/8.1	7.7/—	—	SAM-EL 21025; SAM-EL 16659; [42, 80, 81]
Equus capensis	0.11–0.16	—	—	—	—	—	—	14.1/15.6 (print)	DR-1; [79]
Equus grevyi	0	145.0 (150.0)	ca. 51.4	23.2	26.7	8.6/8.2	6.5/—	8.0/8.0 (hoof)	NMUK-ZD 1923.10.20.16 [82, 83]
Equus quagga burchelli	0	125.5 (123.0–128.0)	47.2 (44.9–49.4)	20.2	22.6	7.5/7.1	5.6/—	7.6 (7.42–7.70)/7.8 (7.38–8.3) (hoof) (9.5/10.0) (print)	PH 6317; [79, 82, 83]
Equus zebra hartmannae (*zebra*)	0	125.5 (124.0–127.0)	ca. 51.7	20.9	23.5	8.1/7.6	5.2/—	(8.8 (7.5, 9.0, 10.0)/ 9.7 (8.0, 10.0, 11.0)) (print)	AM 7691; [79, 82, 83]

Table A3.
Key morphometric parameters of modern Hippotigrine species (useful for estimating height of related fossil species).

Equine group	Height/ cranium	Height/ metacarpal III	Height/ metatarsal III	Height/ proximal (1st) phalanx III (front) (hind)	Height/distal (3rd) phalanx III (front) (hind)	Height/front hoof length (print) (front) (hind)
Equus grevyi	2.82	6.25	5.43	16.86/17.68	22.31/—	18.13/18.13 (—/—)
Equus quagga burchelli	2.66	6.21	5.55	16.73/17.68	22.41/—	16.51/16.09 (13.21/12.50)
Equus zebra hartmannae (*zebra*)	2.43	6.00	5.34	15.49/16.51	24.13/—	—/— (14.26/ 12.94)
HIPPOTIGRINES	2.64	6.15	5.44	16.36/17.29	22.95/—	17.32/17.11 (13.74/12.72)

AM = American Museum of Natural History, New York, USA; NHMUK = British Museum of Natural History, London, UK; PH = Academy of Natural Sciences, Philadelphia, USA; SAM-EL = South African Museum, Cape Town, Republic of South Africa—Elandsfontein Section.

Table A4.
Height/skeletal element ratios (multipliers) for fossil zebras.

Author details

Elise Renders[1] and Alan Vincelette[2]*

1 Faculty of Veterinary Medicine, Department of Functional Morphology, Utrecht University (Ret.), Utrecht, The Netherlands

2 Department of Pretheology, St. John's Seminary, Camarillo, California, USA

*Address all correspondence to: avincelette@stjohnsem.edu

IntechOpen

References

[1] Biknevicius AR, Reilly SM. Correlation of symmetrical gaits and whole body mechanics: debunking myths in locomotor biodynamics. Journal of Experimental Zoology. 2006; **305A**:923-934

[2] Hildebrand M. Analysis of tetrapod gaits: General considerations and symmetrical gaits. In: Herman RM, Grillner S, Stein PSG, Stuart DC, editors. Neural Control of Locomotion. New York: Plenum Press; 1976. pp. 203-236

[3] Hildebrand M. Analysis of asymmetrical gaits. Journal of Mammalogy. 1977;**58**:131-156

[4] Hildebrand M. The adaptive significance of tetrapod gait selection. American Zoology. 1980;**20**:255-267

[5] Robilliard JJ, Pfau T, Wilson AM. Gait characterisation and classification in horses. Journal of Experimental Biology. 2007;**210**:187-197

[6] Starke SD, Robilliard JJ, Weller R, Wilson AM, Pfau T. Walk–run classification of symmetrical gaits in the horse: a multidimensional approach. Journal of the Royal Society Interface. 2009;**6**:335-342

[7] Renders E, Vincelette A. Methodology for the determination of fossil horse gaits. Journal of Paleontological Techniques. 2023;7:1-25

[8] Bertram JEA, Gutmann A. Motions of the running horse and cheetah revisited: Fundamental mechanics of the transverse and rotary gallop. Journal of the Royal Society Interface. 2009;**6**: 549-559

[9] Bertram JEA. Understanding Mammalian Locomotion: Concepts and Applications. Hoboken, NJ: John Wiley; 2016. pp. 27-50

[10] Biancarti CM, Minetti AE. Biomechanical determinants of transverse and rotary gallop in cursorial mammals. The Journal of Experimental Biology. 2012;**215**:4144-4156

[11] Cartmill M, Lemelin P, Schmitt D. Support polygons and symmetrical gaits in mammals. Zoological Journal of the Linnean Society. 2002;**136**(3):401-420

[12] Dagg AE. Gaits in mammals. Mammal Review. 1973;**3**:135-154

[13] Hildebrand M. Walking and running. In: Hildebrand M, Bramble DM, Liem KF, Wake DB, editors. Functional Vertebrate Morphology. Cambridge, MA: Harvard University Press; 1985. pp. 38-57

[14] Hildebrand M. Symmetrical gaits of horses. Science. 1965;**150**:701-708

[15] Serra Bragança FM, Broomé S, Rhodin M, Björnsdóttir S, Gunnarsson V, Voskamp JP, et al. Improving gait classification in horses by using inertial measurement unit (IMU) generated data and machine learning. Scientific Reports. 2020;**10**:17785

[16] Nicodemus MC, Clayton HM. Temporal variables of four-beat, stepping gaits of gaited horses. Applied Animal Behaviour Science. 2003;**80**: 133-142

[17] Nicodemus MC, Clayton HM. 2001. Temporal variables of the Paso Fino stepping gaits. In: Ott E, Stull C, Burns P, Pipkin J, Malinowski K, editors. Proceedings of the 17th Equine Nutrition and Physiology Symposium. Lexington:

Equine Nutrition and Physiology Society, University of Kentucky. pp. 242-247

[18] Feldmann W, Rostock AK. Islandpferde Reitlehre: Leitfaden für Haltung, Ausbildung und Reiten von Islandpferden und anderen Freizeitpferderassen. Bonn: Gestüt Aegidienberg; 1988

[19] Gonçalves Fonseca M. Mangalarga Marchador: Estudo morfométrico, cinemático e genético da marcha batida e da marcha picada. São Paulo, Brazil: Universidade Estadual Paulista; 2018

[20] Muybridge E. Animals in Motion. New York: Dover; 1957

[21] Staiger EA, Abri MA, Silva CAS, Brooks SA. Loci impacting polymorphic gait in the Tennessee Walking Horse. Journal of Animal Science. 2016;**94**: 1377-1386

[22] Renders E, Sondaar PY. Animal prints and trails: Hipparion. In: Leakey MD, Harris JM, editors. Laetoli: A Pliocene Site in Northern Tanzania. Oxnard: Clarendon Press; 1987. pp. 471-481

[23] Renders E. Corrigendum: the gait of Hipparion sp. from fossil footprints in Laetoli, Tanzania. Nature. 1984;**308**:866

[24] Renders E. The gait of Hipparion sp. from fossil footprints in Laetoli, Tanzania. Nature. 1984;**308**:179-181

[25] Vincelette A. Determining the gait of Miocene, Pliocene, and Pleistocene horses from fossilized trackways. Fossil Record. 2021;**24**:151-169

[26] Bishop CW. The horses of T'ang T'ai-Tsung. The Museum Journal. 1918; **9**:244-272

[27] Zyderveld MC. De laterale symmetrische gangen, in het bijzonder die van het paard. Utrecht: Rijksuniversiteit Utrecht; 1991

[28] Dalla Vecchia FM, Rustioni M. Mammalian trackways in the Conglomerato di Osoppo (Udine, NE Italy) and their contribution to its age determination. Memorie di Scienze Geologiche. 1996;**48**:221-232

[29] Lancis C, Estévez A. Las icnitas de mamíferos del sur de Alicante (España). Geogaceta. 1992;**12**:60-64

[30] McNeil PE, Hills LV, Kooyman B, Tolman S. Significance of latest Pleistocene tracks, trackways, and trample grounds from Southern Alberta, Canada. In: Lucas SG, Spielmann JA, Lockley MG. Cenozoic Vertebrate Tracks and Traces. Albuquerque: New Mexico Museum of Natural History Bulletin. 2007;**42**:209-223

[31] Pérez-Lorente F, Serrano F, Rodríguez-Estrella T, Mancheño MA, Romero M. Pisadas fósiles de mamíferos en el Mioceno superior de La Hoya de la Sima (Jumilla, Murcia. España). Memorias de Arqueología. 1997;**12**:15-28

[32] Sarjeant WAS, Reynolds RE. Camelid and horse footprints from the Miocene of California. San Bernardino County Museum Association Quarterly. 1999;**46**:3-19

[33] Pérez-Lorente F, Serrano F, Rodríguez-Estrella T, Mancheño MA, Romero M. Pisadas fósiles de mamíferos en el Mioceno superior de La Hoya de la Sima (Jumilla, Murcia. España). Revista Espanola de Paleontologia. 1999;**14**: 257-267

[34] Renders E, Vincelette A. Laterally coordinated gaits in the modern horse (Equus ferus caballus). In: Kukovics S,

editor. Animal Husbandry. London: IntechOpen; 2022

[35] Leach DH, Ormrod K, Clayton HM. Standardised terminology for the description and analysis of equine locomotion. Equine Veterinary Journal. 1984;**16**:522-528

[36] Chrószcz A, Janeczek M, Pasicka E, Klećkowska-Nawrot J. Height at the withers estimation in the horses based on the internal dimension of cranial cavity. Folia Morphologica. 2014;**73**:143-148

[37] Hayashida S, Yamauchi C. Deduction of withers height from the length of the bone in the horse. Bulletin of the Faculty of Agriculture Kagoshima University. 1957;**6**:146-156

[38] Inoue M, Sakaguchi H. Estimating the withers height of the ancient Japanese horse from hoofprints. Anthropozoologica. 1997;**25-26**:119-130

[39] Onar V, Kahvecioğlu KO, Olğun Erdikmen D, Alpak H, Parkan YC. The estimation of withers height of ancient horse: New estimation formulations by using the metacarpal measurements of the living horse. Revue de Médecine Vétérinaire. 2018;**169**:157-165

[40] Stachurska A, Kolstrung R, Pięta M, Silmanowicz P. Hoof size as related to body size in the horse (Equus caballus). Animal Science Papers and Reports. 2011;**29**:213-222

[41] Eisenmann V. Nouveaux crânes d'hipparions (Mammalia, Perissodactyla) plio-pleistocénes d'Afrique orientale (Ethiopie et Kenia): Hipparion sp., Hipparion cf. ethiopicum et Hipparion afarense nov. sp. Geobios. 1976;**9**(5):577-605

[42] Eisenmann V. Equus capensis (Mammalia, Perissodactyla) from Elandsfontein. Paleontologia Africana. 2000;**36**:91-96

[43] Stock C. Neohipparion leptode (Merriam) from the Pliocene of northwestern Nevada. American Journal of Science. 1951;**249**:430-438

[44] Alexander RM. Estimates of speeds of dinosaurs. Nature. 1976;**261**:129-130

[45] Vilas L, Arias C, Rozycki A, Herrero C, Martínez-Abellán R. El yacimiento de icnitas de vertebrados de La Hoya de la Sima (Miocene Terminal), Jumilla, Murcia, España. De Re Metallica. 2006;**6-7**:1-6

[46] Reynolds RE. Horse hoof prints in the fossil record. In: Reynolds RE, editor. Making Tracks Across the Southwest: The 2006 Desert Symposium, California State University. Desert Studies Consortium and LSA Associates: Zzyzx, California; 2006. pp. 25-28

[47] Janis CM, Bernor RL. The evolution of equid monodactyly: a review including a new hypothesis. Frontiers of Ecology and Evolution. 2019;7:1-19

[48] Alberdi MT, Montoya P. Hipparion mediterraneum Roth & Wagner, 1855 (Perissodactyla, Mammalia) del yacimiento Turoliense inferior de Crevillente (Alicante, España). Mediterranea. 1988;7:107-143

[49] Pesquero MD, Alberdi MT, Alcalá L. New species of Hipparion from La Roma 2 (Late Vallesian; Teruel, Spain): a study of the morphological and biometric variability of Hipparion primigenium. Journal of Paleontology. 2006;**80**: 343-356

[50] Pesquero MD, Alberdi MT, Alcalá L. Remains of Hipparion (Equidae, Perissodactyla) from Puente Minero (Teruel Province, Spain) and their

implications for the systematics of the Turolian Hipparionini. Palaeontology. 2011;**54**:1303-1321

[51] Bernor RL, Tobien H. Two small species of Cremohipparion equidae (Mammalia) from Samos, Greece. Mitteilungen der Bayerischen Staatssammlung für Paläontologie und Historische Geologie. 1989;**29**:207-226

[52] Alberdi MT, Alcalá L. A study of the new samples of the Pliocene Hipparion (Equidae, Mammalia) from Spain and Bulgaria. Transactions of the Royal Society of Edinburgh-Earth and Environmental Sciences. 1999;**89**:167-186

[53] Crusafont M, Sondaar P. Une nouvelle espèce d'Hipparion du Pliocène Terminal d'Espagne. Palaeoverlebrata. 1971;**4**:59-66

[54] Eisenmann V, Mein P. Revision of the faunal list and study of Hipparion (Equidae, Perissodactyla, Mammalia) of the Pliocene locality of La Gloria 4, Spain. Acta Zoologica Cracoviensia. 1996;**39**:121-130

[55] Gromova V. Le genre Hipparion. Annales du Centre d'Ètudes et de Documentation Paleontologiques. 1952;**12**:1-288

[56] Armour-Chelu M, Bernor RL. Equidae. In: Harrison T, editor. Paleontology and Geology of Laetoli: Human Evolution in Context. Vol. 2. Dordrecht, Germany: Springer; 2011. pp. 295-326

[57] Bernor RL, Armour-Chelu M. Later Neogene hipparions from the Manonga Valley, Tanzania. In: Harrison T, editor. Neogene Paleontology of the Manonga Valley, Tanzania: A Window into the Evolutionary History of East Africa. Dordrecht, Germany: Springer; 1997. pp. 219-264

[58] Bernor RL, Armour-Chelu MJ, Gilbert H, Kaiser TM, Schulz E. In: Werdelin L, Sanders WJ, editors. Cenozoic Mammals of Africa. Berkeley, California: University of California Press. Berkeley; 2010. pp. 685-721

[59] Eisenmann V, Geraads D. The hipparion from the late Pliocene of Ahl al Oughlam, Morocco, and a revision of the relationships of Pliocene and Pleistocene African hipparions. Paleontologia Africana. 2007;**42**:51-98

[60] Hooijer DA. Miocene to Pleistocene hipparions of Kenya. Tanzania, and Ethiopia, Zoologische Verhandelingen. 1975;**142**:3-80

[61] Van der Made J. The large mammals of the Plio-Pleistocene of Africa: Afrotheria, Perissodactyla and Artiodactyla I. In: Domínguez Rodrígo M, Baquedano E, editors. The Cradle of Humanity: La cuna de la humanidad. Alcalá de Henares and Burgos: Museo Arquelógico Regional, Alcalá de Henares y Museo de la Evolución Humana, Burgos; 2014. pp. 324-336

[62] Bernor RL, Scott RS, Haile-Selassie Y. A contribution to the evolutionary history of Ethiopian hipparionine horses (Mammalia, Equidae): morphometric evidence from the postcranial skeleton. Geodiversitas. 2005;**27**:133-158

[63] Stoneburg BE, McDonald AT, Dooley AC, Scott E, Hohman CJH. New remains of middle Miocene equids from the Cajon Valley Formation, San Bernardino National Forest, San Bernardino County, California, USA. PaleoBios. 2021;**38**:1-10

[64] Merriam JC. Tertiary mammalian faunas of the Mohave desert. University of California Publications in Geological Sciences. 1919;**11**:437-585

[65] Pagnac D. Scaphohippus: a new genus of horse (Mammalia: Equidae) from the Barstow Formation of California. Journal of Mammalian Evolution. 2006;**13**:37-61

[66] Bernor RL, Kaiser TM, Nelson SV, Rook L. Systematics and paleobiology of Hippotherium malpassii n. sp. (Equidae, Mammalia) from the latest Miocene of Baccinello V3 (Tuscany, Italy). Bollettino della Societa Paleontologica Italiana. 2011;**50**:175-208

[67] Rook L, Bernor RL. Hippotherium malpassii (Equidae, Mammalia) from the latest Miocene (late Messinian; MN13) of Monticino gypsum quarry (Brisighella, Emilia-Romagna, Italy). Bollettino della Societa Paleontologica Italiana. 2013;**52**: 95-102

[68] McNeil PE. Bones and Tracks at Wally's Beach site (DhPg-8): An Investigation of the Latest Pleistocene Mega-Fauna of southern Alberta. Alberta: University of Alberta; 2009

[69] Scott E. The small horse from Valley Wells, San Bernardino, County, California. San Bernardino County Museum Quarterly. 1996;**43**: 85-89

[70] Barrón-Ortiz CI, Rodrigues AT, Theodor JM, Kooyman BP, Yang DY, Speller CF. Cheek tooth morphology and ancient mitochondrial DNA of late Pleistocene horses from the western interior of North America: Implications for the taxonomy of North American Late Pleistocene Equus. PLoS One. 2017; **12**:e0183045

[71] Burke A, Cinq-Mars J. Paleoethological reconstruction and taphonomy of Equus lambei from the Bluefish Caves, Yukon Territory, Canada. Arctic. 1998;**51**:105-115

[72] Forsten A. Equus lambei Hay, the Yukon wild horse, not ass. Journal of Mammalogy. 1986;**67**:422-423

[73] Harington CR, Clulow FV. Pleistocene mammals from Gold Run Creek, Yukon Territory. Canadian Journal of Earth Sciences. 1973;**10**: 697-759

[74] Harington CR, Eggleston-Stott M. Partial carcass of a small Pleistocene horse from last chance Creek near Dawson city, Yukon. Current Research in the Pleistocene. 1996;**13**:105-107

[75] Hay OP. Description of a new species of extinct horse, Equus lambei, from the Pleistocene of Yukon territory. Proceedings of the United States National Museum. 1917;**53**:435-443

[76] Dalquest WW, Hughes JT. The Pleistocene horse, Equus conversidens. American Midland Naturalist. 1965;**74**: 408-417

[77] Azzaroli A. The genus Equus in North America: the Pleistocene species. Paleontolographia Italica. 1998;**85**:1-60

[78] Winans MC. A quantitative study of the North American fossil species of the genus Equus. In: Prothero DR, Schoch RM, editors. The Evolution of Perissodactyls. Oxford: Clarendon Press; 1989. pp. 262-297

[79] Helm C, Carr A, Cawthra H, De Vynck J, Dixon M, Gräbe P, et al. Tracking the extinct giant Cape zebra (Equus capensis) on the Cape south coast of South Africa. Quaternary Research. 2023;**114**:1-13

[80] Hendey QB, Deacon HJ. Studies in palaeontology and archaeology in the Saldanha region. Transactions of the Royal Society of South Africa. 1977;**42**: 371-381

[81] Eisenmann V, Kuznetsova T. Early Pleistocene equids (Mammalia, Perissodactyla) of Nalaikha, Mongolia, and the emergence of modern Equus Linnaeus, 1758. Geodiversitas. 2004;**26**: 535-561

[82] Eisenmann V. Old world fossil Equus (Perissodactyla, Mammalia): extant wild relatives and Incertae Sedis Forms. Quaternary. 2022;**5**:e38

[83] Cirilli O, Pandolfi L, Rook L, Bernor RL. Evolution of Old World Equus and origin of the zebra-ass clade. Scientific Reports. 2021;**11**:e10156

[84] Sondaar PY. The osteology of the manus of fossil and recent Equidae with special reference to phylogeny and function. Verhandelingen der Koninklijke Nederlandse Akademie van Wetenschappen. 1968;**25**:1-76

[85] Thomason JJ. The functional morphology of the manus in tridactyl equids Mercyhippus and Mesohippus: paleontological inferences from neontological models. Journal of Vertebrate Paleontology. 1986;**6**:143-161

[86] Gidley JW. Revision of the Miocene and Pliocene Equidae of North America. Bulletin of the American Museum of Natural History. 1907;**23**:865-934

[87] Scott WB. The mammals of the deep river beds. American Naturalist. 1893;**27**: 659-662

[88] Hermanson JW, MacFadden BJ. Evolutionary and functional morphology of the shoulder region and stay-apparatus in fossil and extant horses (Equidae). Journal of Vertebrate Paleontology. 1992;**12**:377-386

[89] Pajak A, Vincelette A. "Merychippus" stylodontus and "M." intermontanus: Biostratigraphy and basic morphology of Two Barstovian Tridactyl Horses. San Bernardino County Museum Quarterly. 1991;**38**:80-85

[90] Wutke S, Andersson L, Benecke N, Sandoval-Castellanos E, Gonzalez J, Hallsson JH, et al. The origin of ambling horses. Current Biology. 2016;**26**: R697-R699

[91] Casamiquela RM, Chong Diaz G. Icnitas (Mammalia, Equidae?) en rocas dei Plio-Plesitoceno de la costa Prov. de Antofagasta, Chile. Actas del Primero Congreso Argentino de Paleontología y Bioestratigrafía. 1975;**1**(2):87-103

[92] Herrero C, Herrero E, Martín-Chivelet J, Pérez-Lorente F. Vertebrate ichnofauna from Sierra de las Cabras tracksite (Late Miocene, Jumilla, SE Spain): mammalian ichnofauna. Journal of Iberian Geology. 2022;**48**:241-279

[93] Koenigswald WV, Sander PM, Walders M. The upper Pleistocene tracksite Bottrop-Welheim (Germany). Acta Zoologica Cracoviensia. 1996;**39**: 235-244

[94] Morgan GS, Williamson TE. Middle Miocene (Late Barstovian) mammal and bird tracks from the Benevidez Ranch Local Fauna. New Mexico Museum of Natural History and Science Bulletin. 2007;**42**:319-330

[95] Santucci VL, Nyborg T. Paleontological resource management, systematic recording, and preservation of vertebrate tracks within Death Valley National Park, California. San Bernardino County Museum Association Quarterly. 1999;**46**:21-26

Chapter 5

Role of Dopamine Receptors in Olfaction Learning Success

Muhammad Fahad Raza

Abstract

Several biogenic amines neurotransmitters are involved in various social behaviors, including olfaction learning behavior, cast differentiation, generation overlapping and sociability in honeybees. One of the brain's primary functions is remembering and learning the information related to food and odor. Dopamine (DA) is an important signaling molecule derived from the amino acid tyrosine. It is also known as a key neurohormone, neuromodulator and neurotransmitter in vertebrates as well as invertebrates and several studies indicated their important role in olfaction success, rewarding prediction, learning, memory, motor functions, sleep and arousal, aggression, and numerous other behaviors. Evidence suggests that DA plays several roles in honeybees, especially in olfaction success. Three DA receptors, AmDOP1, AmDOP2 and AmDOP3, have been characterized and clones. In this chapter, I focus on the regulation and involvement of the DA in olfactory learning behavior, locomotor function, motivation, and happy memories. This chapter represents an attempt to associate the role of dopamine receptors in olfaction success in honeybees.

Keywords: honeybees, neurotransmitters, dopamine receptors, olfactory learning behavior, olfaction success

1. Introduction

As the population of human grows, habitat loss caused by anthropogenic landscape changes endangers the health and survival of several species. Because of the rising need for food and biofuels due to human population growth, more land must be devoted to agricultural output [1]. To accommodate this need, the usage of land has changed globally, with natural areas and smaller-scale agricultural operations being converted into high-yielding monocultures, but at a cost [2, 3]. Monocultures may significantly affect water, soil, and air quality. When combined with the destruction of natural, noncrop habitats, this type of agriculture has been linked to pollinator population decreases [4]. Concerns have been raised about diminished pollination of crops and wild plants, which might lead to decreased agricultural productivity and ecological service delivery. Honeybees are known as the most economical and important pollinator insects worldwide [5]. Like other pollinating bee species, recently, honeybees faced harsh environmental factors that caused as high as 65% colony losses worldwide. This rate is more significant than apiculturist believes acceptable because of higher expenses for hired pollination services. Several stresses, including genetic, neuroscience, biotic,

abiotic, nutritional shortage, and pesticide exposure, are known as potentially interacting stressors, and all are correlated with anthropogenic influence [6].

All social insects interact with our environment for survival through olfactory learning behavior. Among all social insects, Honeybees are important insects of biodiversity on which our planet depends for survival; they provide us with high-quality food and other product such as royal jelly, honey, pollen, beeswax, bee venom and propolis [7]. The honeybee is an essential pollinator for our planet's survival. Honeybees have olfaction behavior for their survival and food seeking. The seeking of food and water resources exposes honeybees to conspecific competition and predation, leading to learning behavior responses to smell, visual cues, specific locations and other relevant stimuli [8, 9]. The olfactory learning behavior is more critical for the survival of the colony and seeking of nectar, pollen and water. This form of learning plays a significant role in foraging and food collection [10].

2. Types of learning behaviors in honeybees

For neuroethological research, insects are considered favorable organisms due to their nervous system and tiny brain. Insects' central nervous system CNS is highly organized, with distinct separations between multisensory neuropils in the brain and sensory-motor neuropils in the ventral cord [11].

The insects have rich behaviors, including visual, space, time, mechanical communication, chemical communication, and complicated motor functioning for olfactory learning walking, flying, nest building, defense, swimming, learning and memory; however, these behaviors are not generally regarded as strengths of insects [12]. After all, genetically designed neural circuitry frequently considers insect behaviors highly standardized and tightly controlled. This viewpoint, however, does not do credit to the insect group Hymenoptera (wasps, bees, ants). Most insect species of Hymenoptera care for their brood either as a female social group or individual females. Subsequently, they return to their nesting site on a daily basis to protect, feed, store food, feed to larvae and defend themself from unfavorable environmental circumstances [13]. Because they seek food (pollen, prey and nectar on blossoms) in unexpected places, they must learn terrestrial and celestial cues that drive their long-distance foraging trips and enable them to locate their nest locations [14]. The forager's bees learn to position of sun and the pattern of the sky of polarized sunlight to the time of day [15] and locations are remembered in connection to the nesting spot using the time-compensated sun compass. The bees communicate the distance and direction of a food place to colony mates by performing waggle dance (a performed body movement). Associative learning is essential to dance communication and bee foraging activity [15]. Colony mates observing a dance show recognize the odor emitted by the dancing bee and seek it out at the designated food location. Flowers' color, shape and odor are remembered when the individual bees learn this stimulus shortly before discovering water and food (pollen, nectar) [16]. This appetitive form of learning behavior in honeybees has several traits of associative learning famous from research on the learning behavior of mammals [17]. It follows the principles of operant and classical conditions, respectively, so behavioral or stimuli acts are related to evaluating motivation. Because associative learning, particularly classical associative learning, is well explained at the operational and phenomenological levels, it offers a promising strategy in the hunt for the neural substrate underpinning learning and memory [18]. The homeostasis, survival and progress of honeybee colonies always

rely on the coordination's and contribution of each bee in a hive. Several studies have been conducted on the social behavior response of honeybees and also on other Hymenopteran insects [19].

3. Olfactory learning behavior

The appetitive associative behavior type is crucial in foragers' honeybee's species. The foragers' bees quickly learn to associate olfactory and visual stimuli with sugar solution/food reward, establishing a long-lasting remembrance of this association. Under controlled laboratory conditions, the worker bees can also remember/learn to respond to odor stimuli. In what has known as PER paradigm or proboscis extension response [20]. Usually, A bee harnessed in a metal or plastic tube learns to link a sucrose reward with an odor stimulation presented directly before the reward is given. Memory formation is evidenced when the harnessed bee extends its proboscis in response to the learned odor in anticipation of the sucrose reward. This form of classical conditioning has been successfully used to characterize multiple characteristics of associative learning and has shown potential in *Apis florea* and *Apis cerana* [21, 22].

4. Role of biogenic amines in the olfaction success of honeybee

Natural selection has shaped the brain to learn to associate cues that predict the occurrence of nutritious food. Sensory input is organized to produce memory traces for food stored for retrieval when animals are hungry so that animals can identify signals associated with nutritional rewards and avoid irrelevant or intoxication signals. Numerous biogenic amines receptors play a significant role in different types of behavior, such as social behavior [7]; among all biogenic amine receptors, dopamine, octopamine and serotonin receptors are considered primary biogenic amine receptors. The biogenic amines (BAs) neurotransmitters are key modulators and perform biological activities in animals, plants and microorganisms, BAs are responsible for executing and regulating the multiple behavioral and physiological activities in the body of honeybees as neurotransmitters, neurohormones and neuromodulators (**Figure 1**).
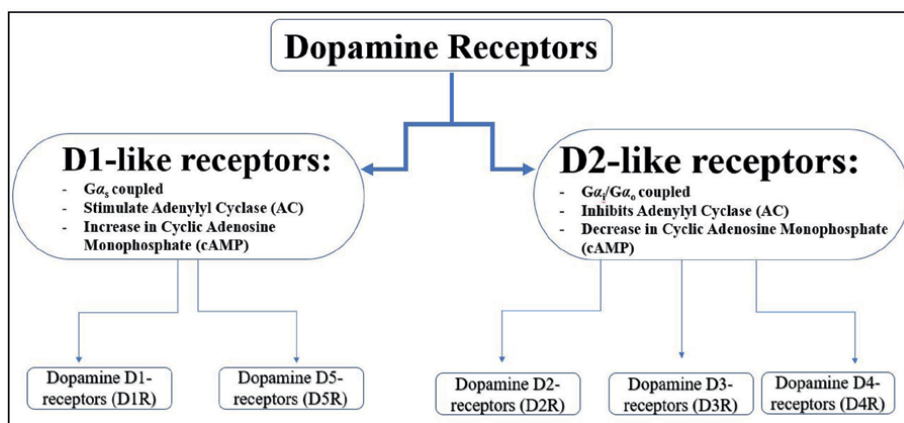

Figure 1.
Schematic diagram of dopamine receptor subtypes.

Receptors	Function	Location	Mechanism	Type	Selective agonist	Selective antagonist
D2	• Reproductive behavior, Locomotion, Sleep, Attention	VTA, Olfactory bulb, Striatum, Cerebral cortex	Increased level of cAMP intracellular by activating adenylate cyclase	Gi-coupled	• Bromocriptine • Pergolide • Cabergoline • Ropinirole	• Haloperidol • Raclopride • Sulpiride • Spiperone • Risperidone
D3	Locomotion, Regulation of food intake, Impulse control, Cognition	Cortex Islands of Calleja Striatum		Gi-coupled	• Nafadotride • GR-103691 • GR-218231 • SB-277011A NGB-2904 • PG-01037ABT-127	• 7-OH-DPAT • Pramipexole • Rotigotine • PD-128907
D4	• Attention • Impulse control • Reproductive behavior	• Hypothalamus • Amygdala • Frontal cortex • Nucleus accumbens		Gi-coupled	• A-381393 • FAUC213L-745,870 • L-750667	• A-412997 • ABT-670 • PD-168077
D1	• Attention • Learning • Locomotion • Sleep • Impulse control • Regulation of renal function • Memory	• Olfactory bulb • Nucleus accumbens • Striatum • Amygdala • Hippocampus • Frontal cortex • Substantia nigra • Hypothalamus	Enhanced intracellular cAMP through activated adenylate cyclase	Gs-coupled	• KF-81297 • SKF-38393Fenoldopa • (SKF-82526)	• SCH-39166 • SKF-83566 • SCH-23390

Receptors	Function	Location	Mechanism	Type	Selective agonist	Selective antagonist
D5	• Motor • Learning • Cognition • Decision • Making • Renin • Secretion	• Hypothalamus • Substantia nigra • Cortex	Adenylate cyclase	Gs-coupled		

Table 1.
Functional and physiological knowledge of dopamine receptors.

Several BAs, such as dopamine, serotonin, octopamine and tyramine, are crucial for olfactory learning behavior in honeybees [23]. Among all these BAs, dopamine is the major receptor and performs a vital role in the olfaction success of honeybees. In both vertebrates and invertebrates of the animal kingdom, dopamine receptors are present in the central nervous system and regulate multiple tasks. The dopamine receptors are divided into two families D1-like family and D2-like families. The D1-like family (D1, D5) and D2-like family (D2, D3, D4) actively regulate and modulate cell proliferation, differentiation, the release of cyclic adenosine monophosphate (cAMP) and other neurotransmitters also [24]. In this chapter, we focused on the learning behaviors of honeybees, especially olfactory learning behavior. Our focus is the practical functions of dopamine receptors, including olfactory learning, motivation, social behaviors, reward system, cognition, movement, emotion, etc., for forming appetitive and aversive learning [25]. Dopamine receptors catecholamine neurotransmitters work as catecholamine release, vascular tone, cardiovascular function, gastrointestinal motility, hormone secretion and renal function. The scientific community has been investigating over four decades that several diseases like schizophrenia, hyperprolactinemia, Tourette's syndrome and Parkinson's disease have been associated with dysregulation (erratic breathing, heart rate, thinking and behavior) of transmission of dopamine neurotransmitters [26].

D1-like receptors (D1 and D5) are located in different body parts. Dopamine D1 receptors are usually located at the Olfactory bulb, nucleus accumbens, striatum, amygdala, hippocampus, frontal cortex, substantia nigra, and hypothalamus and perform various functions, including Attention, learning, locomotion, sleep, impulse control, regulation of renal function and memory. **Table 1** shows the details and knowledge of the function, location, mechanism, type, selective agonist and selective antagonist of all dopamine receptors.

Dopamine receptors control olfactory learning behaviors and insect reproduction [27]. These receptors are responsible for various bodily functions, but dopamine receptors' major functions are reward-seeking, learning and other physiological properties. These receptors have distinct patterns and functional properties to compose the learning and memory in the brain. In insects like honeybees, *Drosophila melanogaster* and rodents, dopamine receptors and the basolateral amygdala are critically important for learning behavior. The mushroom bodies (MB) of *Drosophila melanogaster* and honeybees have a rich center for dopamine for olfactory learning and olfaction success and also provide a tractable mechanism to investigate the interaction between olfactory learning and dopamine receptors [28, 29]. This chapter will provide the basic interaction of dopamine receptors and olfactory learning behavior; olfactory learning behavior is important for colony survival. The functions of dopamine provide concrete evidence of how dopamine receptors are crucial and contribute to honeybees' olfactory behavior. Further study is required to investigate the role of dopamine receptors in managing the pest *varroa* mites of honeybees by using grooming behavior.

Acknowledgements

Author details

Muhammad Fahad Raza
Guangdong Key Laboratory of Animal Conservation and Resource Utilization,
Guangdong Public Laboratory of Wild Animal Conservation and Utilization, Institute
of Zoology, Guangdong Academy of Sciences, China

*Address all correspondence to: fbiuaf91@gmail.com

IntechOpen

References

[1] Muluneh MGJA, Security F. Impact of climate change on biodiversity and food security: A global perspective—A review article. Agriculture & Food Security. 2021;**10**(1):1-25

[2] Hurni H et al. Soil erosion and conservation in global agriculture. Land use and soil resources. 2008;(1):41-71

[3] Barrett CB. Overcoming global food security challenges through science and solidarity. American Journal of Agricultural Economics. 2021;**103**(2):422-447

[4] Kremen C, Miles A. Ecosystem services in biologically diversified versus conventional farming systems: Benefits, externalities, and trade-offs. Ecology and society. 2012;**17**(4):44-48

[5] Paudel YP et al. Honey bees (*Apis mellifera* L.) and pollination issues: Current status, impacts, and potential drivers of decline. Journal of Agricultural Science. 2015;**7**(6):93

[6] El-Seedi HR et al. Bee stressors from an immunological perspective and strategies to improve bee health. Veterinary Sciences. 2022;**9**(5):199

[7] Durazzo A et al. Bee products: A representation of biodiversity, sustainability, and health. Life. 2021;**11**(9):970

[8] Zhang S, Si A, Pahl MJFin. Visually guided decision making in foraging honeybees. Frontiers in neuroscience. 2012;**6**:88

[9] Varnon CA et al. Conspecific and interspecific stimuli reduce initial performance in an aversive learning task in honey bees (*Apis mellifera*). Plos one. 2020;**15**(2):e0228161

[10] Cook CN et al. Individual learning phenotypes drive collective behavior. Proceedings of the National Academy of Sciences. 2020;**117**(30):17949-17956

[11] Huber F, Markl H. Neuroethology and Behavioral Physiology: Roots and Growing Points. Germany: Springer Science & Business Media; 2012

[12] Perry CJ, Barron AB, Chittka LJCOiB. The frontiers of insect cognition. Current Opinion in Behavioral Sciences. 2017;**16**:111-118

[13] Bueno F et al. The queens of the stingless bees: From egg to adult. Insectes Sociaux. 2023;**70**(1):43-57

[14] Netz C et al. Details matter when modelling the effects of animal personality on the spatial distribution of foragers. Proceedings of the Royal Society B. 1970;**2022**(289):20210903

[15] Menzel R. Navigation and dance communication in honeybees: A cognitive perspective. Journal of Comparative Physiology A. 2023: p. 1-13

[16] Farina WM et al. In-hive learning of specific mimic odours as a tool to enhance honey bee foraging and pollination activities in pear and apple crops. Scientific Reports. 2022;**12**(1):20510

[17] Raza MF et al. Biogenic amines mediate learning success in appetitive odor conditioning in honeybees. Journal of King Saud University-Science. 2022;**34**(4):101928

[18] Baracchi D et al. Lateralization of sucrose responsiveness and non-associative learning in honeybees. Frontiers in Psychology. 2018;**9**:425

[19] Siefert P, Buling N, Grünewald BJPo. Honey bee behaviours within the hive: Insights from long-term video analysis. Plos one. 2021;**16**(3):e0247323

[20] Van Nest BN. The olfactory proboscis extension response in the honey bee: A laboratory exercise in classical conditioning. Journal of Undergraduate Neuroscience Education. 2018;**16**(2):A168

[21] Iqbal J et al. Olfactory associative behavioral differences in three honey bee Apis mellifera L. races under the arid zone ecosystem of central Saudi Arabia. Saudi journal of biological sciences. 2019;**26**(3):563-568

[22] Reams T, Rangel JJJoIS. Understanding the enemy: A review of the genetics, behavior and chemical ecology of Varroa destructor, the parasitic mite of Apis mellifera. Journal of Insect Science. 2022;**22**(1):18

[23] Raza M, Su S, Research E. Differential roles for dopamine d1-like and d2-like receptors in learning and behavior of honeybee and other insects. Applied Ecology and Environmental Research. 2020;**18**(1):1317-1327

[24] Scheiner R, Baumann A, Blenau W. Aminergic control and modulation of honeybee behaviour. Current neuropharmacology. 2006;**4**(4):259-276

[25] McQuillan HJ et al. Mushroom bodies of the honeybee brain show cell population-specific plasticity in expression of amine-receptor genes. Learning & Memory. 2012;**19**(4):151-158

[26] Li P, Snyder GL, Vanover KJCtimcE. Dopamine targeting drugs for the treatment of schizophrenia: Past, present and future. Current topics in medicinal chemistry. 2016;**16**(29):3385-3403

[27] Sasaki K, Watanabe TJI. Sex-specific regulatory systems for dopamine production in the honey bee. Insects. 2022;**13**(2):128

[28] Yamada D et al. Hierarchical architecture of dopaminergic circuits enables second-order conditioning in Drosophila. Elife. 2023;**12**:e79042

[29] Tedjakumala SR, Giurfa M. Behavioral and neural analyses of punishment learning in honeybees. In: Handbook of Behavioral Neuroscience. Australia: Elsevier; 2013. pp. 478-486

Edited by Edward Narayan

Animal Science Annual Volume 2023 explores primary research and review papers covering a broad spectrum of topics such as ecology, physiology, anatomy, health, and animal welfare. This volume features five chapters, each providing new insights into relevant areas of study within Animal Science. Topics covered include the ecology of ungulates in the Himalayas, the anatomy of the goat alimentary system, protein misfolding diseases in animals, the study of fossilized horse trackways, and the role of dopamine receptors in olfaction learning success in bees. *Animal Science Annual Volume 2023* will serve as a valuable resource for researchers and educators worldwide.

Rita Payan Carreira,
Veterinary Medicine and Science Series Editor

IntechOpen